Comparative morphology of the forelimb digging apparatus in armadillos (Xenarthra: Cingulata, Dasypodidae)

by

Sarah K. Marshall

Submitted in Partial Fulfillment of the Requirements

for the Degree of

Master of Science

in the

Biological Sciences

Program

YOUNGSTOWN STATE UNIVERSITY

August, 2018

Comparative morphology of the forelimb digging apparatus in armadillos (Xenarthra: Cingulata, Dasypodidae)

Sarah K. Marshall

Signature:

Sarah K. Marshall, Student	Date

Approvals:

Dr. Michael T. Butcher, Thesis Advisor	Date
Dr. Thomas P. Diggins, Committee Member	Date
Dr. Mark D. Womble, Committee Member	Date
Dr. Salvatore A. Sanders, Dean, College of Graduate Studies	Date

ABSTRACT

Armadillos (Family: Dasypodidae) are the most diverse group of the basal superorder Xenarthra, which is evident by their various lifestyles and range of scratch-digging ability. Descriptions of myology and quantifications of osteology reflect adaptations of the post-cranium and are essential for understanding the functional morphology of animal limbs. While there have been several studies on the limb bone proportions in numerous armadillos, limb myology has been reported for a limited number of species. Many of these descriptions need updating, and quantitive muscle data are available for only a single species. The objective of this study is to assess the forelimb myology of the pichi (*Z. pichiy*), screaming hairy (*Cha. vellerosus*), big hairy (*Cha. villosus*), and pink fairy (*Chl. truncatus*) armadillos with comparisons to previous documentations, and evaluate numerous osteological features of the forelimb among multiple species. Several myological features were variable among cingulates, such as the origin of m. trapezius pars cervicalis, variable presence of a distinct m. rhomboideus profundus, and number of heads present for m. triceps brachii and m. flexor digitorum profundus. Multiple osteological traits associated with greater fossoriality were also indicated, including robust limb bones, a prominent olecranon process, and short distal limb elements, which corresponded with the predictions of scratch-digging ability by Discriminant Function Analysis. Strong negative allometry of the humeral mid-shaft width/depth also reinforced the necessity for increased bone robustness as body size increases. These morphological features indicate various scratch-digging specializations among cingulates and their potential reorganization into separate families with future phylogenetic assessments of ancestral versus dervived traits associated with their lifestyles.

ACKNOWLEDEMENTS

I sincerely thank my graduate advisor, Dr. Michael Butcher, for his guidance, patience, and mentoring throughout my Thesis research project and Masters Degree. I thank my graduate committee members, Drs. Thomas Diggins and Mark Womble, for their critical reviews of my Thesis, manuscripts, and helpful comments. I am especially thankful for Dr. Diggins, and the countless hours that he helped with multivariate statistics. I am very grateful to Dr. Mariella Superina for giving me access to frozen armadillo specimens and for allowing me to collect myological data for my Thesis in her laboratory at Instituto de Medicina y Biología Experimental de Cuyo in Mendoza, Argentina. A special thank you to Darren Lunde (National Museum of Natural History), Eileen Westwig (American Museum of Natural History), and Bruce Patterson and Lauren Smith (Field Museum of Natural History) for coordinating access to museum collections in order to take postcranial osteological measurements. I also thank Vincent Village for his contributions to the illustrations included in my Thesis. Last, I am grateful to Marissa Gorvet and Kyle Spainhower, who are both terrific lab mates, and gave me consistent support throughout my tenure at YSU. Support for this research was provided by a Journal of Experimental Biology Traveling Fellowship. The YSU Office of Research and Department of Biological Sciences additionally provided travel funding. Finally, a Cushwa/Commercial Shearing Fellowship award funded my graduate assistantship AY 2017–2018.

DEDICATION

I dedicate this Thesis to my parents, grandparents, and brother who taught me the values of dedication and persistence, and who have always given their love and encouragement. Without the collective support of my family, I would have never been able to earn a Masters Degree in Biological Sciences, let alone, complete this graduate Thesis.

CONICET
IMBECU

Instituto de Medicina y Biología Experimental de Cuyo
Av. Dr. Adrián Ruiz Leal s/n. Parque Gral. San Martín
Dirección postal: Casilla de Correo 855. 5500 –Mendoza,
Argentina. Teléfonos: 54-261-524150/4195
Fax: 54-261-5244001
Correo electrónico: imbecu@mendoza-conicet.gob.ar

IMBecu
Instituto de Medicina y Biología experimental de cuyo

Mendoza (Argentina), August 29, 2017

Re: Journal of Experimental Biology Travelling Fellowship

Dear Review Committee,

It is my pleasure to give Sarah K. Marshall access to legally collected, frozen specimens of different armadillo species at my lab at the Institute of Medicine and Experimental Biology of Cuyo in Mendoza, Argentina. Laboratory space to examine the specimens will be available to Sarah anytime during her time in my facility, which is anticipated to be November and/or December 2017.

By giving her access to these specimens, Sarah will be able to thoroughly dissect their limb musculature and take muscle architectural measurements. I am confident that she will work responsibly and diligently when working with the armadillos as she collects data for her master's thesis research project, which she is carrying out under Dr. Michael Butcher's supervision at Youngstown State University in Ohio.

Furthermore, I am happy to support Sarah's work on her research project, as it is important to expand our knowledge on their limb morphology for scratch-digging and their evolutionary relationships with other xenarthrans.

I look forward to having Sarah in my laboratory and will help her with her project in any way I can.

Please do not hesitate to contact me should the need for additional information arise.

Yours sincerely,

Mariella Superina, Dr.med.vet., Ph.D.
Research Scientist CONICET
msuperina@mendoza-conicet.gov.ar

TABLE OF CONTENTS

LIST OF TABLES

LIST OF FIGURES

INTRODUCTION

Armadillos (Order: Cingulata) are members of the basal superorder Xenarthra, an assemblage which also contains anteaters and sloths (Order: Pilosa) (Superina and Loughry, 2015). In addition to various anatomical (e.g., extra zygapophyseal joints in lumbar vertebrae) and physiological traits (e.g., low resting metabolism) (McNab, 1980; Superina and Loughry, 2012), fossorial habits are considered to be ancestral within The Xenarthra, and are still commonly exhibited by living armadillos (Nyakatura and Fischer, 2011; Olson et al., 2016). The 21 extant species (Family: Dasypodidae) of cingulates demonstrate a gradient of scratch-digging specialization ranging from generalized to semi-fossorial and fossorial forms due to their ability to occupy numerous habitats present broadly throughout the Americas (Nowak, 1999). Importantly, their disparate lifestyles are expected to be reflective of their varying degrees of fossorial ability. For example, the pink fairy armadillo (*Chlamyphorus truncatus*) is found in the dry grasslands and sandy plains throughout Argentina, and it relies heavily on scratch-digging for its burrowing and foraging strategies (Borghi et al., 2011); these behaviors are functionally related to their partial subterranean lifestyle. In contrast, the pichi (*Zaedyus pichiy*), screaming hairy (*Chaetophractus vellerosus*), and large hairy (*Chaetophractus villosus*) armadillos do not exhibit a subterranean lifestyle, but instead are considered semi-fossorial (Superina and Abba, 2014) as related to their wider geographical distribution and mutual preference for arid microhabitats in numerous regions of Argentina and Chile (Superina, 2008; Abba et al., 2012; Polijak et al., 2018).

It has been proposed that adaptations for digging were strongly selected for in the basal stock of xenarthrans (Nyakatura, 2012). Moreover, evolution may have constrained musculoskeletal form for primarily scratch-digging function in all extant species of armadillos despite their broad range of lifestyles. The forelimbs of living armadillos display numerous obvious skeletal modifications for digging behavior, including robust limb bones with large areas for muscle attachment, short, more compact forefeet, and large, sharp foreclaws for piercing soil (Hildebrand, 1985; Olson et al., 2016). Specific modifications to the forelimb skeleton are as follows: enlarged teres process of the scapula; prominent deltoid tuberosity and/or deltopectoral crest of the humerus; wide medial epicondyle of the humerus; shortened and fused radius and ulna; and prominent

olecranon process of the ulna that increases the mechanical advantage of elbow extensor muscles (Miles, 1941; Vizcaíno, 1999; Vizcaíno and Milne, 2002). Armadillos also have well-developed forelimb muscles which provide increased strength (i.e., joint torque) for retraction of the forelimb, extension of the elbow joint, flexion and of the carpus and digits, and stabilization of the shoulder joint (Hildebrand, 1985). The limb retractors, elbow extensors, and digital flexors are typically the most massive functional groups in scratch-diggers (Lagaria and Youlatos, 2006; Rupert et al., 2015; Olson et al., 2016), which is advantageous for exerting high out-force on the substrate.

Limb muscle myology is essential for describing variation in areas of muscle attachment, relative muscle size, and the presence or absence of muscles. These features are often compared across species that share phylogeny to distinguish primitive (ancestral) from adaptive (derived) traits associated with the observed functional habits in extant species (Olson et al., 2016). This type of comparative analysis is critical for xenerthrans having relatively few updated descriptions of postcranial myology and are severely lacking quantitative data on musculoskeletal form. Myological details are available for only six species of armadillo (e.g., Galton 1869; Macalister, 1875; Windle and Parsons, 1899; Miles, 1941); however, the taxonomy of armadillos remains unresolved by a general lack of diversity across which both limb morphology and molecular genomics have been quantitatively evaluated. The current sole family organization is potentially problematic because of the diversity of lifestyles and functional habits observed among the cingulates, and emerging data from analyses of limb functional morphology (e.g., Olson et al., 2016; Butcher et al. unpublished data; Marshall et al. unpublished data) support this supposition. Determining the evolutionary relationships among armadillos is fundamental, as The Cingulata is estimated to have emerged approximately 41 MYA, placing it as one of the earliest orders of placental mammals (Eutheria) to have evolved (Delsuc et al., 2012). Therefore, expanding evaluations of postcranial characters centered on armadillo forelimbs is necessary for improving understanding of the evolutionary history of eutherians. In addition, revisions to forelimb myology of cingulates provide important details for determining the degree of scratch-digging specialization present among different armadillo species.

The main objective of this study is to describe the myology in *Z. pichiy* with morphological comparisons to other rare species of armadillo, including *Cha. vellerosus* *Cha. villosus*, and *Chl. truncatus*; these selected species represent a range of body size and lifestyles. It is hypothesized that differences in forelimb form will be predictive of the lifestyles observed among the cingulates. Specifically, the morphological traits quantified will be predictive of the degree of fossorial ability in armadillos with respect to indicating specialization of their forelimb elements. A secondary goal of this study is to assemble a suite of postcranial anatomical characters to help resolve the influences of morphology vs. phylogeny in the present taxonomic classifications of xenarthrans. It is predicted that armadillos with greater fossorial specialization will have: (1) less complex muscle functional groups by fewer numbers of muscle bellies or heads; (2) limb retractors, elbow extensors, and carpal/digital flexors will account for the greatest muscle mass compared to other functional groups; (3) limb retractors and elbow extensors will have long moment arms (i.e., in-levers) and the capacity for large mechanical advantage at the shoulder and elbow joints, respectively; (4) more robust limb bones for greater relative area of muscle attachment and higher resistance to bending stress; and (5) scratch-digging categorization based on their overall limb morphology and lifestyle. In particular, *Z. pichiy* is expected to be semi-fossorial in its functional habit specialization. This study will improve our understanding of the evolutionary relationships among armadillos, The Xenarthra, and more generally, that of early placental mammals.

MATERIALS AND METHODS

Study specimens

Six forelimbs from *Z. pichiy* (*N*=3), *Cha. vellerosus* (*N*=1), *Cha. villosus* (*N*=1), and *Chl. truncatus* (*N*=1) were dissected and described. Animal origin, sex, age, limb used for dissection, and body mass for all specimens and species studied are reported in Table 1. All individuals were supplied by Mariella Superina, Ph.D. and stored frozen (-20ºC) until observation. Specimens were allowed to thaw 24–36 hours at 4ºC prior to dissection. Systematic dissections were conducted at the Instituto de Medicina y Biología Experimental de Cuyo in Mendoza, Argentina. With the exception of *Z. pichiy*, animals were killed by poachers and confiscated post-mortem by law enforcement authorities of

the Mendoza Province of Argentina. Permission to dissect confiscated armadillos was granted by the Dirección de Recursos Naturales Renovables, Provincia de Mendoza, through Resolutions 794/09, 871/11, 823/13, and 105/16.

Forelimb myology

Muscle myology and nomenclature primarily followed that of Olson et al. (2016) with references to Galton (1869), Macalister (1875), Miles (1941), Murie (1872), and Windle and Parsons (1899). Synonyms of several muscles are provided in the Results section to facilitate comparisons with previous works on armadillo myology. Muscle names and abbreviations are presented in Table 2. Briefly, the carapace was removed, the forelimbs were skinned, and muscles systematically dissected from proximal-to-distal beginning with the extrinsic muscles of the carapace and limb. Muscle bellies were identified (only reduced mm. interossei were observed as intrinsic to the manus) along with the documentation of their origins, insertions, muscle fiber architecture, and actions (see Table 2). Phosphate buffered saline (PBS) was periodically applied to prevent muscle desiccation during dissection (Olson et al., 2016). Several photographs were taken for each muscle belly and at each level of dissection with an α-nex 5 digital camera (Sony, Japan), and these images were used to construct limb muscle maps and produce future illustrations of forelimb muscle topography. Following the removal of each muscle, wet mass was recorded using an analytical balance (Model: Chyo JK-180; Córdoba, Argentina) and fiber archietcure was verified by microdissection.

Bone functional indices

A suite of 29 osteological measurements were taken to the nearest 0.01 mm with digital calipers (Model: CD-8 CSX; Mitutoyo, Japan) from the scapula, humerus, radius, ulna, metacarpal III, first phalanx of digit III, and manus claw of digit III. In addition to the specimens dissected for their myological details, these measurements were taken from the forelimb skeletons of armadillos housed in the collections of the following museums of natural history: The National Musuem of Natural History (NMNH), American Museum of Natural History (AMNH), and the Field Museum of Natural History (FMNH). An additional seven species were observed and included the southern three-banded armadillo (*Tolypeutes matacus*), northern naked-tailed armadillo (*Cabassous centralis*), southern naked-tailed armadillo (*Cabassous unicinctus*), seven-banded armadillo (*Dasypus*

septemcinctus), southern long-nosed armadillo (*Dasypus hybridus*), nine-banded armadillo (*Dasypus novemcinctus*), and giant armadillo (*Priodontes maximus*). Bones were measured for a series of length, width, and depth dimensions, and each metric was recorded three times. All raw measurements were taken with limb long bones oriented in absolute anatomical position relative to the cranial surface of each bone, where dimensions in three planes were orthogonal (Fig. 1). A total of 29 functional indices were calculated from the raw osteological measurements, and these ratios were used to inform quantitative evaluations of scratch-digging ability and specialization of the forelimb for fossorial habits. Abbreviations, formulae, and functional implications of each index are given in Table 3.

Statistical analyses

Descriptive statistics are provided for each muscle/bone measurement, unless otherwise specified. Muscles were categorized into major functional groups for analysis: scapula elevator/rotators, limb retractors, limb protractors, limb adductors, elbow flexors, elbow extensors, carpal flexors, carpal extensors, digital flexors, digital extensors, and pronators. Mass of each functional group was calculated as a percentage total muscle mass and presented as means±s.d. (standard deviation). Allometry of humeral proportions was also statistically assessed, specifically for relationships of humerus length against mass, mid-shaft width, and mid-shaft depth. Raw values for each osteological measurement and individual were log transformed, and fitted with Reduced Major Axis (RMA: Model II) regressions in R Studio (smatr package) to yield the slope (i.e., scaling exponent) of each relationship. Under the null hypothesis of isometry, lengths to scale isometrically with mass (slope=0.33) and length (slope=1.00) (Biewener, 2005). Slopes of the relationships were statistically tested against these isometric predictions. In addition, the 95% confidence intervals about the estimates were determined in R Studio.

Stepwise Discriminant Function Analysis (DFA) was performed in SPSS (V.20: IBM) using all of the functional osteological indices listed in Table 3. This statistical method was utilized to predict substrate use as well as fossorial habit specialization for each armadillo species studied, specifically evaluating how scratch-digging assignment by DFA corresponded to *a priori* substrate use and digging habits based on descriptions of armadillo behavior found in the literature, and these are provided in Table 4. DFA output

(Wilks' Lambda scores and F-statistics) indicated the functional osteological indices that contributed most to the predicted memberships. Significance for all statistical tests was accepted at $p \leq 0.05$.

RESULTS

Forelimb myology is primarily described for *Z. pichiy* with comparisons to *Cha. vellerosus*, *Cha. villosus*, and *Chl. truncatus* where differences are observed. Muscle topography for *Z. pichiy* is illustrated in Figure 2. The origins and insertions of the musculature are shown as a series of limb muscle maps in Figs. 3, 4, 5, and 6. The forelimb of *Z. pichiy* contains 49 muscles (counting multiple heads or parts as separate muscles) that were studied. The species *Cha. vellerosus* also has 49 forelimb muscles, whereas *Cha. villosus* has 51 muscles and *Chl. truncatus* has 44 muscles in total. Muscles and all their actions (estimated from anatomical position and dissection) are organized into muscle functional groups in Table 5.

Muscles of the Carapace

M. Platysma

The m. platysma (or m. platysma pars zygomatica: Zeiger, 1927) originates from the caudal aspect of the zygomatic process of the cranium, immediately ventral to the auditory meatus of the temporal bone. Its origin also extends dorsally to the post-orbital bar except in *Chl. truncatus*, where the muscle belly is notably reduced. M. platysma inserts and/or becomes continuous with the m. panniculus carnosus. The m. platysma is not separable into a second part (m. platysma pars superficialis) and is indistinguishable from the m. panniculus carnosus. Murie (1872) referred to this muscle as the protractor of the scapular (or pectoral) shield of the carapace.

M. Panniculus Carnosus

The m. panniculus carnosus is a thin muscle belly and extremely reduced compared to that observed in *T. matacus* (Murie, 1872; Butcher et al., unpublished data) by being composed of only a single, cranial belly. It has a fleshy origin from the m. platysma and partially from the base of the cranium via the muscle presently identified as the m. trapezius pars cervicalis (see below). In *Chl. truncatus*, the m. panniculus carnosus is very thin and closely adhered to the skin, and therefore reliable descriptions are not

available for comparison. However, Macalister (1875) described two portions of the muscle in *Chl. truncatus*, with one extending from the abdomen to the lateral thigh and the other originating from the scapula and inserting onto the scapular shield. The m. panniculus carnosus inserts onto the dorsolateral aspect of the first dermal ring of the carapace (or movable zone: Murie 1872) just lateral to the origin of m. trapezius pars cercivalis from the carapace. In one individual (Zp 585), it inserts onto the scapular shield of the carapace lateral to the midline. In *Cha. vellerosus*, the insertion extends beyond the scapular shield to the third dermal ring, and in *Cha. villosus* it extends to the fifth dermal ring. Windle and Parsons (1899) reported similar attachments in *Cha. villosus*, although they described the insertion extended to only the fourth dermal ring.

Extrinsic Muscles of the Forelimb

Mm. Trapezius

The mm. trapezius is a broad muscle which is composed of two distinct parts: m. trapezius pars cervicalis and m. trapezius pars thoracica. Windle and Parsons (1899) reported a single muscle, but two distinct and separable bellies were observed in all of the specimens dissected herein. Both parts are located deep relative to the m. panniculus carnosus and variable layers of fat. While the pars cervicalis can be a thick muscle, the pars thoracica has a comparatively thin muscle belly.

- *M. Trapezius pars cervicalis*

The m. trapezius pars cervicalis originates from the first dermal ring of the carapace just lateral to the midline, and the caudolateral aspect of the base of the cranium from the area just caudal to the external auditory meatus. It has no attachments to the thin carapace in *Chl. truncatus*. The belly has an extensive, fleshy insertion that inserts onto the cranial two-thirds (Zp 583, Zp 585) to three-quarters (Zp 582) of the scapular spine and the dorsolateral acromion (Fig. 3a) after merging with m. omotransversarius (see below) near its cranial origin, as well as with m. subclavius via sheath-like tendon onto the distal three-quarters of the clavicle. A slip from the muscle belly additionally passes distal to the acromion (and superficial to the m. deltoideus) to merge with fascia associated with the m. pectoralis superficialis along the medial brachium, and both muscles terminate on the antebrachial fascia. The m. trapezius pars cervicalis, however, has no association with m. subclavius or the clavicle in *Cha. villosus* and *Chl. truncatus*, although a thin insertion

on the lateral clavicle in *Chl. truncatus* was documented by Macalister (1875). Similarly, *Chl. truncatus* is not observed to have the fasical association with the m. pectoralis superficialis. Last, Murie (1872) did not observe a true m. trapezius pars cervicialis in *T. matacus*, instead it is noted that the above descriptions are similar to those reported for two muscles referred to as the (1) protractor of the first movable zone, that also acts to retract the scapula, and the (2) retractor of the scapular shield attaching along the cranial mid-line of scapular shield. An almost indistinguishable condition between muscles of the carapace (Murie, 1872) and the m. trapezius pars cervicalis in specimens dissected herein is duly acknowledged.

- *M. Trapezius pars thoracica*

The m. trapezius pars thoracicia (previously m. trapezius inferior: Macalister, 1875) originates from the spinous processes of thoracic vertebrae T3 (or T4) to T7 (or T8) via fleshy fibers. The belly origin extends to the corresponding ribs in *Cha. villosus*, and via a membranous layer of tissue to T11 in *Chl. truncatus*. It inserts via prominent tendon on the caudal third (Zp 582) to half (Zp 583, Zp 585) of the scapular spine (Fig. 3a). The area of insertion is smaller in *Chl. trucatus* where it approximates the caudal eighth of the scapular spine.

Mm. Rhomboideus

The mm. rhomboideus is composed of a variable number of muscles along with modifications to their origins in all armadillo specimens and species studied. All portions of the muscle complex are found in the dorsal-to-lateral regions of the neck and lie deep to the m. trapezius pars cervicalis and/or the scapula. Three independent bellies are consistently present and include: m. rhomboideus profundus et capitus, m. rhomboideus cervicis, and m. rhomboideus thoracis. The former two muscles are strap-like in their shape, whereas as the m. rhomboideus thoracis has a fan-shaped appearance.

- *M. Rhomboideus profundus et capitus*

The m. rhomboideus profundus et capitus presents as a single belly in all four species. Macalister (1875) also reported that the profundus and capital bellies are fused and referred to the muscle solely as m. rhomboideus capitus; however, Hyrtl (1855) reported separate bellies referred to as m. internus et externus (i.e., m. rhomboideus profundus) and m. extensores capitis (i.e., m. rhomboideus capitus). The m. rhomboideus profundus

et capitus originates from the midline of the base of the cranium on the occipital ridge (Zp 582, Zp 583) or along the lambdoidal crest (Zp 585). In *Cha. villosus*, its arises from fleshy fibers along the lateral occipital ridge and extends to the mastoid process, whereas in *Chl. truncatus*, part of its origin is specifically from the dorsal region of the mastoid process in common with that of the m. cleidocephalicus pars mastoideus (see below) in addition to having an occipital bone attachment. The muscle inserts on the caudal half of the dorsal scapular border and fleshy onto the m. supraspinatus (Fig. 3a), where the two muscles share fibers near the dorsal portion of the caudal border of the scapula. In one individual (Zp 583), both areas of insertion were separable, where the capital belly inserts on the cranial half of the dorsal scapular border in common with m. rhomboideus cervicis and the profundus portion of the belly inserts on the caudal half of the dorsal scapular border. A similar condition is observed in *Cha. villosus* by the capital portion of the belly inserting on the cranial two-thirds of the dorsal scapular border and scapular neck, and the profundus portion of the belly inserting on the caudal third of the dorsal scapular border.

- *M. Rhomboideus cervicis*

The m. rhomboideus cervicis originates primarily from the transverse processes of cervical vertebrae C4–C7. The origin of this muscle also extends to the first rib in one individual (Zp 585), which is also the condition for *Cha. vellerosus* and *Cha. villosus*, whereas in *Chl. trucatus*, it extends to rib 2. Because of these attachments, the m. rhomboideus cervicis is continuous with m. serratus ventralis cervicis along the ribs in *Cha. villosus* and *Chl. truncatus*, which was not reported by either Windle and Parsons (1899) or Macalister (1875), respectively. It has a robust insertion on the medial side of the entire dorsal scapular border where it meets the dorsal region of the belly of m. subscapularis (Fig. 3b). In one individual (Zp 585), its attachment on the dorsal scapular border was more cranial and included the scapular neck, whereas in *Chl. trucatus*, in addition to the entire length of the dorsal scapular border, its insertion includes the dorsal fourth of the medial side of the caudal scapular border. In contrast to the condition observed in other species, the m. rhomboideus cervicis in *Cha. vellerosus* is continuous with m. subclavius (from their origins on rib 1), and notably shares an insertion on the caudal aspect of the clavicle.

- *M. Rhomboideus thoracis*

The m. rhomboideus thoracis originates from the spinous processes of thoracic vertebrae T1–T5, and it shares fibers with the dorsal expanse of the m. latissimus dorsi (see below) as its fan-shaped belly passes ventrally from the vertebral column. The origin of the muscle extended to the spine of T9 in one individual (Zp 583), whereas in *Cha. villosus*, its origin is limited to the spines of T1–T3. Notable muscle slips are observed to arise from each spinous process in *Chl. truncatus*, although these were not described by Hyrtl (1855) or Macalister (1875). It has a fleshy insertion on the medial side of the caudal border of the scapula that extends to the teres process of the scapula (Fig. 3b).

M. Omotransversarius

The m. omotransversarius (previously m. acromio-trachelian: Macalister, 1875) is a thin, strap muscle that originates from the caudal-to-caudolateral base of the cranium, just caudal to the external auditory meatus. In one individual (Zp 585), it also arises from the medial aspect of the mastoid process in common with the origin of the m. cleidocephalicus pars mastoideus (see below), which is also the condition observed in *Chl. truncatus*. Its origin extends further cranially to that of the m. platysma in *Cha. villosus*. The m. omotranversarius joins the belly of the m. trapezius pars cervicalis and both muscles insert on the acromion, just cranial to the origin of m. deltoideus pars acromialis (Fig. 3a). In *Cha. vellerosus* and *Cha. villosus*, its belly appears continuous with a muscular slip given off by the m. trapezius pars cervicalis that, along with the m. pectoralis superficialis, inserts onto the antebrachial fascia. This muscle was reported to be absent by Macalister (1875) and Windle and Parsons (1899).

M. Serratus Dorsalis Thoracis

The m. serratus dorsalis thoracis is not observed in any specimens and species studied. Murie (1872) and Butcher et al. (unpublished data) observed this muscle in *T. matacus.*

M. Serratus Ventralis Thoracis

The m. serratus ventralis thoracis (previously m. serratus magnus: Galton, 1869) is a fan-shaped, thin muscle deep to ventrolateral belly of the m. latissimus dorsi. It has an extensive origin from the ventral-to-ventrolateral aspects of primarily ribs 2–7 and inserts on the medial side of the teres process, ventral to the insertion of m. rhomboideus thoracis (Fig. 3b). In one individual (Zp 585), an additional muscle slip arises from rib 1

and inserts via a tendinous sheath onto the ventral belly region of m. rhomboideus cervicis. In *Cha. vellerosus*, the m. serratus ventralis thoracis arises from only ribs 4–7, whereas in both *Cha. villosus* and *Chl. truncatus*, it arises from ribs 3–8 and specifically inserts on the caudal half of the teres process. The muscle was originally described to originate as seven (Macalister, 1875) or eight (Hyrtl, 1855) separate bellies in *Chl. truncatus* from ribs, as well as from lower cervical vertebrae (Windle and Parsons, 1899).

M. Serratus Ventralis Cervicis

The m. serratus ventralis cervicis (previously levator anguli scapula: Macalister, 1875) is clearly observed in only one individual (Zp 583). It is a small, thin muscle that is closely associated with m. serratus ventralis thoracis that originates from rib 1, the transverse process of cervical vertebrae C7, and the ventrolateral aspect of the sternum. The muscle inserts on the medial side of the teres process cranial to that of m. serratus ventralis thoracis (Fig. 3b). The m. serratus ventralis cervicis arises from ribs 1–3 in *Cha. vellerosus* and ribs 1–2 in *Chl. truncatus*, with no vertebral attachments, and is indistinctive from the m. serratus ventralis thoracis. Accordingly, Macalister (1875) reported this muscle to be indistinguishable from m. serratus ventralis thoracis. However, in *Cha. villosus*, it is observed to have two distinct parts: the first part originates from ribs 2–3 and the transverse processes of cervical vertebrae C4–C7, and the second part from ribs 1–3 that merges with the belly of m. rhomboideus cervicis at rib 1 and the transverse process of C7. Windle and Parsons (1899) described it to be separate from m. serratus ventralis thoracis in *Cha. villosus*, although the number of bellies observed was not reported. Last, the m. serratus ventralis cervicis also shares fibers with m. subscapularis in *Cha. vellerosus*.

M. Latissimus Dorsi

The m. latissimus dorsi consists of dorsolateral and ventrolateral belly portions, and as such has an expansive origin. The dorsolateral expanse of the muscle is relatively thin and arises from the spines of thoracic vertebrae T7–T9 (Zp 583) or T8–T11 (Zp 585) via the thoracodorsal fascia, with muscle fibers that generally overlie the lateral shaft of ribs 8–11 (Fig. 2a). A similar fascial origin is present in Zp 582, although the exact number of lower thoracic vertebrae was not recorded. The ventrolateral portion is well-developed and originates from a variable number of ribs: 5–8 (Zp 585), 5–10 (Zp 583), and 6–11

(Zp 582). Both portions coalesce along the caudal scapular border to form a distinct muscle belly, where the muscle as a whole has an additional origin from the caudolateral aspect of the teres process (Fig. 3a), that is continuous with that of the m. triceps brachii angular head via the m. tensor fasciae antebrahii (see below). The m. latissimus dorsi runs deep along the ventral border of the scapula and distally gives rise to a prominent tendon that inserts onto the medial (Zp 582) to caudomedial (Zp 583, Zp 585) aspect of the proximal humerus (Fig. 4b, d). In one individual (Zp 582), its tendon of insertion lies deep to the tendons of origin for both the m. biceps brachii long head and m. coracobrachialis.

In addition to having similar origins from lower thoracic vertebrae and ribs, the dorsolateral expanse begins more cranially from spine thoracic vertebrae T4 via thoracodorsal fascia in *Cha. villosus*, where it overlaps with the origin of m. rhomboideus thoracis and its fibers further originate from the lateral side of the teres process; the latter condition is also present in *Cha. vellerosus*. A vertebral origin of the dorsolateral expanse is not observed in *Cha. vellerosus*, or *Chl. trunactus*, and arises only from ribs; however, due to prior damage to the *Cha. vellerosus* specimen, the exact number of ribs serving as the origin of this portion could not be determined. In *Chl. truncatus*, the dorsolateral expanse arises from the caudal margins of ribs 7–8 with minimal origin from the teres process. Macalister (1875) also reported two bellies of the m. latissimus dorsi in *Chl. truncatus*, although one was described to originate from the transverse processes of thoracic and lumbar vertebrae, and the second from the five caudal-most ribs and the lateral teres process. The second belly observed corresponds to the distinct ventrolateral portion of the muscle belly. Its insertion on the humerus and is proximal and just cranial to that of m. teres major in *Cha. vellerosus* and *Chl. truncatus*, respectively, whereas it inserts on the craniomedial humerus in *Cha. villosus* via a common tendon with m. teres major.

M. Pectoralis Superficialis

The m. pectoralis superficialis has a broad origin that spans the entire length of the sternum along its midline, and also arises caudally from to the abdominal fascia. The muscle is divisible into two bellies in *Cha. vellerosus* and *Cha. villosus*. Both bellies arise from the sternum in *Cha. vellerosus*, where the cranial belly originates from the cranial

end of the sternum and passes superficial to the sternoclavicular joint, and the caudal belly arises from the sternal midline. However, the m. pectoralis superficialis was not divisible for the right limb of the specimen. In *Cha. villosus*, lateral and ventral bellies arise from the shafts of ribs 5–8 (and abdominal fascia) and the sternal midline, respectively. *Chl. truncatus* has a single belly that originates from the entire breadth of the sternum, although Macalister (1875) indicated additional clavicular and abdominal bellies. The m. pectoralis superficialis inserts via broad tendon on the medial aspect of the deltopectoral crest of the humerus (Fig. 4a, d). It also merges with m. trapezius pars cervicalis to insert on the cranial region of the antebrachial fascia. The latter insertion is absent in *Chl. truncatus*. Specifically, in *Cha. vellerosus*, the cranial belly of the muscle extends to the antebrachial fascia, whereas the caudal belly inserts via a tendon to the craniomedial aspect of the distal deltopectoral crest that passes superficial to the m. biceps brachii long head.

M. Pectoralis Profundus

The m. pectoralis profundus arises from the ventral aspect of ribs 4–8 (Zp 582) and ribs 6–7 (Zp 583); however, it is absent in one individual (Zp 585), as well as being absent in *Cha. vellerosus*, *Cha. villosus*, and *Chl. truncatus*. The muscle was previously reported to be present in both *Cha. villosus* and *Chl. truncatus*, and it was referred to as m. pectoralis minor (Windle and Parsons, 1899) and m. pectoralis quartus (Macalister, 1875), respectively. It inserts on the proximomedial aspect of the deltopectoral crest, proximal to the broad attachment of m. pectoralis superficialis (Fig. 4a, d). In one individual (Zp 582), m. pectoralis profundus inserts onto the proximocranial humerus via a sheet of fascia that overlies the tendon of origin of the m. biceps brachii long head.

M. Subclavius

The m. subclavius (previously m. pectoralis minor: Miles, 1941) originates from the ventral surface of rib 1 and the cranial end of the lateral sternum via fleshy fibers. Notably, no sternal origins are observed in *Cha. vellerosus* or *Cha. villosus*. In *Chl. truncatus*, it originates from rib 1 immediately lateral to the sternoclavicular joint. The muscle inserts on the distal third (Zp 585) to half (Zp 583, Zp 582) of the dorsal surface of the clavicle (Fig. 3a). In *Cha. villosus*, the muscle inserts mainly on the coraco-clavicular ligament via fleshy fibers. Windle and Parsons (1899) and Hyrtle (1855)

described the m. subclavius to have a fascial attachment to m. supraspinatus in *Cha. villosus* and *Chl. truncatus,* respectively. Additionally, it was reported by Macalister (1875) to insert on both the coracoid process and cranial aspect of the acromion in *Chl. truncatus*. The m. subclavius is observed to insert on the craniolateral acromion and the cranial end of the dorsal scapular border in *Chl. truncatus*, but has no obvious attachment to the coracoid process.

M. Sternomastoideus

The m. sternomastoideus is composed of two bellies: sternal and clavicular. The sternal belly arises from the craniomedial sternum, whereas the clavicular belly arises from the proximal end of the clavicle (Fig. 3b). In *Cha. villosus*, the clavicular belly has an additional fibrous attachment to the sternoclavicular joint at its origin. The two bellies fuse prior to its insertion onto the mastoid process via strong common tendon. In one individual (Zp 583) and *Cha. vellerosus*, only one belly is observed. Macalister (1875) documented separate muscles and indicated a single belly in *Chl. truncatus* identified as the m. sternomastoid that originated from only the sternum. The second muscle was identified as the m. cleidomastoid, which was present in the same condition as the m. cleidocephalicus pars mastoidea (see below).

M. Brachiocephalicus

M. brachiocephalicus is a reduced muscle complex in all specimens and species studied. It is variably composed of only one part, the m. cleidocephalicus pars mastoidea. The m. cleidocephalicus pars cervicalis is consistently absent in armadillos (Galton, 1869; Macalister, 1875; Miles, 1941; Murie 1872; Olson et al. 2016; Windle and Parsons 1899).

-*M. Cleidocephalicus pars Mastoidea*

The m. cleidocephalicus pars mastoidea (or m. cleidomastoideus) is a thin, strap muscle that originates from the lateral aspect of the mastoid process immediately caudal to the insertion of m. sternomastoideus (Fig. 3b). It is not clearly observed in two individuals (Zp 583, Zp 582). In *Chl. truncatus*, it originates on the lateral. The belly runs dorsolateral to the m. sternomastoideus to insert on the proximal third of the ventral clavicle.

-*M. Cleidobrachialis*

The m. cleidobrachialis, also referred to as m. deltoideus par clavicularis, is not observed as a belly distinct from the m. deltoideus in all specimens and species studied.

Intrinsic Muscles of the Forelimb

Shoulder Region

M. deltoideus

The m. deltoideus is composed of three parts: pars scapularis, pars acromialis, and pars clavicularis (Fig 4a, d). The m. deltoideus pars scapularis originates via fleshy fibers from the cranial two-thirds of the ventral margin of the scapular spine and fascia overlying the deep m. infraspinatus. In *Cha. villosus*, it originates along the entire length of the ventral scapular spine and a small area approximating the mid-caudal scapular border. In *Chl. truncatus*, the origin of the muscle extends further cranially to the acromion, just caudal to where the pars acromialis takes origin. It inserts via tendinous fibers onto the lateral and distal margins of the deltoid tuberosity of the humerus. The m. deltoideus pars acromialis arises from the ventrolateral aspect of the acromion that is ventral to the acromial insertion of m. trapezius pars cervicalis. In one individual (Zp 583) and *Cha. villosus*, its deep fibers fuse with the thin pars scapularis, and the bellies become tendinous towards their insertion. The muscle inserts on the craniolateral aspect of the distal deltoid tuberosity. In *Chl. truncatus*, its insertion is proximal to that of the pars scapularis. The m. deltoideus pars clavicularis (or m. cleidobrachialis) originates from the distal half (Zp 585) to two-thirds (Zp 583, Zp 582) of the clavicle. In *Chl. truncatus*, the muscle arises from the distal eighth of the clavicle and bony surface of the acromioclavicular joint. It inserts on the craniomedial aspect of the distal deltoid tuberosity intermediate to the pars acromialis and m. pectoralis superficialis. The insertion was partially damaged in *Cha. vellerosus*, but the belly appeared to be continuous with the muscle slip given off by m. trapezius pars cervicalis to the antebrachial fascia with no bony attachment. In *Chl. truncatus*, the insertion on the deltoid tuberosity is distal to that of m. pectoralis superficialis and remains medial to that for both the pars acromialis and pars scapularis.

M. Supraspinatus

The m. supraspinatus has a fleshy origin from the supraspinous fossa of the scapula (Fig. 3a) along with a notable fleshy attachment to the coracoclavicular ligament, which is not observed in *Cha. vellerosus* and *Cha. villosus*. It inserts via tendon on the entire cranial aspect of the greater tubercle proximal to the insertion of m. infraspinatus (Fig. 4a, d). Hyrtle (1855) reported this muscle to be fused with m. teres major in *Chl. truncatus*, but this condition is not observed.

M. Infraspinatus

The m. infraspinatus fossa arises from the infraspinuous fossa of the scapula via fleshy fibers (Fig. 3a), and it inserts on the lateral aspect of the greater tubercle in between the insertion of m. supraspinatus proximally and m. teres minor distally (Fig. 4a, c). The muscle belly consistently has bipennate fiber architecture.

M. Teres Minor

The m. teres minor is a small, strap muscle that has a fleshy origin ventral and partially deep to the belly of m. infraspinatus. It specifically arises from the secondary scapular spine and the cranial half of the ventral scapula border (Fig. 3a). The muscle belly is comparatively reduced in *Cha. vellerosus* and it originates from the cranial half of the secondary scapular spine. In *Cha. villosus*, the origin of m. teres minor extends from the cranial third of the secondary scapular spine to the ventral lip of the glenoid fossa, although the latter attachment was not observed by Windle and Parsons (1899). It inserts just distal to m. infraspinatus on the lateral aspect of greater tubercle of the humerus (Fig. 4a, c).

M. Teres Major

The m. teres major originates from the lateral side of the teres process of the scapula, deep to the origin of the m. triceps brachii caput angulare (Fig. 3b; see below). In *Cha. vellerosus*, its origin is also invested on the cranial half of the ventral scapular border, whereas in *Cha. villosus* and *Chl. truncatus*, its origin is either cranial or dorsal to that of the m. triceps brachii angular head, respectively, along the lateral side of the teres process. Macalister (1875) previously described the origin of this muscle to be ventral to the m. subscapularis from the medial side of the teres process in *Chl. truncatus*. The m. teres major has a tendinous insertion the is generally in common with the m. latissimus

dorsi but onto either the medial (Zp 582) or caudomedial (Zp 583, Zp 585) aspects of the proximal humeral shaft, just distal to the lesser tubercle (Fig. 4b, d). In individual (Zp 582), it is noted as having a prominent tendon of insertion that lies deep to the proximal belly region of both the m. coracobrachialis and m. biceps brachii. In *Cha. vellerosus* it inserts distal to the insertion tendon of m. latissimus dorsi.

M. Subscapularis

The m. subscapularis has a broad, thick belly and a fleshy origin from the entire subscapular fossa of the scapula (Fig. 2b, 3b). It inserts via a thick tendon on the entire lesser tubercle of the humerus, proximal to the insertions of the m. teres major and/or m. latissimus dorsi (Fig. 4a, b, d). Hyrtl (1855) was not able to separate this muscle from m. teres major in *Chl. truncatus* and reported both muscles as the m. subscapularis, whereas Macalister (1875) and Windle and Parsons (1899) reported these two muscles as clearly separable in *Chl. truncatus*, which is consistent with the present condition of these muscles.

Brachium Region

M. Coracobrachialis

The m. coracobrachialis originates via a long, thin tendon from the medial tip of the coracoid process of the scapula (Fig. 2b, 3b). It is absent in one individual (Zp 585) and *Chl. truncatus*, the latter of which is consistent with the accounts of Hyrtl (1855) and Macalister (1875). The muscle runs caudal to the belly of the m. biceps brachii long head, to which it shares some fibers distally, to insert via fleshy fibers on the medial-to-caudomedial aspect of the proximal medial epicondyle of the humerus. In contrast, Windle and Parsons (1899) indicated the m. coracobrachialis is fused proximally with the short head of m. biceps brachii in *Cha. villosus*, and bifurcates prior to the insertion of each belly. In *Cha. villosus*, it inserts via a tendon slip onto the craniomedial aspect of the medial epicondyle, proximal to the origin of m. pronator teres.

M. Articularis Humeri

The m. articularis humeri (or m. coracobrachialis brevis: Ercoli et al., 2015) is not observed in any specimens and species studied. Hyrtl (1855) also did not document this muscle in *Chl. truncatus*, but it was observed by Macalister (1875). Windle and Parsons

(1899) also observed this muscle in *Cha. villosus*, but provided no myological descriptions.

M. Biceps Brachii

The m. biceps brachii primarily has a long head of origin, whereas the short head is only present in *Cha. vellerosus* and *Cha. villosus*. These observations are consistent with Macalister (1875) and Windle and Parsons (1899). The long head (*caput longum*) originates via long tendon from the dorsal lip of the glenoid fossa of the scapula (Fig. 2b, 3b). The tendon of origin travels medially along the proximal, cranial humerus to join the belly of the muscle. In *Chl. truncatus*, the tendon additionally takes origin from a well-developed coraco-clavicular ligament, which was not documented by Macalister (1875). The long head has a tendinous insertion on the ulnar tuberosity of the proximomedial ulna, immediately proximal to the insertion of m. brachialis (Fig. 5b). In *Cha. vellerosus*, *Cha. villosus*, and *Chl. truncatus* it inserts with the m. brachialis via shared tendons and also sends some fibers to the head of the radius. The short head (*caput breve*) originates from the coracoid process. In *Cha. villosus*, it specifically arises from a tendon sheet that envelops the coraco-clavicular ligament. The muscle inserts in common with the long head. In *Cha. vellerosus*, the belly of the short head fuses with the long head just prior to insertion on the proximal ulna.

M. Brachialis

The m. brachialis has an extensive origin in all specimens and species studied except in *C. truncatus*. It arises from the caudolateral aspect of the humerus, just distal to the proximal origin of m. triceps brachii caput laterale (Fig. 4a, b, d; see below), the caudal aspect of the deltopectoral crest, and wraps cranially to further attach to the humeral shaft distal to the deltopectoral crest. Windle and Parsons (1899) reported similar descriptions in *Cha. villosus*. In *Cha. vellerosus*, the muscle arises from the lateral humeral neck and its origin spans the proximal half of the caudal humeral shaft, whereas it arises from only the lateral humeral neck/head deep to the origin of m. triceps brachii caput laterale in *Chl. truncatus*. The m. brachialis inserts distal to m. biceps brachii on the distal end of the ulnar tuberosity (Fig. 5b). In *Cha. vellerosus, Cha. villosus*, and *Chl. truncatus* it inserts in common with the long head of the m. biceps brachii, and also with short head of m. biceps brachii as observed in both *Cha. vellerosus* and *Cha. villosus*.

M. Triceps Brachii

The mm. triceps brachii is a massive and complex muscle that is composed of five distinct muscle heads of origin: angular (*caput angulare*), long (*caput longum*), lateral (*caput laterale*), medial (*caput mediale*), and medial accessory (*caput mediale accessorium*). The angular and long heads arise from the scapula, whereas the lateral and medial heads are situated along the caudolateral and caudomedial aspects of the humerus, respectively. The medial accessory head is the smallest head and arises at the elbow joint. Windle and Parsons (1899) and Macalister (1875) observed four bellies in *Cha. villosus* and *Chl. truncatus* (*caput angulare*, *caput longum*, *caput laterale*, and *caput mediale*), specifically where only one humeral and three scapular bellies were present in *Chl. truncatus*. All heads have similar attachments in the specimens dissected herein.

-*Caput angulare*

The m. triceps brachii caput angulare arises from a heavy investment on the surface of the lateral side of the teres process, superficial to the origin of m. teres major (Fig. 2a, 3a). At its origin, the muscle coalesces with fibers from dorsal expanse and ventrolateral portions of the m. latissimus dorsi via the m. tensor fasciae antebrachii, the latter of which invests to the entire caudal belly of the angular head. In *Cha. villosus*, this head is situated caudal to the origin of m. teres major, whereas in *Chl. truncatus*, its origin is ventral to that of m. teres major at the tip of the teres process, and it is not observed to sharing fibers with the m. latissimus dorsi. This head runs caudal to the long head to insert on the caudolateral aspect of the tip of the olecranon process of ulna (Fig. 5a).

-*Caput longum*

The m. triceps brachi caput longum is a massive muscle which is composed of a medial and lateral belly. One individual (Zp 582) has completely separable bellies, where the medial belly arises via tendon from the ventral lip of the glenoid fossa and the lateral belly (i.e., main belly) from the cranial three-fourths of the ventral secondary scapular spine. It is also present in this condition in *Cha. vellerosus*. In the other two individuals (Zp 583, Zp 585), the origin is similar to that observed for the lateral belly and spans the entire length of the secondary scapular spine and/or ventral scapular border (Fig. 2a,b, 3a). The muscle could be divided into separate bellies which fuse at mid-belly in Zp 583, whereas the bellies are inseparable in Zp 585. In *Cha. villosus* and *Chl. truncatus*, the two

bellies fuse prior to insertion, and their origin extends from the cranial margin of the teres process to the glenoid fossa. Although Macalister (1875) reported three separate scapular bellies for *Chl. truncatus*, those descriptions match the medial and lateral bellies of long head in addition to angular head. The long head inserts on the lateral aspect of the olecranon process, just distal to the insertion of the angular head (Fig. 5a). In Zp 582, the medial belly specifically inserts medially on the olecranon deep to m. tensor fasciae antebrachii. In *Cha. villosus*, the muscle has a cranial insertion on the olecranon process.

-*Caput laterale*

The m. triceps brachii caput laterale has broad origin lateral to medial head which extends from the caudolateral aspect of the humeral neck to the lateral epicondyle via fleshy fibers (Fig. 4b, c). It clearly arises from only the humeral neck in *Cha. vellerosus*, *Cha. villosus*, and *Chl. truncatus*. The muscle inserts on the cranial aspect of the lateral olecranon process distal to the insertion of the long head (Fig. 5b). It is likely that the sole humeral head observed by Macalister (1875) was a fusion of the lateral and medial heads.

-*Caput mediale*

The m. triceps brachii caput mediale arises from the caudal-to-caudomedial aspect of the humerus, distal to the insertion of m. latissimus dorsi and extends to the caudal aspect of the proximal medial epicondyle (Fig. 4b, d). In *Cha. vellerosus*, its origin does not extend as far distally, and the lateral region of its belly is partially deep to the extensive origin of m. brachialis along the caudal humeral shaft. In *Cha. villosus*, its origin extends to the supracondylar ridge of the medial humerus. The muscle inserts on the medial aspect of the olecranon process near the insertion of the caput mediale accessorium (Fig. 5b). Specifcally in *Cha. villosus*, the medial head is observed to insert deep to the medial accessory head.

-*Caput mediale assessorium*

The m. triceps brachii caput mediale accessorium (or m. anconeus internus: Ercoli et al., 2015) is the smallest head of the m. triceps brachii and it arises from the caudomedial aspect of the proximal medial epicondyle, just distal to the insertion of m. coracobrachialis (Fig. 4b, d). In *Cha. vellerosus*, *Cha. villosus*, and *Chl. truncatus* it originates more caudally on the proximal medial epicondyle. The muscle inserts on the medial and caudal surfaces of the olecranon process at its tip (Fig. 5b). In relation to the

muscle belly of the m. triceps brachii medial head, its insertion is distal, but is superficial in *Cha. villosus*, and is proximal in *Chl. truncatus*.

M. Tensor Fasciae Antebrachii

The m. tensor fasciae antebrachii (previously m. dorsi-epitrochlearis; Miles, 1941) has an extensive fleshy origin from fascia on the dorsal belly region of the ventrolateral portion of m. latissimus dorsi. Previously, Windle and Parsons (1899) observed it to also arise from the insertion of m. latissimus dorsi at the humeral neck in *Chl. truncatus*. Along the caudoventral border of the teres process, its muscle fibers become superficial to the scapular origins of both the m. latissimus dorsi and m. triceps brachii angular head. Distally, its thin muscle belly invests the entire caudal belly of the angular head and the m. tensor fasciae antebrachii inserts via fleshy fibers onto antebrachial fascia overlying the medial tip of the olecranon (Fig. 5a). It is noted that the muscle was nearly inseparable from m. triceps brachii angular head in most specimens. The muscle also has a small area of insertion on the proximolateral olecranon just distal to that of the angular head, whereas no olecranon insertion is observed in *Cha. vellerosus* and *Cha. villosus*, and it inserts medially on the olecranon process in *Chl. truncatus*. Macalister (1875) additionally described the muscle to insert on the medial epicondyle in *Chl. truncatus*.

M. Anconeus

The m. anconeus (or m. anconeus externus: Ercoli et al., 2015) is a triangular-shaped muscle which originates from the entire expanse of the olecranon fossa on the caudodistal humerus (Fig. 4b, c). It inserts on the craniolateral aspect of the olecranon process of the ulna either distal (Zp 583, Zp 585, *Cha.* vellerosus, *Cha. villosus*,) or deep (Zp 582, *Chl. truncatus*) to the insertion of the m. triceps brachii lateral head (Fig. 5a).

Antebrachium Region

M. Pronator Teres

The m. pronator teres originates on the medial epicondyle of the humerus, where it specifically arises immediately medial to the supracondyloid foramen (Fig. 4a). However, the muscle originates from the medial supracondylar ridge in *Chl. trunatus*, consistent with the observations reported by Macalister (1875). It has a membranous insertion on the distal end of the medial radius in an area that is distal to the broad origin of the m.

flexor digitorum profundus caput radiale (Fig. 5d; see below). In *Chl. truncatus*, it inserts similarly, but its radial attachment is cranial to the origin of m. flexor digitorum profundus radial head.

M. Flexor Carpi Ulnaris

The m. flexor carpi ulnaris originates from the caudomedial aspect of the olecranon process deep to the insertion of all heads of the m. triceps brachii (Fig. 5b), and from the caudomedial aspect of the medial epicondyle via short tendon (Fig. 4b, d). In *Cha. vellerosus* and *Cha. villosus*, it arises only from the caudal tip of the medial olecranon and is not positioned deep to m. triceps brachii. In *Chl. truncatus*, the muscle arises from the caudodistal medial epicondyle and the medial olecranon process in common with m. flexor digitorum superficialis, where the bellies of both muscles separate just distal to their origin. It inserts via a prominent layer of tendon onto the accessory carpal bone (pisiform) (Fig. 6a). In *Cha. villosus*, the muscle insertion continues distally to the lateral aspect of the manus via palmar fascia. It displays a tendinous inscription which runs the entire length of the belly.

M. Flexor Carpi Radialis

The m. flexor carpi radialis arises via a tendon from the medial epicondyle of the humerus, medial to the origin of m. pronator teres and always proximal to the origin of all humeral heads of the m. flexor digitorum profundus (Fig. 4a, d). In *Cha. vellerosus*, *Cha. villosus*, and *Chl. truncatus*, the origin is distal to the origin of m. pronator teres. It inserts via a thin tendon onto a portion of the trapezium (Fig. 6a), in addition to inserting onto the palmar aspect of the base of metacarpal I in *Chl. truncatus*. Both insertions are observed in *Cha. villosus*.

M. Palmaris Longus

The m. palmaris longus is not observed in any specimens and species studied. This muscle was previously reported to be fused with m. flexor digitorum superficialis in *Cha. villosus* (Windle and Parsons, 1899) and *Chl. truncatus* (Macalister, 1875). Specifically, the m. palmaris longus in *Cha. villosus* was described as superficial fibers arising from m. flexor digitorum superficialis and passing to the annular ligament of the radius, whereas in *Chl. truncatus*, it was described as a separate belly that is orientated close to the both origin and medial margin of the m. flexor digitorum ulnaris.

M. Flexor Digitorum Superficialis

The m. flexor digitorum superficialis (previously m. flexor digitorum sublimis: Macalister, 1875) originates from the distal, caudal tip of the medial epicondyle of the humerus (Fig. 4b). In *Cha. vellerosus*, it also shares a small tendon with m. flexor carpi ulnaris at the origin. In *Chl. truncatus*, its association with the belly of m. flexor carpi ulnaris is fleshy, but the muscle partially arises from the medial olecranon. This condition was similarly observed by Macalister (1875). Distally, two thin tendons emerge from the muscle belly. The medial tendon inserts on the palmar aspect of the proximal phalanx of digit II, while the lateral tendon passes to the proximal phalanx of digit III. The latter tendon also sends a minor slip to the lateral base of the intermediate phalanx of digit IV, which was only observed in *Z. pichiy* (Fig. 6a). In *Cha. vellerosus*, the medial tendon emerges from the muscle belly as a thinner tendon that to inserts on digit III, which sends a thicker tendon to digit II. In *Chl. truncatus*, its tendons insert on the base of the intermediate phalanges of digits I and III rather than inserting on digit II, although Macalister (1875) indicated insertion onto the palmar aspect of an internal ossicle. Windle and Parsons (1899) reported this muscle to have only a single tendon inserting on digit III in *Cha. villosus*.

M. Flexor Digitorum Profundus

The mm. flexor digitorum profundus is a large and complex muscle that is primarily composed of two heads with humeral origins (*caput humerale mediale* and *humerale laterale*), a third head that takes origin from the ulna (*caput ulnare*), and a fourth head that arises from the radius (*caput radiale*). *C. villosus* is the only species observed to have a third head arising from the humerus (*caput humerale profundus*), whereas *Chl. truncatus* has only one head that arises from the humerus (*caput humerale*). Overall, it is the deepest muscle in the medial and caudal regions of the antebrachium, and it is the largest muscle of the entire distal forelimb. Macalister (1875) previously described this muscle as having only radial and ulnar heads in *Chl. truncatus*.

The humeral medial head (*caput humerale mediale*) has a tendinous origin on the medial tip of the medial epicondyle, distal to the origins of both m. pronator teres and m. flexor carpi radialis (Fig. 4a, d). In *Chl. truncatus*, the muscle is closely associated with the radial head at its origin. The humeral lateral head (*caput humerale laterale*) arises

from the caudodistal edge of the medial epicondyle (Fig. 4b), intermediate to the origin of the humeral medial head (medial) and the trochlea of the humerus (lateral). It shares fibers with the ulnar head at its origin and along three-fourths of its belly length. In *Cha. villosus* and *Cha. vellerosus*, it arises more cranially from the craniodistal surface of the medial epicondyle. The humeral profundus head (*caput humerale profundus*) originates from the distal tip of the cranial medial epicondyle in between the origin for the humeral lateral and medial heads. The ulnar head (*caput ulnare*) is the largest of all heads of m. flexor digitorum profundus. It has an extensive origin on the medial and caudal aspects of the entire ulna, including the olecranon (Fig. 5b). In *Chl. truncatus*, it originates from the entire caudal margin of the ulna, whereas Macalister (1875) described this head to arise from only the olecranon. The radial head (*caput radiale*) originates from the medial mid-shaft of the radius and the interosseous membrane (Fig. 5d). In one individual (Zp 583), this head is also observed to take origin from the medial epicondyle via tendon superficial to the m. pronator teres and additionally from the caudomedial aspect of the ulna.

All four muscle heads merge together to form a broad, thick common tendon that contains two large sesamoid bones. In *Cha. vellerosus*, *Cha. villosus*, and *Chl. truncatus*, as well as other armadillos (*D. novemcinctus*: Olson et al., 2016; *T. matacus*: Butcher et al., unpublished data), only one sesamoid bone is present. Specifically, the portion of the common tendon from the humeral medial and ulnar heads contains to the medial sesamoid bone, while the portion from the humeral lateral and radial heads contain the lateral sesamoid bone. Distal to the sesamoid bone(s), the common tendon divides into four tendons of insertion, which continue throughout the palmar aspect of the manus to insert onto the distal phalanges at the base of the claw of digits II–V: the medial tendon to digit V, the lateral tendon to digit II, and two central tendons to digits III and IV (Fig. 6a). The two lateral-most tendons run deep to both tendons of m. flexor digitorum superficialis. In *Cha. vellerosus*, five tendons are present, where the tendon slip to digit I is miniscule, and they each insert on the intermediate phalanges. Four tendons are observed in *Cha. villosus*, although they similarly insert onto the intermediate phalanges.

M. Pronator Quadratus

The m. pronator quadratus is not observed in any specimens and species studied except *Cha. villosus*. It is the deepest muscle of the medial antebrachium, and it originates from

the whole of the midshaft of the medial ulna and inserts on approximately the middle third of the caudomedial radius. The muscle also attaches to the interosseous membrane. Windle and Parsons (1899) reported the m. pronator quadratus was absent in *Cha. villosus*, whereas Macalister (1875) observed it to be a small, fibrous band in *Chl. truncatus*.

M. Brachioradialis

The m. brachioradialis, also referred to as m. supinator longus, is absent in armadillos (Galton, 1869; Macalister, 1875; Miles, 1941; Murie 1872; Olson et al. 2016; Windle and Parsons 1899).

M. Extensor Carpi Radialis

The m. extensor carpi radialis arises primarily from the entire supracondylar ridge of the humerus, proximal to the origins of both the m. extensor digitorum communis and m. extensor digitorum lateralis (Fig. 4a, c; see below). Additionally, its fibers take origin from the craniolateral edge of the radius. In one individual (Zp 583), it has two bellies, longus and brevis, where the long belly arises from the proximolateral aspect of the supracondylar ridge and the short belly arises from the craniodistal aspect. The two bellies fuse immediately distal their respective humeral origins. There are also two bellies observed in *Cha. villosus*, which merge near the origin and separate toward the distal end of the muscle. The m. extensor carpi radialis passes along the craniomedial-to-cranial radius, superficial to m. abductor digiti I longus, and it gives rise to a single tendon of insertion that passes deep to the belly of m. abductor digiti I longus where that muscle crosses over the styloid process of the radius. Its tendon inserts on the dorsomedial base of metacarpal III (Fig. 6b). In *Cha. vellerosus* and *Cha. villosus*, the muscle belly has minimal attachment to the distal radius, and its common tendon which gives rise to two tendons that cross the carpal joint and insert on the base of metacarpal II and mid-shaft of metacarpal III. In *Chl. truncatus*, it has no discernable tendons to the digits and the belly appears to become continuous with the m. abductor digiti I longus. Hyrtl (1855) and Macalister (1875), however, observed this muscle to insert on digit II.

M. Extensor Carpi Ulnaris

The m. extensor carpi ulnaris primarily originates from the lateral edge of the ulna extending from the olecranon to its distal end, as well as partially from some tendinous

fibers attaching to both the distal lateral epicondyle and humeroulnar (collateral) ligament (Fig. 5a). In one individual (Zp 585), the muscle originates from only the lateral olecranon and ulnar shaft. In *Cha. vellerosus*, *Cha. villosus,* and *Chl. truncatus* it mainly arises from the craniodistal aspect of the lateral epicondyle via a common extensor tendon, in addition to fleshy fibers along the lateral olecranon and ulnar shaft. A deep tendon runs throughout the muscle belly and emerges as a broad tendon of insertion just proximal to the carpus, which then inserts onto the dorsolateral aspect of the base of metacarpal V (Fig, 6b).

M. Extensor Digitorum Communis

The m. extensor digitorum communis originates via a common extensor tendon from the lateral epicondyle immediately proximal to the origin of m. extensor digitorum lateralis (Fig. 4a, c). In one individual (Zp 582), it also arises in part from the proximal half of the lateral radial shaft, which extends to the distal third of the lateral radius in *Cha. vellerosus.* In *Cha. villosus*, the muscle arises from the supracondylar ridge, immediately distal to the origin of m. extensor carpi radialis, and from fibers on the proximal half of the cranial radius. A thick tendon emerges from the distal muscle belly and passes deep to the extensor retinaculum, along with the deep tendon of m. extensor digiti II, and splits into two tendons of insertion. These two tendons primarily insert onto the dorsal aspect of the proximal phalanges of digits III and IV. The tendon to digit III sends a tendinous slip that inserts on the cranial aspect of the proximal phalanx of digit II, while the tendon to digit IV sends a tendinous slip to the proximal phalanx of digit III (Fig. 6b). In addition, the digit IV tendon sends another slip to the base of the intermediate phalanx of digit III, although this condition is not observed in Zp 585. In *Cha. vellerosus*, the m. extensor digitorum communis inserts on digits II–IV, whereby a single tendon of insertion to intermediate phalanx of digit III sends tendon slips to the same phalanges of digits II and IV. In *Cha. villosus*, except a notable tendon inserts onto the proximal phalanges of digits III and IV while a second, smaller tendon attaches to the proximal phalanx of digit II. In *Chl. truncatus*, one tendon of inserts on the proximal phalanges of both digits II and III, and the second tendon inserts on only the proximal phalanx of digit IV.

M. Extensor Digitorum Lateralis

The m. extensor digitorum lateralis (previously m. abductor digiti V longus: Olson et al. 2016) also originates via a common extensor tendon from the lateral epicondyle of the humerus in close association with m. extensor digitorum communis (Fig. 4a, c). In one individual (Zp 582), its origin is separate and immediately distal to that of m. extensor digitorum communis, which is also condition observed in *Cha. vellerosus* and *Cha. villosus*. In *Chl. truncatus*, its origin is shared with m. extensor digitorum communis and proximal to the humeral origin of m. abductor digiti I longus (see below). Distally, the muscle belly gives rise to two tendons of insertion, which then passes deep to the extensor retinaculum of the carpal joint to enter the manus. One tendon carries fleshy muscle fibers and inserts onto the dorsolateral base of the proximal phalanx of digit IV, and also sends a tendon slip to the dorsolateral mid-shaft to the proximal phalanx of digit V. The second tendon is more prominent and attaches onto the dorsal base of metacarpal V (Fig. 6b). In *Cha. vellerosus*, the belly of the m. extensor digitorum lateralis sends a single tendon (along with fleshy fibers) that inserts on dorsolateral aspect of the proximal phalanx of digit V, as well as the fascia overlying the dorsal aspect of metacarpal V. In *Chl. truncatus*, two tendons also serve digits IV and V, but they insert on dorsal aspect of the distal end of the intermediate phalanges near the base of the claw.

M. Extensor Digiti II

The m. extensor digiti II (or m. extensor digiti I et II: Ercoli et al. 2015) is a small muscle that originates from the craniolateral aspect of the ulnar shaft, immediately medial to the distal line of origin for m. extensor carpi ulnaris (Fig. 5a). In *Cha. vellerosus*, the muscle belly is reduced, and it originates from only the distal fourth of the cranial aspect of olecranon, whereas it is absent in *Cha. villosus.* In contrast, the m. extensor digiti II has an extensive origin in *Chl. truncatus*, where it arises from the distal quarter of the craniolateral ulna, the proximal half of the lateral radial shaft deep to the m. abductor digiti I longus, and the interosseous membrane. Its tendon passes deep to the extensor retinaculum to enter the manus and inserts on the dorsal aspect of the mid-shaft of both metacarpal II and III in one individual (Zp 582) and the distal end of only metacarpal III in two individuals (Zp 583 and Zp 585) (Fig. 6b). Because of its insertion onto metacarpal III in *Z. pichiy*, this muscle can also be referred to as m. extensor digiti II et

III. In *Cha. vellerosus*, a thin tendon is sent from the muscle belly to insert to the midshaft of metacarpal II, and further to the distal end of metacarpal II in *Chl. truncatus*.

M. Abductor Digiti I Longus

The m. abductor digiti I longus origin extends from the lateral olecranon to the proximocranial ulnar shaft, the interosseous membrane, and the lateral radius (Fig. 5c), deep to m. extensor carpi radialis. In *Cha. vellerosus* and *Cha. villosus*, its origin is similar, but it is positioned slightly more laterally to also be deep to that of m. extensor carpi ulnaris. In *Chl. truncatus*, the muscle is not well-developed, and it originates from the distal tip of the lateral epicondyle and lateral ulnar shaft. The m. abductor digiti I longus crosses over the craniodistal end of the radius and/or radial ridge, superficial to passage of the insertion tendon of m. extensor carpi radialis, and inserts onto metacarpal I (Fig. 6b).

Intrinsic Manus

M. Flexores Breves

The m. flexores breves are not observed in any of the specimens and species studied. Murie (1872) and Windle and Parsons (1899) observed this muscle in *T. matacus* and *Cha. villosus*, respectively, but provided no myological descriptions.

Mm. Interossei

The mm. interossei are observed in all specimens and species studied, and are extremely reduced. Their attachments could not be described. Macalister (1875) observed the m. interossei in *Chl. truncatus*, but provided no myological descriptions. Windle and Parsons (1899) indicated the m. interossei insert on digits II and III, while the lateral- and medial-most interossei were described as fibrous bands.

Mm. Lumbricales

The mm. lumbricales are absent in armadillos (Galton, 1869; Macalister, 1875; Miles, 1941; Murie 1872; Olson et al. 2016; Windle and Parsons 1899).

Limb Muscle Mass Distribution

The forelimb of *Z. pichiy* contains 17 extrinsic and 32 intrinsic muscles (counting each head of the m triceps brachii and m. flexor digitorum profundus separately) that were studied. Means (±s.d.) of muscle mass are reported in Table 5. Mean total forelimb mass

(excluding the mass of m. platysma, m. panniculus carnosus and m. sternomastoideus) for *Z. pichiy* is 42.63±6.27 g, which accounts for 5.5±0.5% of total body mass. Muscles are organized into functional groups based on their main actions (Table 6) and their percentage distribution for *Z. pichiy* is shown in Fig. 7a. The limb retractors are the most massive group, accounting for 46.4±1.45% of total forelimb muscle mass. The m. latissimus dorsi, m. triceps brachii long head, and m. pectoralis superficialis are the major mass contributors to this group. The second most massive groups are the scapular elevators/rotators (mean: 25.1±0.54%) and the limb protractors (mean: 25.1±2.23%) that have equivalent percentages relative to total forelimb muscle mass (Fig. 7a). The m. rhomboideus profundus et capitus, m. rhomboideus cervicis, and m. omotransversarius are categorized in both functional groups, and the sum of the remaining muscles in both groups also have similar masses. The elbow extensors account for 19.5±1.26% of total forelimb muscle mass and contain four relatively massive heads of the m. triceps brachii, along with its small medial accessory head, the m. anconeus, and the thin m. tensor fasciae antebrachii (Tables 5, 6). The limb adductors also account for an appreciable amount of total forelimb muscle mass (mean: 16.9±1.55%) due to the inclusion of the large m. pectoralis superficialis and thick m. subscapularis, which contributes the most mass to this functional group. The digital flexors account for a moderate amount of total forelimb muscle mass with a mean of 5.20±0.61%, and are collectively the most massive functional group of the antebrachium, while the two synergistic carpal flexors, the m. flexor carpi radialis and m. flexor carpi ulnaris, only account for 1.35±0.22% (Fig. 7a).

The percentage distribution of muscle functional groups in *Z. pichiy* is shown relative to those of *Cha. vellerosus*, *Cha. villosus*, and *Chl. truncatus* in Fig. 7b. Overall, the relative mass of each muscle functional group is similar across the armadillos sampled. Most notably, *Z. pichiy* has the lowest limb retractor mass compared to the other three species, whereas *Cha. vellerosus* and *Chl. truncatus* have the greatest values, both approximating mass distributions of 51.0% of total forelimb muscle mass. Similarly, *Z. pichiy* and *Chl. truncatus* have comparatively the smallest and largest mass distributions, respectively, for percentage of total forelimb muscle mass accounted for by the digital flexors. However, *Chl. truncatus* has the lowest relative elbow extensor mass with a value of 18.5%, which is slightly less than that of *Z. pichiy*, while *Cha. villosus* has the

greatest mass distribution at 21.5% (Fig. 7b). The massive m. triceps brachii long head (two bellies) in the latter species (13.2 g; Table 5) is the major contributor to this muscle functional group. Last, similar to the digital flexors, the distributions of the carpal flexors show little variability in relative mass (~1.0%) across all four armadillo species; *Z. pichiy* has the largest muscle mass distribution, *Cha. vellerosus* and *Cha. villosus* are equal and intermediate, and *Chl. truncatus* has the smallest mass distribution at 0.88% (Fig. 7b).

Allometric Relationships

Figure 8 shows size scaling relationships for humeral dimensions and bone mass. Relative to bone mass, humerus length scales with slight positive allometry (Fig. 8a). The relationship slope is 0.35 and differs significantly ($p<0.001$) from the null hypothesis of isometry. The relationships between humerus length and mid-shaft width (slope: 0.73, $p=0.02$) and mid-shaft depth (slope: 0.65, $p<0.001$) scale with significant negative allometry (Figs. 8b, c) compared with the isometric prediction of a slope of 1.0.

Functional Osteological Indices

Means (±s.d.) of the raw ostelogical measurements are presented in Table 7 while means (±s.d.) of the functional indices are presented in Table 8. Numerous functional indices (e.g., EI, HRI, IFA) have been previously calculated and interpreted for the forelimb bones of armadillos (Hildebrand, 1985; Vizcaíno et al., 1999; Vizcaíno and Milne, 2002; Olson et al., 2016). The same functional indices were calculated for the specimens and species studied herein and are consistent with these prior reports. The following selected functional indices have either not been calculated or are infrequently reported for armadillos, while several others contribute significantly to DFA predictions (see below).

Scapular index (SI) scores range from 0.62–0.89 (Table 8), where *T. matacus* has the lowest value and *Chl. truncatus* and *P. maximus* have the greatest values of 0.86 and 0.89, respectively, indicative of a more prominent teres process. However, due to the prior damage to *Cha. vellerosus*, the acromion of this specimen was completely fractured, and scapula length for it is a conservative measurement (Table 7). Glenoid fossa shape index (GFSI) indicates relative width of the glenoid fossa, and is the highest in *Ca. unicinctus* (value 0.79) and lowest in the smallest (*Chl. truncatus*) and largest (*P. maximus*) armadillos sampled, whereas scapulohumeral index (SHI) ratios areÃ≥1.0 in all armadillo species regardless of body size, reflecting their shorter, more robust humeri.

Shoulder moment index (SMI) scores range from 0.47–0.67 (Table 8), where *Ca. centralis* has the highest value and *D. hybridus* has the lowest value. The species *Z. pichiy* and *Chl. truncatus* have similar values for SMI of 0.52 and 0.53, respectively, indicating similar mechanical advantage of m. deltoideus to flex the shoulder joint. Brachial index (BI), for which a low score is related to greater limb mechanical advantage, is lowest in *Chl. truncatus* and *P. maximus,* and highest in *T. matacus* (value: 0.78) due to its longer distal limb bone proportions (Table 7). Correspondingly, humerus-radial length index (HRLI) relating the opposite proportions is the highest in *Chl. truncatus* and *P. maximus,* and it is lowest in *T. matacus*. Finally, ulnar trochlea notch length index (UTLI) scores have a narrow range from 0.12–0.22 (Table 8), with *Ca. unicinctus* and *Cha. vellerosus* having the greatest values.

Olecranon length index (OLI) is highest in *Chl. truncatus* (value: 0.45) and the lowest in *T. matacus* (value: 0.26), with *Z. pichiy* (value: 0.27) having a comparably low ratio (Table 8). The pink fairy armadillo also has the largest values for three robustness metrics, including the humeral (HRI), radial (RRI), and ulnar (URI) robustness indices, as well as the ulnar shape index (USI), which all indicate bone bending resistance and large areas for muscle attachment. The species *Ca. centralis*, *Ca. unicinctus, D. novemcinctus*, and *P. maximus* similarly have high values for these indices, whereas *Z. pichiy* has intermediate scores (Table 8). Metacarpal III robustness index (MCRI) was substantially large in *P. maximus* (value: 1.05), while both *Chl. truncatus* and *P. maximus* have large manus proportions index (MPI) ratios >1.0, collectively emphasizing their short metacarpal III length (Table 7). Lastly, all armadillos, except *D. septemcinctus* and *Cha. vellerosus*, also have large relative manus claw length index (CLAW) ratios >1.0, indicating longer claws relative to stout manus elements. Again, fracture to the third claw of *Cha. vellerosus* resulted in a low score.

Digging Specialization

Figure 9 shows the results of DFA for predicted substrate use and digging habit memberships. Both predicted substrate use (Fig. 9a) and digging habits (Fig. 9b) groups show 100% assignment to the *a priori* memberships for all armadillo species sampled (see Table 4). For substrate use, six functional indices have significant Wilk's Lambda values that determine these categorizations and include the BI ($p=0.012$), as well as the

USI ($p<0.001$), RRI ($p<0.001$), SMI ($p<0.001$), OLI ($p<0.001$), and SHI ($p<0.001$) (Table 9). For digging habit specializations, there are also six functional indices for the forelimb bones with significant Wilk's Lambda values that determine these categorizations. Again, BI has the highest single value at 0.157 ($p=0.001$) followed by the HRLI ($p<0.001$), UTLI ($p<0.001$), CLAW ($p<0.001$), MCRI ($p<0.001$), and GFSI ($p<0.001$) (Table 10).

DISCUSSION

The results strongly support the hypothesis that postcranial morphological characteristics are predictive of scratch-digging ability. Among the specimens and species studied, several features were distinctive and numerous quantitative bone metrics were related to scratch-digging ability, thus providing remarkable independent verification of previous reports of lifestyles in armadillos based on qualitative accounts of their respective behaviors (Nowak, 1999; Vizcaíno and Milne, 2002). The arrangements of the forelimb musculature, functional osteological indices, and DFA predictions determined for *Z. pichiy*, *Cha. vellerosus*, and *Cha. villosus* all provide critical evidence for their level of scratch-digging ability related to a shared semi-fossorial lifestyle, whereas the pink fairy armadillo has several other forelimb modifications which reflect greater fossorial ability, and their specialization for a fossorial lifestyle. All four species have generally similar myological features of the forelimb, especially for *Z. pichiy*, *Cha. vellerosus*, and *Cha. villosus*. These observations combined with their forelimb skeletal proportions may be additionally reflective of their sympatric home ranges, similar habitat use, and current taxonomic classification (Family: Dasypodidae; Tribe: Euphractini), as well as potential close phylogenetic relationship (see below) compared with other living cingulates.

The major findings are also in accord with several specific expected outcomes. For example, *Chl. truncatus* has only three separate heads of m. flexor digitorum profundus, including a sole humeral head, and yet the lack of complexity by having fewer muscle heads of its digital flexors does not limit mass in this functional group. Indeed, the digital flexors of the pink fairy armadillo account for a slightly greater percentage of total forelimb muscle mass distribution compared with the members of the Euphractini Tribe, and this feature may indicate greater force production required for its fossorial

specialization as a burrower. Muscle complexity is also related to fiber pennation, and quantifications of muscle architectural properties in pennate digital flexors that provide calculations of physiological cross-sectional area (PCSA) are needed to test this hypothesis across species. Other functional groups demonstrate a surprising number of muscle bellies, which potentially weakens the argument that fossorial species have less complex muscles by fewer heads or bellies. The majority of specimens and species observed have six distinct heads of m. triceps brachii, including two separate bellies of TBLO and a medial accessory head. However, while this condition of m. triceps brachii may provide fine joint position control at the elbow joint (Ercoli et al., 2015), the forelimb motion of armadillos is largely restricted to flexion/extension in the sagittal plane during scratch-digging (Moore et al., 2013). Thus, having robust m. triceps brachii in general, likely may be an ancestral retention for concentrating muscle mass in the elbow extensors in all extant species. Mass distributions in the forelimb are also concentrated in the limb retractor, elbow extensor, and digital flexor functional groups, which is similarly observed in other scratch-diggers (Warburton et al., 2013; Rupert et al., 2015; Olson et al., 2016). This specific distribution of muscle mass along the forelimb is necessary for applying large force to the substrate during the power stroke of scratch-digging. Last, the limb protractors have relatively large muscle mass, especially in *Z. pichiy*, which is not typical of scratch-diggers, and was not expected. Enhanced limb protractor mass could be functionally related to the terrestrial walking/running habits of a given species, or possibly the presence/absence of selected muscles (see subsection: Comparative Myology Perspectives) may be more indicative ancestral or derived traits associated with restrictions on pectoral girdle motion.

The osteological features of *Z. pichiy*, as well as those from the forelimb skeletons of the majority of armadillo species sampled, demonstrate long in-lever and short out-lever lengths (e.g., high SMI and IFA, low BI: Vizcaíno et al., 1999; Vizcaíno and Milne, 2002) for large joint torque application, and robust limb bones (e.g., high HRI, URI/USI, RRI: Milne et al., 2011; Olson et al., 2016) for enhanced resistance to bending stresses and greater area for attachment of large muscles. In addition, most armadillos have a prominent medial epicondyle of the humerus (high EI) and strong joint articulations (e.g., high UTLI) that restrict motion to a single plane. Several of the collective functional

osteological indices are related of fossorial ability, and in particular, those metrics indicating overall limb mechanical advantage (e.g., BI) are strongest predictors in accordance with initial expectations. For example, the smallest (*Chl. truncatus*) and largest (*P. maximus*) armadillos, which are both categorized as fossorial diggers, have long in-levers and robust limb bones which correspond to stronger scratch-digging ability, whereas less prominence of these skeletal features in *T. matacus* are associated with generalized habits and much less frequent digging for foraging, thermoregulation, or protection for predators (Nowak, 1999; Smith, 2007). In the following subsections, selected myological and osteological features are evaluated in greater detail with respect to scratch-digging function and their potential phylogenetic significance.

Comparative Myology Perspectives

Comparisons of forelimb myology of *Z. pichiy* to that of other armadillos furthers understanding of proximate relationships within the family Dasypodidae, in addition to identifying traits that indicate specialization in scratch-digging mammals (Olson et al., 2016). Table 11 summarizes numerous traits obtained from data in the present study and all previous documentations of armadillo myology (e.g., Galton, 1869; Macalister, 1875; Windle and Parsons, 1899; Miles, 1941; Olson et al., 2016). Such information is essential for future phylogenetic recontructions of Family Dasypodidae, Order Cingulata, and The Xenarthra as a clade. Moreover, the proposed meta-analysis should include cranio-dental characteristics, molecular genomic evidence, as well as key features derived from studies of postcranial morphology, (Milne et al., 2011; Nyakatura, 2012; Olson et al., 2016). Several notable features are observed among seven species of cingulates for which descriptions are available, including (1) modification of the origin/insertion of m. trapezius pars cervicalis, (2) presence/absence of m. omotransversarius, m. brachiocepahlicus and m. brachioradialis, and (3) number of bellies of the mm. rhomboideus, m. triceps brachii, and m. flexor digitorum profundus.

The m. trapezius pars cervicalis does not have a consistent origin. It originates from the carapace in some species (e.g., *Z. pichiy* and *Cha. villosus*) and from the vertebrae and/or cranium in others (e.g., *Chl. truncatus* and *D. novemcinctus*). An origin from the rigid carapace might restrict this part of the m. trapezius to primarily act as a scapular elevator and stabilizer. When m. trapezius pars cervicalis contracts, it could also draw the

scapular shield of the carapace closer to the body, which may play a role in protection when armadillos are threatened by a potential predator. Specifically, both *Z. pichiy* and *Cha. villosus* have been observed to lay flat against the substrate with their limbs completely retracted under the carapace as a defense mechanism, and thus heavily rely on their carapace for protection from predators (Krieg, 1961; Nowak, 1991; Smith, 2008*a*; Superina and Abba, 2014). In contrast, *Chl. truncatus* has a thin and flexible carapace (Superina and Loughry, 2012), and its lack of rigidity may explain why m. trapezius pars cervicalis does not originate from the carapace in this species. A cranial origin of the m. trapezius pars cervicalis would additionally allow this muscle to act as a limb protractor, which might permit stronger or more rapid cycling of the limbs (Carrier et al., 2008).

Pink fairy armadillos burrow quickly as their main mode of predatory defense (Vizcaíno and Milne, 2002) despite having large mechanical advantage about the shoulder and elbow joints (i.e., large SI and IFA, respectively; see subsection: Functional Osteological Indices and Scratch-digging Function). However, *Chl. truncatus* frequently burrows in loose sandy soil (Borghi et al., 2011), which would facilitate fast scratch-digging by the substrate offering little resistance to large amount of out-force being applied by the forelimbs. Expression of fast myosin heavy chain (MHC) isoforms 2X and 2B in muscles with long, parallel fascicles enhances contractile velocity and may permit more rapid cycling of their limbs during burrowing behaviors. Beyond burrow construction, a potentially large distribution of fast MHC-2X and -2B fibers may be critical to thermoregulation in *Chl. truncatus* and is expected for mammals of their diminutive body size. Observations of pink-colored forelimb muscles with a majority having parallel fiber architecture (Marshall et al. unpublished data) help support these functional interpretations. Last, rapid predatory escape behaviors (e.g., vertical leaping and quick zig-zag walk-run locomotion) are also documented in *D. novemcinctus* (Talmage and Buchanan, 1954), which share a similar origin of the m. trapezius pars cervicalis with *Chl. truncatus* and have been shown to retain expression of the fast MHC-2B isoform (Olson et al., 2016). Intrinsically fast-contracting muscles generate high power that could act as mechanical trade-off with mechanical advantage in selected muscle groups, including limb protracators and elbow flexors.

All specimens and species observed have an m. omotransversarius, and this muscle is

also present in *E. sexcinctus* (Galton, 1869) (Table 11). In addition to its purported function in limb protraction (Ercoli et al., 2015), this muscle may also provide stability to the pectoral girdle due to its modified origin from the base of the cranium and its insertion on the acromion in common with the m. trapezius pars cervicialis. In *Cha. villosus* and *Cha. vellerosus*, the m. omotranversarius is continuous with both m. trapezius pars cervicalis and m. pectoralis superficialis via a muscle slip along the brachium that inserts onto the antebrachium; in *Z. pichiy* and *Chl. truncatus*, this complex only involves the latter two extrinsic muscles. This muscle complex formed has enhanced mechanical advantage of each muscle to extend the shoulder joint and flex the elbow joint. Although this complex is not well-developed in armadillos, the ability of these three extrinsic muscles to effect action at the both the shoulder and elbow joints is reminiscent of a similar muscular arrangement observed in Chinese pangolins (*Manis pentadactyla*) (Kawashima et al., 2015) and that among the mm. pectoralis, deltoideus, and biceps brachii in two-toed sloths (*Choloepus*) (Nyakatura and Fischer, 2011; Spainhower et al., unpublished data). In pangolins, the analogus muscle the muscle/fascia slip observed in the armadillos was described as the m. supinator longus with a purported function to facilitate protraction of the forelimb in coordination contralateral flexion of the neck during walking, whereas the mechanical linkage of muscles in sloths is viewed a modification for climbing.

Similar to the overlapping scales in pangolins, the carapace in armadillos may pose some restriction of forelimb movement, and the ability of extrinsic muscles to act further distally has evolved to overcome a parallel limitation. Stability of the shoulder joint is essential for scratch-digging, and the presence of m. omotransversarius, which serves as a linkage muscle, is most likely a derived feature common to members of the Tribe Euphractini because a similar arrangement is not observed in the fossorial *Chl. truncatus*. The pink fairy armadillo is the only species in the present for which the trapezius lacked an origin from carapace, and this condition may also affect modification of the shoulder girdle musculature in species that exhibit greater dependence on scratch-digging. Furthermore, the m. omontransversarius is absent in semi-fossorial *D. novemcintus* (Olson et al. 2016), and *T. matacus* (Butcher et al., unpublished data) and this condition could also be derived for a greater range of motion of the forelimb for terrestrial

locomotor behavior associated with more generalized habits (Vizcaíno and Milne, 2002). Indeed, the latter two species depend less on scratch-digging for foraging, predator evasion, and independent burrow construction (Nowak, 1999; Smith, 2007).

Three-banded armadillos are also the only species in which a separate m. rhomboideus profundus and m. rhomboideus capitus has been documented (Murie, 1872; Butcher et al., unpublished data). Having distinct bellies not only provides greater positional control of the scapula, but also provides a longer moment arm for the m. rhomboideus profundus by way of an insertion that is further caudal on the scapula. This arrangement provides an overall greater mechanical advantage of the mm. rhomboideus (collective: profundus, capital, and cervical bellies) about the shoulder joint for stronger protraction of the pectoral girdle (and limb), and is may be a modification associated with cursorial habits in *T. matacus*. Additional studies of postcranial myology in this and other species of armadillos (e.g., *D. hybridus*) are needed to support this hypothesis. In contrast, the profundus and capital bellies of mm. rhomboideus are fused in *Z. pichiy*, and are either fused or absent in other semi-fossorial-to-fossorial armadillos for which data is available (see Table 11). Less complexity by fusion of muscle bellies is most likely the common condition in armadillos and may be more strictly ancestral and related to scapular stabilization during the power stroke, and to a lesser extent, limb protraction during the recovery stroke of scratch-digging. The antagonistic limb retractors are considerably more massive compared to the other functional groups (Fig. 7a, b) and have a long flexor moment arm about the shoulder joint due to the enlargement of the teres process (high SI). Thus, the majority of the mm. rhomboideus muscle mass has an important functional role to counterbalance flexor torque application at the shoulder joint.

Despite these various modifications in limb protractors, the m. cleidocephalicus pars cervicalis is consistently absent in all observed armadillos (Table 11). Because of the lack of limb protraction during the power stroke, this trait may be ancestral due to the fossorial behaviors of the basal xenarthrans (Nyakatura and Fischer, 2011; Olson et al., 2016). The presence of other limb protractors which are more developed (e.g., mm. rhomboideus pars cervicis, subscapularis) may also contribute to the absence of m. cleidocephalicus pars cervicalis. In addition, the armadillo's inability to gallop due to the extra constraint and mass from the carapace results in less utilization of limb protraction. Similar to the

absence of m. cleidocephalicus pars cervicalis, the m. cleidobrachialis is observed as indistinct from m. deltoideus pars clavicularis in our specimens and species in this study as well as in *D. novemcinctus* (Olson et al., 2016) and *E. sexcinctus* (Galton, 1869). However, Butcher et al (unpublished data) describes the m. cleidobrachialis interchangeably for the m. deltoideus pars clavicularis, which is also the case for myological descriptions of the lesser grison (*Galictis cuja*, Ercoli et al., 2015). Other studies only report the m. cleidobrachialis being present with similar attachments as m. deltoideus pars clavicularis (Fisher et al., 2009). These inconsistent descriptions make it difficult to directly compare the presence or absence of these muscles with some of the historical descriptions in dasypodids. However, both muscles have been reported as separate and distinct in some species of scratch-digging sciurids (Thorington et al., 1997). Similarly, we consider m. cleidobrachialis and m. deltoideus pars clavicularis as separate muscles in all our studied specimens and species until further observations in other armadillos can determine the presence or absence of m. cleidobrachialis.

An essential modification for scratch-digging in the brachium of armadillos is a well-developed m. triceps brachii. The presence of three massive biarticular bellies of the m. triceps brachii heads substantially contribute to large mass limb retractor and elbow extensor mass. A medial accessory head of the m. triceps brachii was also observed in *T. matacus* (Murie, 1872) and *E. sexcincutus* (Galton, 1869), whereas the latter species and *D. novemcinctus* are the only armadillos for which distinct bellies of the long head are not documented. In particular, despite only having four separate heads of the m. triceps brachii, the elbow extensors in *D. novemcinctus* account for a greater percentage of total forelimb muscle mass (Olson et al., 2016) compared to armadillos in the present study. Moreover, have just four massive heads of the m. triceps brachii is similar to the condition observed in other strong scratch-digging taxa such as badgers (*Taxidea taxus*, Moore et al., 2013) and bandicoots (*Isoodon obesulus*, Warburton et al., 2013).

The relative findings for *Chl. truncatus* are surprising since they are considered to be fossorial rather than semi-fossorial as is *D. novemcinctus* (Borhi et al., 2011; Delsuc et al., 2012; Olson et al., 2016), and point to fossorial adaptation being more of a collective assemblage of traits versus the arrangement and mass of a single muscle group in the forelimb system. At this time, muscle mass has not been statistically evaluated as a

continuous variable in DFA analysis, and mass of the m. triceps brachii may be a selected step-wise variable that helps explain a a significant portion of the variance. Future DFA predictions of functional habit memberships in armadillos should include muscle mass as a factor. Nevertheless, *Chl. truncatus* has several skeletal features (i.e., limb mechanics) that are broadly indicative of large extensor torque application about the elbow joint, including a prominent olecranon process (high IFA and OLI) and short distal forelimb elements (low BI) (see subsection: Functional Osteological Indices and Scratch-digging Function). These traits are more evident in this species compared to the rest of the armadillos sampled, including *D. novemcinctus*, and are more reflective of the highly fossorial lifestyle of *Chl. truncatus* (Hildebrand, 1985; Borghi et al., 2011; Moore et al., 2013; Rupert et al. 2015). The relatively greater elbow extensor mass in *D. novemcinctus* could be a compensatory modification for a less prominent olecranon process, which is predictive of a more semi-fossorial lifestyle (Olson et al., 2016). However, the pichiy, screaming hairy, and large hairy armadillos all have lower IFA and OLI values compared to *D. novemcincus*, and relating shorter in-lever length with lower elbow extensor mass may indicate that these species exert weaker elbow extension during scratch-digging, despite sharing a semi-fossorial designation. Thus, multiple combinations of postcranial traits, along with functional trade-offs between out-force and range of limb motion, are related to lifestyle and frequency of scratch-digging in armadillos.

Another muscle which is consistently absent among all dasypodids observed is the m. brachioradialis (Table 11) which acts in elbow flexion and antebrachial supination (Ercoli et al., 2015). Elbow flexor muscles typically have a low muscle mass distribution among scratch-diggers (Moore et al., 2013; Warburton et al., 2013; Rupert et al., 2015; Olson et al., 2016) since these muscles are utilized as agonists during the recovery stroke of scratch-digging. Lower levels of activation during the power stroke may have been a selective pressure that ultimately lead to the absence of m. brachioradialis in armadillos. In addition, and perhaps more important, is that armadillos have a permanently pronated limb posture and a high degree of fusion between the radius and ulna (Olson et al., 2016), which results in an inability to supinate the antebrachium. The lack of rotation of the radius coupled with the robustness of the distal elements is considered to be reflective of their fossorial ancestry (Nyakatura, 2012). Armadillos mainly consume insects and

vegetative forage and have reduced dentition, thus they do not require their forelimb limbs to manipulate prey. These factors are more strongly suggestive that the absence of m. brachioradialis may be ancestral, and the additional absence (Macalister, 1875; Windle and Parsons, 1899; Olson et al., 2016) or reduction (Galton, 1869; Murie, 1872) of the m. supinator may have followed as a derived feature. A m. supinator is only observed in *T. matacus* and *E. sexcinctus*, although its function is not known.

Last, the digital flexors are the most well-developed group of muscles in the distal forelimb, which is associated with having a prominent medial epicondyle (high EI) for more relative area available for attachment (Vizcaíno and Milne, 2002; Rose et al., 2014; Olson et al., 2016). Namely, the m. flexor digitorum profundus accounts for the majority of the digital flexor mass distribution. Specifically, *Chl. truncatus* has the highest muscle mass for the m. flexor digitorum profundus compared to the rest of the specimens and species for this study (Fig. 7b) despite having fewer heads (Table 11). This is associated with greater out-force exertion and the ability to maintain strong flexion throughout the power stroke (Olson et al., 2016). Moreover, it is expected that mass of the digital flexors would contribute significantly to revised DFA predictions of digging specialization, such as the fossorial habit in *Chl. truncatus* as well as the naked-tailed armadillos. Future studies of forelimb myology and muscle mass distribution are aimed at members of the Genus Cabassous to confirm this possibility. However, mass alone is not sufficient to determine the force production capacity of the digital flexors. Quantifications of muscle architecture are needed evaluate muscle length (i.e., shortening velocity) and PCSA (i.e., isometric force) properties of armadillo muscles. These data will indicate which bellies are capable of muscle exertion for mechanical work and power versus force production for joint stability.

The number of digits served by m. flexor digitorum superficialis also varies among armadillo species (Table 11). The pichi has the greatest number of served digits compared to the other species sampled in the present study. Additional tendon slips, to multiple digits is associated with fine motor control of the digits (Ercoli et al., 2015; Olson et al., 2016), and this feature may result in more effective object and prey manipulation compared to other species. Therefore, these actions may contribute to the foraging strategies of the pichi for successfully subduing prey, as this species has been

reported to consume larger specimens (e.g., scorpions and lizards) in addition to insects (Superina et al., 2009; Superina and Abba, 2014). The number of digits present on the manus also could be a factor involved with the degree of digital control. Digit number on the forefeet typically ranges between four and five in armadillos for which published observations are available (e.g., Galton, 1869; Macalister, 1899; Olson et al., 2016). All specimens and species in the present study have five digits, and yet a variable number of digits served by m. flexor digitorum superficialis is observed. In contrast, *T. matacus* has either three or four digits on their manus (Murie, 1872; Butcher et al., unpublished data), which is another modification associated with their potential cursorial habits compared to the majority of extant armadillos (Nowak, 1999; Vizcaíno and Milne, 2002; Smith, 2007). A greater number of digits is useful for more effective removal of dirt and debris during scratch-digging, and this would be expected in species that exhibit more frequent scratch-digging behavior compared to *T. matacus* (Hildebrand, 1985; Elissamburu and De Santis, 2011; Rose et al., 2014). On the other hand, longer and fewer distal limb elements are typical cursorial adaptations to increase velocity of limb excursion and stride length (Hildebrand, 1985).

Functional Osteological Indices and Scratch-digging Function

Beyond myology, functional osteological indices of the forelimb are essential for indicating fossorial specialization in scratch-diggers based on multiple limb bone proportions (Hildebrand, 1985; Sargis, 2002; Salton and Sargis, 2008; Rose et al., 2014). Specifically, armadillos have numerous adaptations for scratch-digging behavior exhibited in their forelimbs (Vizcaíno et al., 1999; Vizcaíno and Milne, 2002; Olson et al., 2016), and several indices are strongly predictive of fossorial ability using DFA (Tables 9 and 10). The advantage of DFA is that it determines only the most essential factors from multiple independently measured continuous variables that explain the greatest amount of variance for predicting outcome memberships. One of these factors in the index GFSI, which is indicative of the range of motion about the glenohumeral (shoulder) joint (Salton and Sargis, 2008). A dorsoventrally narrow glenoid fossa (low GFSI) likely reflects restricted movement (i.e., small range of motion) or motion limited to flexion/extension at the shoulder joint, and it has been previously observed in other scratch-diggers (Reed, 1951; Sargis, 2002; Stein, 2002). However, direct comparisions of

index values across taxa (e.g, armadillo versus shrew) are often not practical and are rarely useful for indications of relative function in mammals (Rose et al., 2014). The power stroke of scratch-digging is typically limited to the sagittal plane (Hildebrand, 1985; Moore et al., 2013), which may explain the low GFSI values in the species of armadillo sampled herein. Specifically, *Chl. truncatus* and *P. maximus* have the lowest values in correspondence with their strong fossorial ability (Silverira et al., 2009; Borghi et al., 2011). It should also be noted that our sample size for *Chl. truncatus* is small (*N*=2) due to lack of availability of this species, although the osteological features of *C. truncatus* reported by Vizcaíno and Milne (2002) have high correspondace to the values reported in the present study.

Shoulder moment index (SMI) is another strong predictor of substrate use and fossorial ability. The high values of *Ca. centralis* and *P. maximus* indicate the ability of their m. deltoideus to exert high torque about the shoulder joint during limb retraction and shoulder flexion (Hildebrand, 1985; Vizcaíno and Milne, 2002; Rose et al., 2014). Surprisingly, *Z. pichiy*, *Chl. truncatus*, and *T. matacus* all have similar (and low) SMI scores, despite their different substrate use and functional habit categorizations (Tables 9 and 10). Since both *Z. pichiy* and *Chl. truncatus* scratch-dig in sandy soils (Abba and Vizcaíno, 2011; Borghi et al., 2011; Superina and Abba, 2014), less torque may be required to excavate the substrate compared that needed for compact soils, and this functional difference may have constrained their skeletal morphology for a less prominent deltopectoral crest with a more distally displaced deltoid tuberosity. A similar constraint is also likely to be related to the generalized behaviors of *T. matacus*.

Conversely, the high values of the robustness indices (e.g., HRI, URI/USI, and RRI) are associated with the enhanced size of the skeletal elements in digging taxa (Rose et al., 2014; Olson et al., 2016), and in particular, the mid-shaft cross-sectional area of the long bones in armadillos. Large robustness ratios correspond to the negative allometric relationships between humerus length and humerus width and depth (Figs. 7b, c). Robust limb skeletons provide resistance to bending and shearing stresses/strains which occur during scratch-digging (Samuels et al., 2013; Rose et al., 2014), and also considered to be ancestral features among cingulates, and The Xenarthra, stemming from their basal fossorial habits as a clade (see above). Furthermore, the strong negative allometry

discovered in armadillos also is likely to be associated with support for the carapace, which places greater axial loads on the limb bones (Milne et al., 2011; Superina and Loughry, 2012). The combination of elevated axial loading (i.e., carapace mass and body weight support) superimposed on both bending and shear stresses is expected to result in overall large cross-sectional area to resist loading from multiple orientations. Still, preferential patterns of bone loading change the shape of long bones, and those in armadillos display curvature matched with the typical loading orientations (Marshall et al., unpublished data). Despite not having to support a carapace, other scratch-digging taxa are also reported to have robust limb bones (Lagaria and Youlatos, 2006; Rose et al., 2014) relative to cursorial and selected arboreal mammals the have more gracile limb bones (Samuels and Van Valkenburgh, 2008; Samuels et al., 2013).

BI is highly predictive of both substrate use and functional habit assignments of armadillos, which is reflective of its importance in determining fossorial ability. The high values of BI in *T. mataus* indicate a longer distal out-lever length for greater limb excursion and rotational velocity compared to the other armadillos sampled, and again this limb mechanical design is most often observed in mammals that exhibit cursorial habits (Salton and Sargis, 2002; Samuels et al., 2013). Alternatively, each other species have shorter distal skeletal elements, and their greater limb mechanical advantage results in greater out-force exerted at the substrate (Rose et al., 2013; Olson et al., 2016). Furthermore, the range BI values calculated are directly related to the fossorial ability of the cingulates (e.g., low BI for *Chl. truncatus* versus intermediate BI for *Z. pichiy*). The fossorial armadillos also have a prominent olecranon process length (high OLI) compared to *T. matacus* (Tables 7, 8). It is interesting to note that this index is strongly predictive of fossorial ability whereas IFA, which indicates in-lever length relative to distal out-lever length (Vizcaíno et al., 1999; Vizcaíno and Milne, 2002; Rose et al., 2014), does not contribute significantly to the predicted memberships (Tables 9, 10). Although OLI does not directly determine in-lever length of the m. triceps brachii, it compares olecranon length relative to the greatest ulna length and indicates the amount of relative area available for attachment of the elbow extensors (Sargis, 2002). Thus, more massive elbow extensors are expected to correspond with OLI, though PSCA and muscle fiber

pennation will further validate the amount of total force produced by the m. triceps brachii.

Several species of armadillo have high ulnar trochanter length index (UTLI) values (e.g., *Z. pichiy*, *Cha. vellerosus*, *Cha. villosus*, and *Ca. unicinctus*). The lower UTLI scores observed for *Chl. truncatus* and *P. maximus* indicate a less robust articulation between the humerus and ulna at the elbow joint by comparison (Szalay and Sargis, 2001; Sargis, 2002), which is not expected for species with fossorial habit specialization. However, UTLI and GFSI may correlate with regard to the narrowness of the shoulder and elbow joint articulations previously associated with scratch-digging ability. The relationship between these features need further evaluation to understand their functional significance. Lastly, the large CLAW scores determined for nearly all armadillos indicates the maintenance of long, sharp claws, which are advantageous for initially piercing the substrate and loosening soil during excavations of burrows and/or foraging behavior (Hildebrand, 1985; Olson et al., 2016). It is interesting to note that both the southern and northern naked-tailed armadillos have several high index values (e.g., IFA, SMI) similar to the species categorized as fossorial (*Chl. truncatus*, *P. maximus*), yet they are predicted to be semi-fossorial (Fig. 9b). Because several studies have indicated that these species are fossorial (Pine, 1973; Vizcaíno et al., 2003; Hayssen et al., 2013; Hayssen, 2014), myological descriptions of these species will further verify their scratch-digging specializations for foraging and burrow construction.

Conclusions

Post cranial morphology is critical for determining the level of fossorial specialization among armadillos, and can provide important anatomical characteristics for assessing their evolutionary history. In addition to having robust limb bones and long in-lever lengths, armadillos have well-developed limb retractors, elbow extensors, and digital flexors, which are all essential for high torque during the power stroke. Many of these features are more prominent in species with stronger fossorial ability (e.g., *Chl. truncatus*), whereas more semi-fossorial species have more intermediate traits (e.g., *Z. pichiy*). Furthermore, architectural properties are essential for determining force and power exersion from muscles, and can further verify scratch-digging ability in armadillos in future studies. Lastly, the similar myological traits observed for the pichi, screaming

hairy, big hairy, and six-banded armadillos provide further support of their previous categorization into the Tribe Euphractini. However, updated morphological descriptions for the six-banded armadillo and comparisons to other armadillos will be needed to evaluate these phylogenetic relationships. Further studies and comparisons of the forelimb myology will provide further indication of scratch-digging specialization, and help determine if certain armadillo species belong in separate families or sub-families along with additional molecular and cranial data in a meta-analysis.

REFERENCES

Abba, A. M., Vizcaíno, S. F., and Cassini, M. H. (2007). Effects of land use on the distribution of three species of armadillos in the Argentinian Pampas. *J. Mammal.* **88**, 502-507.

Abba, A. M. and Vizcaíno, S. F. (2011). Distribución de los aramdillos (Xenarthra: Dasypodidae) en la provincial de Buenos Aires, Argentina. *Mastozool. Neotrop.* **18**, 185-206.

Abba, A. M., Tognelli, M. F., Seitz, V. P., Bender, B., and Vizcaíno, S. F. (2012) Distribution of extant xenarthrans (Mammalia: Xenarthra) in Argentina using species distribution models. *Mammalia* **76**, 123-136.

Alexander, R. M., Brandwood, A., Currey, J. D. and Jayes, A. S. (1984). Symmetry and precision of control of strength in the limb bones of birds *J. Zool.* **203**, 135-143.

Ancona, K. A. and Loughry, W. J. (2009). Time budgets of wild nine-banded armadillos. *Southeast. Nat.* **8**, 587-598.

Biewener, A. A. (1989). Scaling body support in mammals: limb posture and muscle mechanics. *Science* **4913**, 45-48.

Biewener, A. A. (2005). Biomechanical consequences of scaling. *J. Exp. Biol.* **208**, 1665-1676.

Borghi, C. E., Giannoni, S. M., and Roig, V. G. (2002). Eye reduction in subterranean mammals and eye protective behavior in *Ctenomys*. *J. Neotrop. Mammal.* **9**, 123-134.

Borghi, C. E., Campos, C. M., Giannoni, S. M., Campos, V. E., and Sillero-Zubiri, C. (2011). Updated distribution of the pink fairy armadillo *Chlamyphorus truncatus* (Xenartha, Dasypodidae), the world's smallest armadillo. *Edentata* **12**, 14-19.

Carlini, A. A., Soibelzon, E., and Glaz, D. (2016). *Chaetophractus vellerosus* (Cingulata: Dasypodidae). *Mamm. Species* **48**, 73-82.

Carrier, D. R. Deban, S. M., and Fischbein, T. (2008). Locomotor function of the forelimb protractor and retractor muscles of dogs: evidence of strut-like behavior at the shoulder. *J. Evol. Biol.* **211**, 150-162.

Copploe, J.V., Blob, R. W., Parrish, J. H. A., and Butcher, M. T. (2015) In vivo strains in the femur of the nine-banded armadillo (*Dasypus novemcinctus*). *J. Morph.* **276**, 889-899.

Delsuc, F., Scally, M., Madsen, O., Stanhope, M. J., Jong, W.W., Catzeflis, F.M., Springer, M.S., and Douzery, E. J. P. (2002). Molecular phylogeny of living xenarthrans and the impact of character and taxon sampling on the placental tree rooting. *SMBE* **19**, 1656-1671.

Delsuc, F., Stanhope, M. J., and Douzery E. J. P. (2003). Molecular systematics of armadillos (Xenarthra, Dasypodidae): contribution of maximum likelihood and Bayesian analyses of mitochondrial and nuclear genes. *Mol. Phylogenet. Evol.* **28**, 261-275.

Delsuc, F., Vizcaíno, S. F., and Douzery, E. J. P. (2004). Influence of Tertiary paleoenvironmental changes of the diversification of South American mammals; a relaxed molecular clock study within xenarthrans. *BMC Evol. Biol.* **4**, 11.

Delsuc, F., Superina, M., Tilak, M., Douzery, E. J. P., and Hassanin, A. (2012). Molecular phylogenetics unveils the ancient evolutionary origins of the enigmatic fairy armadillos. *Mol. Phylogenet. Evol.* **62**, 673-680.

Delsuc, F. and Douzery, E. J. P. (2008) Recent advances and future prospects in Xenarthran molecular phylogenetics. In: *The Biology of the Xenarthra* (ed., S. F. Vizcaíno and W. J. Loughry), pp. 11-23. Gainsville: University of Florida Press.

Elissamburu, A. and De Santis, L. (2011). Forelimb proportions and fossorial adaptations in the scratch-digging rodent *Ctenomys* (Caviomorpha). *J. Mammal.* **92**, 683-689.

Eng, C. M., Smallwood, L. H., Rainiero, M. P., Lahey, M., Ward, S. R., and Lieber, R. L. (2008). Scaling of muscle architecture and fiber types in the rat hindlimb. *J. Exp. Biol.* **211**, 2336-2345.

Ercoli, M. D., Álvarez, A., Stefanini, M I., Busker, F., and Morales, M. M. (2015). Muscular anatomy of the forelimbs of the lesser grison (*Galictis cuja*), and a functional and phylogenetic overview of Mustelidae and other Caniformia. *J. Mammal. Evol.* **22**, 557-91.

Fariña, R. A. and Blanco, R. E. (1996). *Megatherium*, the stabber. *Proc. R. Soc. B* **263**, 1725-1729.

Fisher, R. E., Adrian, B. Barton, M., Holmgren, J., and Tang, S. Y. (2009). The phylogent of the red panda (*Ailurus fulgens*): evidence from the forelimb. *J. Anat.* **215**, 611-635.

Galton, J. C. (1869) The muscles of fore and hind limbs in *Dasypus sexcinctus*. *Trans. Linn. Soc.* **26**, 523–565.

Garland, T and Janis, C. M. (1993). Does metatarsal/femur ratio predict maximal running speed in cursorial mammals? *Zool. Soc. Lond.* **229**, 133-151.

Gaudin, T. J. and Croft, D. A. (2015). Paleogene Xenarthra and the evolution of South American mammals. *J. Mammal.* **96**, 622-634.

Greegor, G. H. (1980). Diets of the little hairy armadillos, *Chaetophractus vellerosus*, of Northwestern Argentina. *J. Mammal.* **61**, 331-334.

Hamlett, G. W. D. (1939). Identity of *Dasypus septemcinctus* Linnaeus with notes on some related species. *J. Mammal.* **20**, 328-336.

Hayssen, V., Ortega, J., Morales-Leyva, A., and Martínez-Mendez, N. (2013). *Cabassous centralis* (Cingulata: Dasypodidae). *J. Mammal.* **45**, 12-17.

Hayssen V. (2014). *Cabassous unicinctus* (Cingulata: Dasypodidae). *J. Mammal.* **46**, 16-23.

Hildebrand, M. (1985) Digging of quadrupeds. In: *Functional Vertebrate Morphology* (ed. M. Hildebrand, D. M. Bramble, K. F. Liem, and D. B. Wake), pp 89–109. Cambridge: Harvard University Press.

Hildebrand, M. and Goslow, G. E., (2001). Digging and crawling without appendages. In: *Analysis of Vertebrate Structure* (ed. M. Hildebrand and G. Goslow), pp. 455-474. New York: John Wiley & Sons, Inc.

Hill, A. V. (1938). The heat of the shortening and the dynamic constants of muscle. *Proc. R. Soc. B.* **126**, 136-195.

Hyrtl, J. (1855). Chlamydophori truncate cum Dasypode gymnuio comparatum Examen Anatomicum. *Denkschr. d. k.-k. Akad. d. Wissensch.* **9**, 1-66.

Kardong, K. V. (2013) The Muscular System. In: *Vertebrates: Comparative Anatomy, Function, Evolution* (ed. K. V., Kardong), pp. 372-412. New York: McGraw-Hill Education.

Kawashima, T., Thorington, R. W., Bohaska, P. W., and Chen, Y. (2015). Anatomy of the shoulder girdle muscle modifications and walking adaptation in the scaly Chinese pangolin (*Manis pentadactyla pentadactyla*: Pholidota) compare with the partially osteoderm-clad armadillos (Dasypodidae). *Anat. Rec.* **298**, 1217-1236.

Kley, N. J. and Kearney, M. (2007). Adaptations for digging and burrowing. In: *Fins into Limbs: Evolution, Development, and Transformation* (ed. B. K. Hall), pp. 284-310. Chicago: The University of Chicago Press.

Krieg, H. 1961. Das verhalten der Gürteltiere (*Dasypodidae*). In: *Handbuch der Zoologie* (ed. J.G. Helmcke, H. v. Lengerken, and D. Starck), pp. 24-31. Berlin: Walter de Gruyter & Co.

Lagaria, A. and Youlatos, D. (2006). Anatomical correlates to scratch digging in the forelimb of European ground squirrels (*Spermophilus citellus*). *J. Mammal.* **87**, 563-570.

Lieber, R. L. (2012). Skeletal muscle anatomy. In: *Skeletal muscle structure, function, and plasticity: the physiological basis of rehabilitation* (ed. R. L. Lieber), pp. 1-41. Phliadelphia Lippincott Williams and Wilkins.

Macalister, A. (1875). A monograph of the anatomy of *Chlamyphorus truncates* (Harlan), with notes on the structure of other species of Edentata. *Trans. R. Irish Acad.* **25**, 219-278.

McKenna, M. C. (1975). Toward a phylogenetic classification of the Mammalia. In: *Phylogeny of the Primates* (ed. W. P. Luckett and F. S. Szalay), pp. 21-46. New York: Plenum Press.

McNab, B. K. (1980). Energetics and the limits to a temperate distribution in armadillos. *J. Mammal.* **61**, 606–627.

Miles, S. S. (1941). The shoulder anatomy of the armadillo. *J. Mammal.* **22**, 157-169.

Milne, N., Toledo, N., and Vizcaíno S. F. (2011). Allometric and group differences in the Xenarthran femur. *J. Mammal. Evol.* **19**, 199-208.

Moore, L. A., Budny, J. E., Russel, A. P., and Butcher, M. T. (2013). Architectural specialization of the intrinsic thoracic limb musculature of the American badger. *J. Morph.* **274**, 35-48.

Murie, J (1872). On the habits, structure, and relations of the three-banded armadillo (*Tolypeutes conurus, Is. Geof.*). Trans. Linn. Soc. **30**, 1-132.

Nowak, R. M. (1991). *Walker's Mammals of the World*. 5th Edition. Baltimore: Johns Hopkins University Press.

Nowak, R. M. (1999). *Walker's Mammals of the World*. 6th Edition. Baltimore: Johns Hopkins University Press.

Nyakatura, J. A. and Fischer, M. S. (2011). Functional morphology of the muscular sling at the pectoral girdle in tree sloths: convergent morphological solutions to new functional demands" *J. Anat.* **219**, 360-374.

Nyakatura, J. A. (2012). The convergent evolution of suspensory posture and locomotion in tree sloths. *J. Mammal. Evol.* **19**, 225-234.

Olson, R. A., Womble, M. D., Thomas, D. R., Glenn Z. D., and Butcher, M. T. (2016). Functional morphology of the forelimb of the nine-banded armadillo (*Dasypus novemcinctus*): comparative perspectives on the myology of Dasypodidae. *J. Mammal.* **23**, 49-69.

Olson, R. A., Glenn, Z. D., Cliffe, R. N., and Butcher, M. T. (2017). Architectural properties of sloth forelimb muscles (Pilosa: Bradypodidae) *J. Mammal. Evol.* doi: 10.1007/s10914-017-9411-z.

Pine, R. H. (1973). Mammals (exclusive of bats) of Belém, Pará, Brazil. *Acta Amazon.* **3**, 47-79.

Polijak, S., Ferruri, A. M., Chiappero, M. B., Sánchez, J., Gabrielli M., and Lizarralde, M. S. (2018). Phylogeography of screaming hairy armadillo *Chaetophractus vellerosus*: successive disjunctions and extinctions due to cyclical climatic changes in southern South America. *PLoS One* **13**, e0190944.

Price, M. V. (1993) A functional-morphometric analysis of forelimbs in bipedal and quadrupedal heteromyid rodents. *Biol. J. Linnean. Soc.* **50**, 339-360.

Rose, J., Moore, A., Russell, A., and Butcher M. (2014). Functional osteology of the forelimb digging apparatus of badgers. *J. Mammal.* **95**, 543-558.

Rupert, J. E., Rose, J. A., Organ, J. M., and Butcher, M. T. (2015). Forelimb muscle architecture and myosin isoform composition in the groundhog (*Marmota monax*). *J. Exp. Biol.* **218**, 194-205.

Sargis, E. J. (2002). Functional morphology of the hindlimbs of tupaiids (Mammalisa, Scandentia) and its phylogentic implications. *J. Morph.* **254**, 149-185.

Samuels, J. X., and Van Valkenburgh, B. (2008). Skeletal indicators of locomotor adaptations in living and extinct rodents. *J. Morph.* **269**, 1387-1411.

Samuels, J. X., Meachen, J. A., and Sakai, S. A. (2013). Postcranial morphology and the locomotor habits of living and extinct Carnivorans. *J. Morph.* **274**, 121-146.

Schaller, G. B. (1983). Mammals and their biomass on a Brazillian ranch. *Arg. Zool.* **31**, 1-36.

Silverira, L., Almeida Jácomo, A. T., Furtadp, M. M., Torres, N. M., Sollmann, R., and Vynne, C. (2009). Ecology of the giant armadillo (*Priodontes maximus*) in the grasslands of central Brazil. *Edentata* **8-10**, 25-34.

Smith, P. (2007). Southern three-banded armadillo *Tolypeutes matacus*. In: *FAUNA Paraguay Handbook of the Mammals of Paraguay, Volume 2* (ed. P. Smith), pp. 84-91.

Smith, P. (2008*a)*. Greater Hairy Armadillo *Chaetopractus villosus*. *FAUNA Paraguay Handbook of the Mammals of Paraguay, Volume 2* (ed. P. Smith.), pp. 17-22.

Smith, P. (2008*b*). Lesser Hairy Armadillo *Chaetopractus vellerosus*. *FAUNA Paraguay Handbook of the Mammals of Paraguay, Volume 2* (ed. P. Smith), pp. 11-16.

Stein, B. R. and Casinos, A. (1997). What is a cursorial mammal? *Zool. Soc. Lond.* **242**, 185-192.

Stein, B. (2002). Morphology of subterranean rodents. In: *Life Underground: The Biology of Subterranean Rodents* (ed. E. A. Lacey, J. L. Patton, and G. N. Cameron) Chicago: University of Chicago Press.

Superina, M. (2008). The natural history of the pichi, *Zaedyus pichiy*, in western Argentina. In: *Biology of the Xenarthra* (ed. S. F., Vizcaíno and W. J. Loughry), pp. 313-318. Gainsville: University of Florida Press.

Superina, M., Campón, F., Stevani, E. L., and Carrara, R. (2009). Summer diet of the pichi *Zaedyus pichiy* (Xenarthra: Dasypodidae) in Mendoza Province, Argentina. *J. Arid. Environ.* **73**, 683-686.

Superina, M. and Loughry, W. J. (2012). Life on the half-shell; consequences of a carapace in the evolution of armadillos (Xenarthra: Cingulata). *J. Mammal.* **19**, 217-224.

Superina, M., and Abba, A. M. (2014). *Zaedyus pichiy* (Cingulata: Dasypodidae). *Mamm. Species* **46**, 1-10.

Superina, M. and Loughry, W. J. (2015). Why do Xenarthrans matter? *J. Mammal.* **96**, 617-621.

Szalay, F. S. and Sargis, E. J. (2001). Model-based analysis of postcranial osteology of marsupials from the Palaeocene of Itaboraí (Brazil), and the phylogenetics and biogeography of Metatheria. *Geodiversitas* **23**, 139-302.

Taber, F. W. (1945). Contribution on the life history and ecology of the nine-banded armadillo. *J. Mammal.* **26**, 212-226.

Talmage, R. V. and Buchanan, G. D. (1954). The armadillo (*Dasypus novemcinctus*): a review of its natural history, ecology, anatomy and reproductive physiology. *The Rice Institute Pamphlet, Monograph in Biology* **41**, 1-135.

Thorington, R. W., Darrow, K., and Betts A. D. K. (1997). Comparative myology of the forelimb of squirrels. *J. Morph.* **234**, 155-182.

Toledo, N., Bargo, M. S., Cassini, G. H., and Vizcaíno, S. F. (2012). The forelimb of early Miocene sloths (Mammalia, Xenarthra, Folivora): morphometrics and functional implications for substrate preferences. *J. Mammal. Evol.* **19**, 185-198.

Vassallo, A. I. (1998). Functional morphology, comparative behaviour, and adaptation in two sympatric subterranean rodent genus *Ctenomys* (Caviomorpha: Octodontidae). *Zool. Soc. Lond.* **244**, 415-427.

Vaughn, T. A., Ryan J. M., and Czaplewski, N. J. (2015). *Mammalogy.* Burlington: Jones & Barlett Learning.

Vizcaíno S. F., Fariña, R. A., and Mazzetta, G. V. (1999). Ulnar dimensions and fossoriality in armadillos. *Acta Theriol.* **44**, 309-320.

Vizcaíno, S. F. and Mine, N. (2002). Structure and function in armadillo limbs (Mammalia: Xenarthra: Dasypodidae). *J. Zool. Lond.* **257**, 117-127.

Vizcaíno, S. F., Milne, N., and Bargo M. S. (2003). Limb reconstruction of *Eutatus seguini* (Mammalia: Xenarthra: Dasypodidae). Paleobiological implications. *Rev. Asoc. Paleontol. Argent.* **40**, 89-101.

Warburton, N. M., Grégoire, L., Jacques, S., and Flandrin, C. (2013). Adaptations for digging in the forelimb muscle anatomy of the southern brown bandicoot (*Isoodon obesulus*) and bilby (*Macrotis lagotis*). *Aust. J. Zool.* **61**, 402-419.

Windle, B. C. A. and Parsons, F. G. (1899). On the myology of the Edentata. *Proc. Zool. Soc. Lond.* **1899**, 314–339.

APPENDIX

Origin and Evolution

Placental (eutherian) mammals are arranged into four major clades: Afrotheria (e.g., aardvarks and elephants), Xenarthra (e.g., armadillos and anteaters), Euarchontoglires (e.g., rodents and primates), and Laurasiatheria (e.g., carnivores and ungulates) (Delsuc et al., 2002). Among these groups, the superorder Xenarthra may represent the most basal clade from which eutherians evolved, a hypothesis that is primarily supported by paleontological evidence (i.e., fossil crania), biogeographical data, and molecular genomic analyses (Delsuc et al., 2002). The Xenarthra emerged ~100 million years ago in present day South America (Vizcaíno et al., 2012) and were among the most diverse and abundant genera distributed throughout this land mass (Superina and Loughry, 2015). Currently, The Xenarthra consists of only 31 extant species categorized into two monophyletic orders: Cingulata and Pilosa. The Cingulata contains 21 species of armadillos (Family: Dasypodidae) while the Pilsoa contains 4 species of anteaters (subfamily: Vermilingua) and 6 species of tree sloths (subfamily: Folivora) (Delsuc et al., 2002; Superina and Loughry, 2015). Overall, their genetic composition and morphological characteristics are fundamentally important for determining the phylogeny and origins of placental mammals (Delsuc et al., 2003, 2004). To this end, data provided by the outcomes of the studies proposed herein will contribute anatomical characters to help re-evaluate the taxonomic classification of cingulates.

Xenarthrans have numerous distinctive structural and physiological traits. For example, each species has a lower basal metabolism and body temperature than those typical of eutherian mammals (McKenna, 1975; Gaudin and Croft, 2015), and these features are viewed as plesiomorphic (i.e., ancestral) traits among placental mammals (Delsuc and Douzery, 2008). Xenarthrans exhibit various functional habits such as burrowing to help compensate for their poor ability to internally thermoregulate (Superina and Loughry, 2012). Also, xenarthrans generally have robust skeletons that show the following morphological characteristics: 1. xenarthrous (i.e., extra) zygapophyseal joints in their lumbar vertebrae for reinforced trunk stability (Nowak, 1999); 2. a secondary scapular spine (Rose and Archibald, 2005) for enhanced shoulder muscle attachment; 3. a large third trochanter (T3) the of femur for increased weight

support at the hip joint; and 4. reduced (e.g., sloths and armadillos) or completely absent (e.g., anteaters) dentition (Vizcaíno, 2009) due to their restricted diets.

Despite sharing a number of exclusive morphological traits, extant xenarthrans additionally possess anatomical structures that differ among sloths, anteaters, and armadillos, and these are reflective of lifestyle and/or niche occupied (Nyakatura, 2012). The Xenarthra is particularly interesting because of the variety of **substrate preferences** and **substrate uses** observed in such a small clade of mammals. The extreme ranges of substrate preference and use, respectively, include: arboreal locomotion and suspension for sloths; arboreal/semi-arboreal locomotion and hook-and-pull digging for anteaters; and ground-dwelling locomotion and scratch-digging for armadillos (Nowak, 1999). Specifically, adaptation for substrate use (described in detail below) posed morphological constraints in their limbs, which resulted in notably different musculoskeletal features over time (Nyakatura and Fischer, 2011). As evidence of this type of selection, anteaters and armadillos have both robust limb bones and muscles capable of high out-forces (i.e., mechanical advantage) during digging, whereas sloths have adapted a derived form of long, more gracile limb bones and low muscle mass beneficial for suspensory function (Nyakatura, 2012). In addition, several muscle attachments differ throughout their fore and hind limbs (Macalister, 1875). One notable example are the origins of their extrinsic forelimb musculature that are often different among xenarthran species. Muscle attachments (e.g., mm. trapezius and rhomboideus) range from various levels of thoracic and cervical vertebrae as well as from heavy-to-no attachment to the occiput of the cranium depending on the functional habit exhibited (Miller, 1935; Nyakatura and Fischer, 2011). These variations in musculoskeletal form not only should indicate which locomotor habits are utilized, but also inform the overall functional specialization of the limbs.

Irrespective of the described differences in selected anatomical features, modifications for digging behavior, or **fossorial habit**, is evidenced by the remains of the last common ancestor of all extant xenarthrans, and thus is considered to be the ancestral form representative of the superorder (Nyakatura and Fischer, 2011; Olson et al., 2016). Within The Xenarthra, fossorial habits are ancestrally associated with scratch-digging behavior. In particular, armadillos still exhibit scratch-digging, where it plays a major

role in the niches they occupy. Important to this review/proposal is the following description of **scratch-digging**: a mode of digging when armadillos alternately flex and extend their forelimbs repeatedly in a sagittal plane to excavate earth (Hildebrand, 1985). There are two limb phases to scratch-digging: power stroke and recovery stroke. The power stroke begins when the foreclaws pierce and loosen the soil, followed by sequential extension of the elbow joint and ventral retraction of the forelimb to move debris either behind or caudolateral to the animal (Vassallo, 1998; Hildebrand and Goslow, 2001). The recovery stroke begins at the end of the power stroke and involves recycling the forelimb by protraction to return it to a position in front of the animal to begin the next digging cycle. The **ecomorphology** of armadillos was likely constrained for scratch-digging due to the fossorial ancestry among The Xenarthra (Olson et al., 2016). Therefore, analysis of their limb form will help remedy the gaps in our knowledge about functional morphology and evolutionary relationships among xenarthans, and basal placental mammals at large.

Ecology and Speciation

Armadillos are the most widely distributed of all xenarthrans. They are found throughout South and Central America, Mexico, and the southern and eastern regions of the United States (Nowak, 1999; Vaughn et al., 2015). Ranges of their dispersal greatly vary among genera and species. For example, long-nosed armadillos (Genus: *Dasypus*) show an extensive distribution from the USA through Central America to southern Argentina. In contrast, pichi armadillos (Genus: *Zaedyus*) and hairy armadillos (Genus: *Chaetophractus*) are only found in a few South American countries, including Chile and Argentina (Smith, 2008*b*; Superina and Abba, 2014). Numerous species of armadillo prefer to inhabit the Neotropical regions of the Americas, but they can occupy a variety of habitats (Vaughn et al., 2015) that can range from scrubby grasslands and xeric areas (Borghi et al., 2011) to rainforests.

Armadillos display low levels of activity and have some of the lowest basal metabolic rates among placental mammals (McNab, 1980). Therefore, conservation of metabolic energy and body heat is essential to their survival during bouts of activity, which is why they are typically active during warmer periods of day or active at night depending on the species (Taber, 1945; Schaller, 1983). During the few hours/day that they are active,

armadillos mainly forage (Ancona and Loughry, 2009) and dig burrows for shelter (Superina and Loughry, 2011; Superina and Abba, 2014). Some species of armadillo prefer to scavenge or share burrows rather than exert the energy to dig their own as a means to further conserve energy. However, armadillos do not often associate with other individuals when active. Solitary habits are commonly observed among armadillos with the exception of periods of mating and caring for offspring (Superina and Loughry, 2011; Superina and Loughry, 2015).

To search for food armadillos will slowly walk with their snout in the soil and/or leaf litter (Superina and Loughry, 2011). Once their food source is located, they will clear the area by scratching their long, sharp foreclaws, or excavate to find the food source by scratch-digging (Hildebrand and Goslow, 2001). Whereas most species of armadillo utilize scratch-digging, many species also exhibit myrmecophagy (i.e., feeding on ants and termites) (Superina and Loughry, 2011). Typical food sources include various invertebrates (e.g., scorpions and beetles) small vertebrates (e.g., birds and lizards), and vegetation (e.g., tubers and fruit) (Superina and Abba, 2014; Carlini et al., 2016). Their diets may change seasonally depending on availability of familiar food sources.

Predation is not a major threat to armadillos because they are active outside of their burrows only a few hours at a time. The presence of a bony carapace is also a critical deterrent for predators (Superina and Loughry, 2011). However, armadillos face depredation from an assortment of carnivores, including jaguars, pumas, foxes, various eagles (e.g., the crowned eagle: *Harpyhaliaetus coronatus*), and domestic dogs (Smith 2008*a*; Superina and Abba, 2014). Armadillos exhibit several behaviors when threatened by approaching predators, and these include leaping upward (Talmage and Buchanan, 1954), quickly digging or retreating to burrows, 'running' in zig-zag patterns (Superina and Abba, 2014), and retracting their limbs into the pectoral and pelvic shields of their carapace (Nowak, 1999). At least two species of three-band armadillo (Genus: *Tolypeutes*) are capable of fully retracting their limbs and flexing their entire body into a spherical confirmation, and thus rely heavily on their armor for protection from predators (Nowak, 1999).

As a result of armadillos being the most speciose among The Xenarthra (Superina and Loughry, 2015), they have a broad range of lifestyles, body sizes, and digging

specializations. It is of particular interest to compare traits present among armadillos in light of the limited available data on their functional morphology. Three representative species have been selected to continue quantitative sampling for the range of diversity in the cingulates: the pichi armadillo (*Zaedyus pichiy*), the screaming hairy armadillo (*Chaetophractus vellerosus*), and the pink fairy armadillo (*Chlamyphorus truncatus*). These selected species will be central to the focus of this review/proposal.

Zaedyus. pichiy mainly inhabits arid and semi-arid microenvironments of Chile and Argentina (Superina, 2008) that have firm, but sandy soils. It frequently employs scratch-digging to construct burrows for shelter and thermoregulation. *Z. pichiy* is diurnal, and is also the only known extant xenarthran to go undergo daily torpor, as well as prolonged periods of hibernation when ambient temperatures become too low (Superina and Boily, 2007; Superina and Abba, 2015). Furthermore, it is omnivorous and consumes a variety of invertebrate and plant material. *C. vellerosus* is known for emitting loud scream-like vocalizations, which is the origin of its common name. Its diet changes seasonally, with more vegetation consumed in winter months versus more insects during the summer (Greegor, 1980; Carlini et al., 2016). Similar to *Z. pichiy*, *C. vellerosus* inhabits more xeric environments, and tends to construct burrows in native woodlands and areas with calcareous soil (Abba et al., 2007). Last, *C. truncatus* has a partially subterranean lifestyle and relies more heavily on scratch-digging for constructing burrows and foraging compared with the other two species (Borghi et al., 2002). *C. truncatus* also is the smallest species of the armadillo with a body mass of ~120 g and body length of 90–115 mm (Borghi et al., 2011). Its habitat consists of dry grasslands and sandy plains within central Argentina. Although each of these species exhibit scratch-digging behavior, their distinctive lifestyles reflect the varying degrees of fossorial ability present among armadillos. More specifically, understanding the relationship between resource acquisition and selection for morphological traits that improve fitness (i.e., ecomorphology) is essential for this taxon. The study proposed herein will explore how morphological traits of three wild species of armadillo relate to differences in scratch-digging specialization.

Functional Morphology

Digging behavior is both phylogenetically and functionally important to diverse taxa spanning generalized digging, semi-fossorial, fossorial, and subterranean lineages (Moore et al., 2013; Rose et al., 2014). Digging plays an essential role in the lifestyles of fossorial specialists, where it provides microhabitats to numerous activities such as socialization, caring for offspring, protection from predators, and catching of food. Again, armadillos commonly utilize scratch-digging when foraging for food, escaping predators, and burrow construction for thermoregulation (Superina and Loughry, 2011; Olson et al., 2016). The following sub-sections highlight available functional morphology in family Dasypodidae by reviewing digging behavioral classification, musculoskeletal modifications, lever mechanics, limb myology, muscle architectural properties, and bone functional indices.

Behavioral Categories

All armadillos are ground-dwelling mammals and they are limited to this substrate preference. There are three categories for which to characterize the functional behavior of armadillos that reflect their substrate use: generalized, semi-fossorial, and fossorial (Vizcaíno et al., 2012). First, armadillos that exhibit generalized habits (e.g., Genus: *Tolypeutes*; three-banded armadillos) typically engage in terrestrial locomotion (walking and 'running') as their main functional behavior rather than scratch-digging (Nowak, 1999). Second, armadillos categorized as semi-fossorial (e.g., Genera: *Dasypus*, *Zaedyus,* and *Chaetophractus*) do not dig frequently, and have fewer limb modifications for fossorial ability compared to armadillos that rely more on their high degree of fossorial ability (Smith, 2008*b*). While scratch-digging may be used less frequently when foraging, digging is often exhibited during burrow construction. Third, armadillos categorized as fossorial (e.g., *C. truncatus* and the giant armadillo, *Priodontes maximus*) employ scratch-digging as their primary strategy for constructing burrows and foraging. Moreover, these two species of armadillo display more extreme modifications for fossorial ability in their forelimb morphology (Hildebrand, 1985). In addition, *C. truncatus* and *P. maximus* also represent the extremes of armadillo body size with pink fairy armadillos as the smallest species and giant armadillos as the largest species (~60 kg).

Musculoskeletal Features

The forelimbs of armadillos display numerous skeletal modifications for scratch-digging behavior, including robust bones with large areas for muscle attachment, short, more compact forefeet, and large, sharp foreclaws. These gross musculoskeletal features strongly contribute to their ability to utilize scratch-digging (Vizcaíno and Milne, 2002; Vizcaíno et al., 2012). Specific modifications to the forelimb skeleton include an enlarged teres process of the scapula, a prominent deltoid tuberosity and/or deltopectoral crest of humerus, a wide medial epicondyle of humerus, and foreshortened and fused radius and ulna (Vizcaíno, 1999). Perhaps the most notable feature of the forelimb skeleton of diggers is a prominent olecranon process of ulna (e.g., 30–90% of ulna length) for increasing the mechanical advantage (see sub-sections below: *Lever Systems* and *Bone Functional Indices*) of the elbow extensor muscles (Miles, 1941; Vizcaíno and Milne, 2002; Olson et al., 2016). Moreover, well-developed muscles of the forelimb provide increased strength in retraction of the limb, extension of the elbow joint, flexion and of the carpus and digits, and stabilization of the shoulder joint (Hildebrand, 1985). Compared to the forelimbs, the hindlimbs are often associated more with weight bearing (depends on body size), stability, and posture during scratch-digging (Milne et al., 2011). Armadillos with a larger body mass typically have a large medial femoral condyle and a more distal third trochanter (T3) to compensate for greater bending (tensile) stresses on the lateral cortex of the femoral shaft (Copploe et al., 2015). In addition, large armadillos have a more proximal (larger) greater trochanter for a more upright posture of the hindlimb (Talmage and Buchanan, 1954), and a deeper knee joint and wider patellar surfaces for increased leverage in knee extension (Sargis, 2002). All armadillos generally have a robust and fused tibia-fibula (tibiofibula) for greater stabilization and body weight support during scratch-digging (Vizcaíno and Milne, 2002) or other load-bearing behaviors. Many of these skeletal features observed in armadillos are suggested to be the ancestral retentions for fossorial habits (Milne et al., 2011; Nykatura and Fischer, 2011; Olson et al., 2016).

Lever Systems

A lever system has three components: (1) a fulcrum, or pivot point, (2) the effort, or force applied, and (3) the load, or resistance to the effort (Alfaro et al., 2004; Vogel, 2013). The

different categories of lever systems depend on the arrangement of the fulcrum, site of applied effort, and site of load. In a **first class lever** system, the effort and load are positioned on either side of the fulcrum (Vogel, 2013). If the fulcrum is arranged closer to the point of load application, then this will result in a longer in-lever length (length between effort and fulcrum) relative to out-lever length (length between load and fulcrum), as well as a greater mechanical advantage (Vogel, 2013). However, the out-lever length will increase if the fulcrum is positioned closer to the site of applied effort, resulting in a greater velocity advantage. In a **third class lever** system, the position of the applied effort falls between the fulcrum and the point of the load. A shorter distance between the fulcrum and the site of applied effort (i.e., in-lever) results in a greater velocity advantage due to the shorter in-lever length relative to out-lever length (Vogel, 2013). However, due to the arrangement of this lever system, out-lever length is unaltered regardless of the distance between the applied effort and the fulcrum. In a **second class lever** system, the applied effort and fulcrum are at both ends of the lever system with the load site in between them (Vogel, 2013). A shorter distance between the fulcrum and the load (i.e., out-lever) results in a shorter out-lever relative to in-lever and overall, great mechanical advantage. In contrast to a third class lever system, the *in-lever* length is unaltered regardless of the distance between the load and fulcrum in this lever arrangement. Unlike first/third class lever systems, second class levers are not naturally found in animal musculoskeletal systems (Vogel, 2013).

In a musculoskeletal lever system, the joint is the fulcrum, the applied effort is the muscle force produced, and the load is the body mass of the animal or that of another object, which depends on the type of activity (e.g., manipulation of objects, postural, or locomotor). However, the distance of these components relative to the fulcrum determines the length of the muscle moment arm (i.e., the in-lever; L_i) and that of the load (i.e., the out-lever; L_o). L_i is defined as the perpendicular distance between the muscle line of action (the axis of muscle force production) and the joint center of rotation, whereas the L_o is the distance between the joint and where the load is applied (Vogel, 2013). Importantly, the product of L_i and muscle force produced results in the magnitude of **joint torque** (rotational force, or moment) applied at a given joint. The joint torque applied in a lever system obeys a simple rule: the product of muscle in-force

(F_i) and in-lever (L_i) must equal the product of load out-force (F_o) and out-lever (L_o) (Vogel, 2013). This principle is known as the torque balancing equation ($F_iL_i=F_oL_o$). Conceptually, the arrangement of the out-lever and in-lever lengths and their ratio (L_o/L_i) determines the function of a lever system and the amount of mechanical advantage.

Lever lengths can be manipulated to result in either mechanical or velocity advantage of the lever system. A lever system with high **mechanical advantage** must have long in-lever length and/or short out-lever length (e.g., small L_o/L_i) (Rose et al., 2014). Moreover, this lever system results in a functional tradeoff of lower joint rotational velocity for higher **out-force** (Vogel, 2013). In general, scratch-diggers have several musculoskeletal features associated with increased limb mechanical advantage and out-force applied to the substrate. Armadillos have both long in-lever lengths (e.g., olecranon process) and short out-lever lengths (e.g., foreshortened ulna and metacarpals) in their forelimbs, which leads to greater joint torque application during scratch-digging (Vizcaíno and Milne, 2002; Olson et al., 2016). An example of this are the elbow extensors acting about the elbow joint as a first class lever system. In contrast, a lever system with a **velocity advantage** must have longer out-lever lengths relative to in-lever lengths (e.g., large L_o/L_i), resulting in a tradeoff between higher joint velocity and lower out- force (Vogel, 2013). Most often these are third class lever systems. For example, cursorial mammals (e.g., ungulates) typically have a much longer radius-ulna and metacarpals relative to L_i lengths of the muscles that flex/extend these limb segments, which is associated with greater joint rotational velocity during running behaviors.

Limb Myology

While the structure of a lever system indicates either a mechanical advantage or velocity advantage at a limb joint, limb myology is foremost for describing variation in areas of muscles attachment, relative muscle size, and the presence or absence of muscles. These trends are often compared among species that share ancestry to decipher phylogenetic (ancestral) relationships from adaptive (derived) morphology associated with the observed functional habits in extant species. This type of comparative analysis is particularly critical for species with few descriptions of myology and/or quantitative data on limb musculoskeletal form. Postcranial data are only available for a limited number of species of armadillo (e.g., Galton 1869; Macalister, 1875; Windle and Parsons, 1899;

Miles, 1941); however, the nomenclature used in these reports is antiquated and in need of updating. A recent study (Olson et al., 2016) in nine-banded armadillos (*Dasypus novemcinctus*) began the process of comparing historic anatomical reports to more current literature in order to facilitate future functional morphological studies among cingulates. In this section, general trends in forelimb myology will be described using any data available from selected species, including *D. novemcintus* (Macalister, 1875; Miles, 1941; Olson et al., 2016), *Euphractus sexcinctus* (Galton, 1869), *C. truncatus* (Macalister, 1875; Windle and Parsons, 1899), and *Chaetophractus villosus* (Windle and Parsons, 1899).

a. Extrinsic Musculature

The mm. trapezius, rhomboideus, subclavius, and serratus ventralis are all involved in either scapular stabilization, rotation, or elevation. Additionally, mm. trapezius and rhomboideus act in scapular (and limb) protraction and retraction (Olson et al., 2016). M. trapezius is composed of pars cervicalis and pars thoracica as reported for *D. novemcintus*, *E. sexcinctus*, *C. truncatus*, and *C. villosus* (Galton, 1869; Macalister, 1875). The cervical part generally arises from the cervical vertebrae in addition to the occiput in *C. truncatus*, which is distinctive among this species (Macalister, 1875). The origin for m. trapezius pars thoracica is extensive for *E. sexcinctus* and *C. villosus*, where it spans C4-T12 (Galton, 1869; Windle and Parsons, 1899). However, its origin in *D. novemcintus* includes all thoracic vertebrae but does not attach to the cervical vertebrae (Olson et al., 2016). M. rhomboideus profundus was found to be present in *T. matacus* (Butcher et al., unpublished observations), but no presence was described for *D. novemcintus*, *E. sexcinctus*, *C. truncatus*, or *C. villosus*. The capital and cervical heads of m. rhomboideus are distinctive from one another in *E. sexcinctus* and *C. truncatus*, resulting in two separate muscles (m. rhomboideus capitis and m. rhomboideus cervicalis) (Galton, 1869; Macalister, 1875). In *D. novemcintus*, these heads are less distinguishable, and the observed fused muscle is referred to as m. rhomoboideus cervices et capitis (Olson et al., 2016). The number of bellies for m. serratus ventralis can vary depending on the species. For example, it was reported that *C. villosus* had two muscle bellies (Windle and Parsons, 1899) whereas Macalister (1875) reported 7-8 muscle bellies in *C. truncatus*.

The mm. latissimus dorsi and pectoralis superficialis primarily act in humeral retraction, where the latter muscle also acts as a humeral adductor (Olson et al., 2016). *C. truncatus* was reported to have two portions of m. latissimus dorsi: one arising from the lumbar vertebrae and inserting on the inferior scapular spine, and a second portion arising from the five caudal-most ribs (Macalister, 1875). The other species for which myology is available were reported to have only one main portion of m. latissimus dorsi, where its insertion was similar to the second portion observed in *C. truncatus* on the craniomedial aspect of the proximal humerus. M. pectoralis superficialis consists of a clavicular belly, sternal belly, and abdominal belly in *C. truncatus*, which are easily separable (Macalister, 1875). Macalister (1875) also reported that this muscle is trifid in *D. novemcintus*, whereas Olson et al. (2016) observed only the sternal belly to be present. Similarly, Galton (1869) reported that m. pectoralis superficialis is only composed of the sternal head in *E. sexcinctus*. M. pectoralis profundus, which has similar actions as m. pectoralis superficialis, is absent in *D. novemcintus* (Olson et al., 2016) and *E. sexcinctus* (Galton, 1869). It was reported to be present in *C. truncatus* and was referred to as m. pectoralis quartus (Macalister, 1875). However, Macalister (1869) mainly discussed his observations in human anatomical terms as opposed to comparative anatomical terms, which could be associated with less reliable descriptions for m. pectoralis profundus.

b. Intrinsic Musculature

The mm. deltoideus, infraspinatus, and teres major all act in scapular flexion and humeral retraction. M. teres minor, which has similar actions, was reported to be absent in *D. novemcintus* (Olson et al., 2016), but Miles (1941) reported it as being highly fused with m. infraspinatus. Macalister (1875) reported m. teres minor as large and distinctive in *C. truncatus*, whereas Galton (1869) reported it as being less broad in *E. sexcinctus*. M. deltoideus is generally trifid, where it is composed of pars scapularis, pars acromialis, and pars clavicularis. The latter two parts are reported to be fused in *E. sexcinctus*, *D. novemcintus*, and *C. truncatus*. The insertion for m. teres major is similar in *E. sexcinctus*, *D. novemcintus*, and *C. truncatus*, where it is associated with the insertion of m. latissimus dorsi (Galton, 1869; Macalister, 1875; Olson et al., 2016). The origin of m. teres major (i.e., the lateral teres process of scapula) and the attachments of m.

infraspinatus (origin: infraspinatus fossa of scapula; insertion: near or on greater tubercle of humerus) are reported as being generally similar among these four armadillo species.

The shoulder extensors (limb protractors) include mm. supraspinatus and subscapularis, which are also involved in humeral stabilization and adduction, respectively (Olson et al., 2016). M. supraspinatus originates from the supraspinuous fossa of the scapula and inserts on the greater tubercle, whereas the m. subscapularis originates on the subscapular fossa and inserts on the lesser tubercle of the humerus. Overall, the origins and insertions of these muscles are similar based on available descriptions. Windle and Parsons (1899) and Macalister (1875) additionally reported that m. supraspinatus is larger than m. infraspinatus. M. subscapularis is divided into three portions by internal tendinous inscriptions in *C. truncatus* and *D. novemcintus*. However, this separation was not reported by Galton (1869) for *E. sexcinctus*.

The brachial muscles of the forelimb consist of elbow flexors (mm. biceps brachii and brachialis) and extensors (mm. triceps brachii and anconeus). Both heads of m. biceps brachii (long and short head) are present in *C. villosus* (Windle and Parsons, 1899) and *D. novemcintus* (Olson et al., 2016). However, Macalister (1875) reported that no distinct short head was present in *D. novemcintus*. The presence of the long and short head may vary among species, as the short head was reported to be absent in both *E. sexcinctus* and *C. truncatus*. M. brachialis typically inserts with (e.g., *C. truncatus*) or near (e.g., *D. novemcintus* and *E. sexcinctus*) the m. biceps insertion onto the ulna (Galton, 1869; Olson et al., 2016). Mm. triceps brachii is reported to have four distinctive heads in all four species for which data is available, which includes the angular, long, lateral, and medial heads; the latter head is often fused with any reported accessory heads. There are two heads with scapular origins present in *C. villosus*, *D. novemcintus*, and *E. sexcinctus*, but the number of heads present with this condition may be variable in *C. truncatus* (Macalister, 1875; Olson et al., 2016). m. anconeus was reported in all four species for which data is available (Macalister, 1875; Windle and Parsons, 1899; Olson et al., 2016); however, some confusion arises as it may be described as the m. epitrochleo-anconeus in some reports (e.g., Galton, 1869).

The m. coracobrachialis, which is also identified as m. coracobrachialis longus, is present in *D. novemcintus*, *C. villosus*, and *E. sexcinctus* (Galton, 1869; Olson et al.,

2016), and reported as variably present in *C. truncatus* depending on the specimen (Macalister, 1875). This muscle acts in limb protraction and adduction. The presence of m. coracobrachialis brevis, which is also referred to as m. articularis humeri, may be variably present in *D. novemcintus*, although Olson et al. (2016) reported it as absent. Macalister (1875) also reports this muscle as variably present in *C. truncatus*, but it was found to be present in both *E. sexcinctus* (Galton, 1869) and *C. villosus* (Windle and Parsons, 1899). M. cleidobrachialis has been used interchangeably with m. deltoideus pars clavicularis in recent publications (e.g., Ercoli et al., 2015), making it difficult to compare it to other (historical) myology descriptions where two muscles with similar orientations may be present. Since the presence of this muscle remains uncertain in armadillos, it is considered to be absent until further observation (Olson et al., 2016).

Extensors of the carpus and digits include mm. extensor carpi ulnaris, extensor carpi radialis, extensor digiti II, and extensor digitorum communis. M. extensor carpi ulnaris has little variation of attachments among armadillos for which data is available. Olson et al. (2016) reported that *D. novemcintus* distinctively has a small slip associated with this muscle, which originates from the humeral lateral epicondyle and runs distally with m. extensor carpi ulnaris along the ulnar ridge and styloid process of the ulna. The size of m. extensor carpi ulnaris is not reported for any of the four armadillo species described, although Macalister (1875) reported this muscle as "weak" in *C. truncatus*. Insertions of m. extensor carpi radialis are variable among armadillo species. For example, this muscle inserts on metacarpals II and III in *D. novemcintus* (Olson et al., 2016), but it is also reported to insert on metacarpals I and II in *C. truncatus* (Macalister, 1875). The insertion for m. extensor digiti II, which was referred to as m. extensor indicis by Galton (1869) and Macalister (1875), may be modified for *D. novemcintus* (Olson et al., 2016). It inserts only onto the distal phalanx of digit II in nine-banded armadillos, whereas it inserts onto both digits I and II in *E. sexcinctus* (Galton, 1869) and *C. truncatus* (Macalister, 1875). These same two species also have similar insertions for m. extensor digitorum communis, whereby its tendons attach to digits II–IV. However, the tendons for m. extensor digitorum communis insert onto digits III and IV only (no digit V) in *D. novemcintus* (Olson et al., 2016).

The flexors of the carpus include mm. flexor carpi radialis and flexor carpi ulnaris. M. flexor carpi radialis is another example of a muscle with variable insertions described among armadillos. It inserts on the trapezium in *E. sexcinctus* (Galton; 1869) and *C. villosus* (Windle and Parsons, 1899), but *C. truncatus* (Macalister, 1875) and *D. novemcintus* (Olson et al., 2016) have insertions onto metacarpal I and/or II. M. flexor carpi ulnaris is reported to have two separate heads in *C. truncatus* and *D. novemcintus*, but this was not reported in *E. sexcinctus* by Galton (1869). The digital flexor muscles of the antebrachium include m. flexor digitorum superficialis (also reported as m. flexor sublimis digitorum) and mm. flexor digitorum profundus. M. flexor digitorum superficialis primarily acts in flexion of digits I–III for *D. novemcintus* (Olson et al., 2016), digits II and III for *E. sexcinctus* (Galton, 1869), and only digit III for *C. villosus* (Windle and Parsons, 1899). The number of digits served by this muscle were not described for *C. truncatus*. Mm. flexor digitorum profundus is generally composed of humeral (multiple bellies), ulnar, and radial heads (Olson et al., 2016). The tendons of this muscle insert on the distal phalanges of digits II–IV in *D. novemcintus*, whereas the tendons of mm. flexor digitorum profundus serve all digits in *E. sexcinctus* (Galton, 1869). The mm. flexor digitorum profundus is the strong flexor of the digits in addition to being a notable flexor of the carpus.

Abductors of the digits include mm. abductor digiti I longus and abductor digiti V longus, which is also known as m. extensor digiti lateralis. M. abductor digiti V longus acts on only digit IV in *D. novemcintus* (since there is no digit V observed on this species) (Olson et al., 2016), and digits IV and V in *E. sexcinctus* (Galton, 1869), *C. truncatus* (Macalister, 1875), and *C. villosus* (Windle and Parsons, 1899). M. abductor digiti I longus acts on digit I in all for species of armadillo for which myology data is available. This muscle can serve to digit II in addition to digit I in certain species (e.g., *C. villosus*).

Lastly, the presence of several muscles of the antebrachium remain difficult to resolve in armadillos. M. brachioradialis is reported to be absent in armadillos (Galton, 1869; Macalister, 1875; Olson et al., 2016), but it may be present in *T. matacus* (Butcher et al. unpublished data). M. pronator quadratus is also generally reported as absent, but Macalister (1875) observed it as notably reduced in size in *D. novemcintus* and *C.*

truncatus. M. palmaris longus was reported as absent in *D. novemcintus* (Olson et al., 2016), while a described superficial portion of m. flexor digitorum superficialis may represent a rudimentary m. palmaris longus, which was observed in *E. sexcinctus* (Galton, 1869) and *C. villosus* (Windle and Parsons, 1899). If this form is also present in *D. novemcintus*, then the fiber divisions of m. flexor digitorum superficialis may be the remnant of m. palmaris longus. The presence of m. supinator is variable in *E. sexcinctus* (reduced when reported present) and *C. villosus*, but absent in *C. truncatus* (Macalister, 1875) and *D. novemcintus* (Olson et al., 2016). A reduced m. supinator is also present in *T. matacus* (Butcher et al. unpublished data). Last, the intrinsic muscles of the manus have been difficult to describe. This has often been due to either the fixed condition of the specimens, degree of fusion of the skeletal elements, or number of digits on the forefeet. As previously indicated, *D. novemcintus* has four digits on its forefeet (digits I–IV), while the reported number of digits present for *C. villosus* ranged from 3–5 (Windle and Parsons, 1899). Five digits were reported to be present in *E. sexcinctus* (Galton, 1869) and *C. truncatus* (Macalister, 1875).

Muscle Architectural Properties

The force and velocity of contraction produced by limb muscles are largely influenced by their architectural properties (Eng et al., 2008; Lieber, 2012). Muscle architecture is defined as the orientation of muscle fibers relative to the axis of muscle force production (Kardong, 2013). Multiple fiber arrangements are typically observed within a limb which results in a range of functional capabilities. In general, fiber architecture ranges from parallel-to-pennate-fibered muscles (Kardong, 2013). **Parallel-fibered muscles** have long myofibers arranged in parallel with the line of action, and often have a measurable pennation angle of <15° (Moore et al., 2013). Due to these properties, parallel-fibered muscles have enhanced shortening capability (i.e., greater length excursion and velocity) and can exert force over a large range of joint motion (Rupert et al., 2015). Limb muscles with this form are most often paired with short muscle moment arms (in-levers), and these muscle-tendon units (MTU) have the capacity to rotate joints with a velocity advantage through a large range of motion (ROM) (Olson et al., 2017). Parallel-fibered muscles are also associated with greater muscle work and power output (Rupert et al., 2015).

In contrast, **pennate-fibered muscles** have short myofibers that are oriented at a larger angle to the line of action, and have pennation angles in the range of 15–55° (Moore et al., 2013). An important principle to understand is that muscle fibers become progressively shorter in length as pennation angle increases (Vogel, 2013), and therefore pennate-fibered muscles are best designed for force production at the expense of work/power performance (Kardong, 2013). Pennate-fibered muscles are categorized into the following four fiber architectures depending on the organization of the myofibers relative to the tendon of insertion or intramuscular tendinous inscriptions: unipennate, bipennate, multipennate, and circumpennate. Unipennate muscles have myofibers orientated on only one side of the tendon of insertion, where the fascicles (bundles of myofibers) are appreciable in length and have modest pennation angles. Bipennate muscles have myofibers orientated on both sides of the tendon of a single, central tendinous inscription, where the fascicles are moderate in length and have moderate-to-high pennation angles. Moreover, bipennate muscles take on the characteristic appearance of a feather from which their name is derived (Kardong, 2013). Multipennate muscles have myofibers orientated on either side of multiple tendinous inscriptions, where the fascicles are short in length and have high pennation angles. Muscles with multipennate architecture are highly specialized for force production due to having large **physiological cross-sectional area** (PCSA), which represents the cross-sectional area of all muscle fibers orthogonal to their longitudinal axes (Kardong, 2013). Circumpennate muscles have myofibers radially orientated to a central tendon of insertion, where the fascicles are short and take on the orientation of spokes in a bicycle wheel. Muscles with circumpennate architecture are uncommon (e.g., m. supraspinatus) in mammal limbs (Kardong, 2013). Overall, pennate-fibered muscles have a lower shortening velocity, but greater isometric force compared to parallel-fibered muscles (Vogel, 2013). Limb muscles with pennate architectures are most often paired with long muscle moment arms (in-levers), and these MTU's have the capacity to rotate joints slower with greater mechanical advantage (Olson et al., 2017).

Evaluation of muscle architectural properties provides insight into fossorial specialization by indicating how muscle structure affects force, joint torque, and power output (Moore et al., 2013; Rupert et al., 2015). Quantification of muscle architectural

properties involves measurement of the following geometric dimensions: moment arm length (r_m), MTU length, muscle belly mass (MM), muscle belly length (ML), fascicle length (L_F), pennation angle (θ). These metrics are used to calculate PCSA and estimates of **maximum isometric force** (F_{max}), joint torque (T), and power (W). In addition to these estimates, architectural indices (AI) are often calculated as series of ratios, and include L_F/ML to indicate muscle shortening capacity, PCSA/MM to indicate size-scaled force capability, and L_F/r_m to indicate the ability of a muscle to rotate a joint through a large ROM. AI further indicate the functional capacity of limb muscles (Moore et al., 2013; Rupert et al., 2015). A brief explanation of selected architectural properties will follow along with their functional implications as related to armadillo digging behavior.

A functional distribution of forelimb **muscle mass** indicates the relative investment of muscle group mass and the degree of utilization of group action (e.g., limb retraction/shoulder flexion) throughout the power stroke (Moore et al., 2013). The limb retractors, elbow extensors, and carpal/digital flexors (e.g., m. flexor digitorum profundus) are typically the most massive functional groups among scratch-diggers (Lagaria and Youlatos, 2006; Rupert et al., 2015; Olson et al., 2016). In addition, some scratch-diggers, including the nine-banded armadillo and groundhog (Rupert et al., 2015), have other functional groups that were found to be massive, such as the scapular elevator/stabilizers which facilitate limb retraction. Collectively, large masses in these groups contribute to greater PCSA. **PCSA** is one of the most important architectural properties for scratch-digging taxa because it is proportional to muscle force production (Alexander et al., 1984), and to the application of out-force to the substrate.

Muscle groups with substantial summed PCSA often act in limb joint stabilization, application of large joint torque, or generation of appreciable joint power (Moore et al., 2013; Rupert et al., 2015). This is because individual muscles from these functional groups display a range of architectural properties. The mm. latissimus dorsi, pectoralis superficialis, teres major, and triceps brachii (angular and/or long head), in particular, have long fascicles but also large PCSA due to their hypertrophied muscle mass (Moore et al., 2013). These muscles, among others, additionally have long r_m at the joints that they span, and therefore have large mechanical advantage for joint position control. For example, the long head of m. tricieps brachii has the largest PCSA of all muscles in the

groundhog forelimb (Rupert et al., 2015), and it is capable of substantial joint torque application about both the shoulder and elbow joints during scratch-digging. Other forelimb muscles (e.g., subscapularis, supraspinatus, and flexor digitorum superficialis) may be less well-developed, but have short fascicles with notable pennation and, consequently have large PCSA. Thus, there are several combinations of architectural properties that result in substantial PCSA, isometric force, and joint torque application (Rupert et al., 2015).

Among scratch-digging taxa, the carpal/digital flexors are observed to have relatively high PCSA/MM and low L_F/ML ratios, which indicates large F_{max} produced to be applied to joint torque at carpometacarpal and interphalangeal joints. Notably, some heads of the digital flexor complex have moderate L_F/ML indicating the ability to shorten to flex the digits to enable the long, sharp foreclaws to pierce the soil (Moore et al., 2013). Other heads of the carpal/digital flexors have little ability to shorten and act to strongly maintain the flexed position of the carpus and digits as the forelimb is retracted during the power stroke (Moore et al., 2013; Rupert et al., 2015). Scratch-diggers also have several muscles with high L_F/r_m ratios, which indicates the ability of the muscle or functional group to rotate the joint through a broad ROM. However, muscles with greater joint rotation are generally associated with low joint torque application (Rupert et al., 2015). For example, mm. infraspinatus and biceps brachii, were found to have a high L_F/r_m in the American badger (Moore et al., 2013). Finally, there are also several examples of scratch-digging taxa that have muscles with large F_{max} as well as an appreciable range of contraction. This combination of architectural properties is demonstrated by the medial and lateral heads of m. triceps brachii of badgers that have large PCSA as well as high L_F/ML (Moore et al., 2013). These muscles exemplify high power generation at the elbow joint (Moore et al., 2013). This is because W is the product F_{max} and contractile velocity, which is proportional to muscle length.

Bone Functional Indices

There are numerous functional indices that can be used to indicate fossorial ability in armadillos based on their limb bone proportions (Rose et al., 2014). Such indices can infer the presence of specializations for scratch-digging, namely in-lever and out-lever lengths, and the resulting mechanical advantage (Fariña and Blanco, 1996; Vizcaíno et

al., 1999; Vizcaíno and Milne, 2002). Overall, multivariate statistical assessment of functional indices can help determine fossorial specializations that were selected for in armadillos based on their lifestyles, and how they can be observed through morphological variation in forelimb bone proportions. Definitions, relative values, and functional implications of selected indices used in determining fossorial ability are summarized for the forelimb in **Table 1** and the hindlimb in **Table 2** (see below).

A. Forelimb proportions

A large scapular shape index (SSI) is associated with increased area for muscle attachment and development. By extension, an enlarged scapula is also related to greater ability for humeral retraction (and shoulder joint stabilization) and application of greater out-force to the substrate during scratch-digging (Rose et al., 2014). For example, a large teres process of scapula that is present in armadillos, provides a greater area of origin for m. teres major as well as a longer r_m for substantial flexor torque application at the shoulder joint (Olson et al., 2016), and thus stronger humeral retraction (Hildebrand, 1985; Kley and Kearney, 2007; Rose et al., 2014). Values of SSI approaching 1.0 are reflective of greatly enlarged scapular width due to elongation of the hook-like teres process.

The glenoid fossa shape (GFI) humeral head shape indices (HHSI) both indicate the articulation strength about the shoulder joint as defined in **Table 1**. Moreover, the relative values of these indices are reflective of the degree of joint rotation capable during limb protraction and retraction, in that articular robustness limits joint rotation. A strong articulation by a more secure fit of an enlarged humeral head in a deeper glenoid fossa can withstand high levels of joint loading during scratch-digging. Greater fossorial ability is similarly indicated by articular strength at the elbow joint by the humeral trochlea/capitulum length index (HTCLI), which involves the articulation of the humerus with the proximal radius and ulna, and the humerus. Robust articulations at the radiohumeral and ulnarhumeral joints are also associated with a more restricted axis of rotation, or smaller ROM, which is advantageous for larger application of out-force to excavate earth during scratch-digging activity (Salton and Sargis, 2008).

The shoulder moment index (SMI) indicates the mechanical advantage of m. deltoideus acting at the shoulder joint to either retract the forelimb or stabilize the

shoulder joint (Hildebrand, 1985; Vizcaíno and Milne, 2002; Rose et al., 2014). Large values for SMI result from a more distal position of an enlarged deltoid tuberosity, thus increasing the in-lever length of the deltoids and consequently, their application of flexor torque for stronger humeral retraction. In contrast, scratch-diggers often have small values for the brachial index (BI), which is associated with having shorter distal limb lengths relative to humeral length (Vizcaíno and Milne, 2002; Rose et al., 2014) and greater limb mechanical advantage. For perspective, species adapted for running (and speed) have a high BI due to elongated distal limbs for increased stride length and higher joint rotational velocity (Stein and Casinos, 1997), and resulting in greater mobility of their limbs. Armadillos have robust distal limb elements and little ability to cycle their limbs quickly (Vizcaíno and Milne, 2002) implying morphological specialization to use their stout limbs to translate high out-force during scratch-digging. An extreme example of this limb form is observed in the giant armadillo that has a BI of 0.55 (Vizcaíno and Milne, 2002) compared to a cheetah with a BI greater than 1.0.

A large humeral epicondylar index (EI) is often strongly correlated with fossorial ability (Hildebrand, 1985; Rose et al., 2014; Olson et al., 2016). Armadillos have a wide medial epicondyle for greater relative area of attachment of the carpal/digital flexors and pronators of the antebrachium (Olson et al., 2016). In addition, a large HEI is associated with greater muscle mass in the distal and medial aspects of the antebrachium (Vizcaíno and Milne, 2002). Hypertrophied muscle mass (or greater number of muscle bellies) in the distal forelimb is related to greater PCSA for these muscles to produce large force for maintaining flexion of the carpus and digits during scratch-digging. Well-developed carpal/digital flexors are important distinctive features in the distal limbs of scratch-diggers (Moore et al., 2013).

Indices of robustness for the humerus (HRI), radius (RRI), and ulna (URI) all indicate the ability to resist shearing and bending loads, where higher values infer greater bone strength and stiffness (Rose et al., 2014). Bending/shearing stresses are caused by both substrate reaction forces (SRF) and muscular forces experienced by these bones during the power stroke. Thus, it is critical for armadillos to maintain robust bones to minimize stress and strain (Moore et al., 2013). Cursorial mammals have more gracile limb bones, although they are exposed to similar magnitudes of bone stress as scratch-diggers

(Samuels et al., 2013). This is only possible by a shift to upright limb posture that increases the effective mechanical advantage of their limbs (Biewener, 1989). Armadillos have short, stout limbs and crouched limb posture requiring that their muscles apply larger torque to maintain joint position. Coupled with substantial SRF during digging, their limb bones must be more robust to avoid fracture. Moreover, high robustness indices are also associated with larger relative area available for muscle development and attachment (Rose et al., 2014; Olson et al., 2016).

The index of fossorial ability (IFA) is the most well-established indicator of fossorial ability (Hildebrand, 1985; Rose et al., 2014). A high value for IFA is associated with a long olecranon process length relative to functional ulna length, as well as greater relative area for elbow extensor attachment (Olson et al., 2016). Armadillos have a particularly well-developed olecranon and an IFA that ranges from 0.3 to 0.9 (Hildebrand, 1985). An olecranon that approximates greater than half the length of the ulna/radius greatly increases the mechanical advantage of the elbow extensors. Most importantly, a more prominent olecranon is proportional to the out-force applied to the substrate (Rose et al., 2014). The triceps metacarpal out-force index (TMOI) estimates the out-force applied at the distal end of the metacarpals relative to the m. triceps brachii in-force (force produced by the muscles) during scratch-digging (Price, 1993; Lagaria and Youlatos, 2006). Specifically, a longer olecranon relative to metacarpal length results in substantial downward force due to the overall increase in limb mechanical advantage (Olson et al., 2016). IFA and TMOI are closely related, as they both are associated with features for enhancing out-force applied to the substrate (Lagaria and Youlatos, 2006).

The manus proportions index (MANUS) relates the lengths of the metacarpal III and proximal phalanx of digit III (Samuels and Van Valkenburgh, 2008). For example, *D. novemcinctus* have a relatively short metacarpal III and long proximal phalanx, and a resulting MPI of approximately 0.5 (Olson et al., 2016). A large MANUS value is yet another metric associated with enhanced mechanical advantage for the application of out-force to the substrate during scratch-digging (Olson et al., 2016). Lastly, most armadillos have longer foreclaws relative to their hind claw length, and this proportion is related by the claw length index (CLAW) (Samuels and Van Valkenburgh, 2008). Because a larger portion of scratch-digging activity is performed by the forelimbs, having longer, sharper

foreclaws is advantageous for initially piercing and loosening the soil during excavations of burrows and/or foraging behavior.

Table 1. Forelimb indices: formulae and functional significance

Index	Definition
Scapular Shape Index (SSI)	Scapular dorsoventral width divided by scapular craniocaudal length (SW/SL). Indicates relative scapular width available for intrinsic muscle attachments associated with humeral retraction and shoulder joint stabilization.
Glenoid Fossa Shape Index (GFSI)	Scapular glenoid fossa mediolateral width divided by scapular craniocaudal length (SGFW/SGFL). Indicates relative size of glenoid fossa and humeral head articulation.
Humeral Head Shape Index (HHSI)	Humeral head mediolateral width divided by craniocaudal depth (HHW/HHD). Indicates relative size of glenoid fossa and humeral head articulation.
Shoulder Moment Index (SMI)	Delto-pectoral crest proximodistal length (or deltoid tubercle) divided by greatest humerus length (DPCL/HL). Indicates degree of mechanical advantage of the shoulder joint musculature and the ability to strongly retract the humerus.
Humeral Robustness Index (HRI)	Humerus mid-shaft mediolateral width divided by greatest humerus length (HW/HL). Indicates robustness of humerus its ability to resist bending stress-strain, and relative area available for muscle attachment.
Humeral Epicondyle Index (HEI)	Humeral distal epicondylar mediolateral width divided by greatest humeral length (HDEW/HL). Indicates relative area available for the origins of carpal and digital flexors and antebrachial pronator musculature.
Humeral Epicondyle Width Index (HEWI)	Humeral distal articular mediolateral width divided by humeral distal epicondylar mediolateral width (HDAW/HDEW). Indicates relative size between the epicondyles and the trochlea and capitulum.
Humeral Trochlea/Capitulum Length Index (HTCLI)	Humeral trochlea proximodistal length divided by capitulum proximodistal length (HTL/HCL). Indicates relative size between the capitulum and trochlea and the area available for articulation the radius and humerus and the ulna and humerus.
Brachial Index (BI)	Greatest radius length divided by greatest humerus length (RL/HL). Indicates distal out-lever length and overall mechanical (or velocity) advantage of the forelimb.
Radial Robustness Index (RRI)	Radius mid-shaft mediolateral width divided by greatest radial length (RW/RL). Indicates robustness of radius and its ability to resist bending stress-strain, and relative area available for attachment of carpal and deep digital flexors.

Fossorial Ability Index (IFA)	Functional olecranon length divided by functional ulna length [FOL/(FUL-OTL)]. Indicates in-lever length and mechanical advantage of elbow extensors to apply large out-force during elbow extension.
Ulnar Robustness Index (URI)	Ulnar mid-shaft mediolateral width divided by greatest ulna length (UW/UL). Indicates robustness of ulna and its ability to resist bending stress-strain, and relative area available for the attachment of carpal and digital flexors and extensors.
Triceps Metacarpal Out-force Index (TMOI)	Functional olecranon length divided by the sum of the functional ulna and metacarpal III length (FOL/FUL+ML). Indicates amount of out-force applied at distal end of metacarpals per unit triceps in-force.
Manus Proportions Index (MANUS)	Proximal phalanx length of digit III divided by metacarpal III length (PPL/MCL). Indicates relative size of phalanges, metacarpals, and palmar surface of manus.
Relative Manus Claw Length (CLAW)	Manus claw length of digit III divided by the sum of metacarpal III length and proximal phalanx length of digit III [MnCL/(MCL+PPL)]. Indicates relative proportions of the manus.

B. Hindlimb proportions

Armadillos with lower body mass typically have a smaller hip moment index (HMI). In contrast, armadillos with higher body mass have a larger HMI value due to greater hip leverage for overall hindlimb support in extension (i.e., more upright limb posture). Ratios of 0.42 and 0.56 have been reported for the smallest and largest species of armadillo, respectively (Vizcaíno and Milne, 2002). A larger HMI is representative of greater stabilization of the hindlimb, which is advantageous during fossorial activity. Moreover, it indicates the relative position of T3, which needs to be more distal in larger armadillos for enhanced weight-bearing and stabilization at the hip (Milne et al., 2011). Armadillos are also notably associated with having greater HMI values compared to the ratios seen with cursorial and/or arboreal adapted mammals. Differences in limb form emphasize mechanical advantage about the hip joint that may be required during scratch-digging. Importantly, increased leverage of the hindlimbs translates to greater out-force exerted by the forelimbs to excavate earth. Similarly, larger armadillos were previously found to have higher intermembral index (IMI) ratios indicative of greater hind limb size relative to the forelimb. Armadillos only as large as *Z. pichiy* may have IMI values significantly greater that those of *C. truncatus,* and this is often interpreted as larger armadillos tending to have more hindlimb dominance because of the greater role in weight-bearing support by their hindlimbs (Vizcaíno and Milne, 2002).

A high value for femoral head depth index (FHDI) indicates a strong articulation between the femoral head and the acetabulum. However, there is also limited mobility about the hip joint due the greater stability implied by this ratio. Similarly, the femoral condylar index (FCI) indicates the strength of the articulation between the femoral and tibial condyles. Large armadillos have a greater relative area between these articular surfaces. This could be associated with a more upright limb posture to compensate for higher stresses on their hindlimb bones due to their increased body mass (Milne et al., 2011).

The tibial tuberosity index (TTI) is associated with mechanical advantage of the knee extensors acting across the knee joint (Samuels and Van Valkenburgh, 2008). In addition to joint stabilization, a large TTI value indicates high out-force of these extensor muscles due to their increased mechanical advantage. Greater limb mechanical advantage is also

conferred by having shorter distal limb length. This lever ratio is calculated as the crural index (CI) and is analogous to BI for the forelimb. In contrast to cursorial species adapted for a joint velocity advantage, scratch-diggers generally have a low CI (Vizcaíno and Milne, 2002). Specifically, armadillos were reported to have CI values of ~0.80, which are much lower compared with values greater than 1.0 that are typical for generalized terrestrial, and cursorial and arboreal adapted mammals. Armadillos have a shorter tibiofibula length compared to their femur length, in addition to fused and reduced bony elements in their hindfeet. Collectively, these modifications provide a shorter distal limb length and modulate their L_o/L_i ratio for higher out-force application to the substrate by the hindlimbs (Vizcaíno and Milne, 2002).

Similar to the forelimb robustness indices, the femoral robustness index (FRI) and tibial robustness index (TRI) are related to resistance to shearing and bending loads during scratch-digging (Samuels et al., 2013). In general, armadillos have high robustness indices, which indicate greater bone strength and stiffness, as well as the amount of relative bone width available for muscle attachment (Rose et al., 2014). Increased area for attachment of well-developed hip extensors and knee flexors/extensors is correlated with greater fossorial ability (Eliassamburu and Vizcaíno, 2004).

The calcaneus length index (CLI) relates the tibiofibula length to calcaneus length, and it is indicative of out-force applied by the ankle extensors (e.g., m. gastrocnemius). Since the tibiofibula length is reduced in armadillos (Vizcaíno and Milne, 2002), the calcaneus is relatively longer, and therefore more out-force is produced with ankle joint extension. CLI is often paired with the ankle extensor index (AEI) to evaluate mechanical advantage at the ankle joint. Scratch-diggers generally have a large AEI due to having a more compact hindfoot and a long calcaneus. Again, a favorable out-lever (metatarsals and phalanges) to in-lever (calcaneus) ratio increases mechanical advantage about the ankle joint and allows the hindlimb to apply higher out-force to the substrate. The opposite form is generally observed in cursorial species, where having longer foot elements is advantageous for ankle joint rotational velocity, resulting in smaller AEI values (Stein and Casinos, 1997). Accordingly, cursorial species also have an overall larger pes length index (PES) compared to non-cursorial species due to their long

metatarsals (Garland and Janis, 1991). Thus, armadillos are expected to have comparatively small values for PES.

Table 2. Hindlimb indices: formulae and functional significance

Index	Definition
Femur Head Depth Index (FDHI)	Femur head proximodistal length divided by femur head mediolateral width (FHL/FHW). Indicates relative size of articulation between acetabulum and femoral head.
Hip Moment Index (HMI)	Proximal femur length divided by greatest femur length (PFL/FL). Indicates mechanical advantage of m. gluteus superficialis during hip extension.
Greater Trochanter Height Index (GTHI)	Greater trochanter length divided by greatest femur length (GTL/FL). Indicates mechanical advantage of the gluteal muscles during rotation of the hip joint as well as the posture of the hindlimb.
Femur Robustness Index (FRI)	Femoral mid-shaft mediolateral width divided by greatest femur length (FW/FL). Indicates robustness of the femur and its ability to resist strain-inducing bending stress.
Femoral Condylar Index (FCI)	Femur condylar mediolateral width divided by greatest femur length (FCW/FL). Indicates relative area of articulation between the femoral and tibial condyles.
Crural Index (CI)	Greatest tibia length divided by greatest femur length (TL/FL). Indicates relative proportions of the proximal and distal aspects of the hindlimb.
Fibula Length Index (FLI)	Greatest fibula length divided by greatest tibia length (FBL/TL). Indicates the relative proportions between the fibula and tibia.
Tibia Robustness Index (TRI)	Tibial mid-shaft mediolateral width divided by greatest tibia length (TW/TL). Indicates robustness of tibia and its ability to resist strain-induced bending stress.
Tibial Tuberosity Index (TTI)	Proximal tibial tuberosity length divided by greatest tibia length (TTL/TL). Indicates mechanical advantage of the knee joint.
Medial Malleolus Index (MMI)	Medial malleolus mediolateral width divided by greatest tibia length (MMW/TL). Indicates size of medial malleolus relative to the tibia and ankle joint mobility.
Intermembral Index (IMI)	The sum of the greatest humerus length and functional ulna length divided by the sum of the greatest femur length and greatest tibia length [HL+(UL-OL)/FL+TL]. Indicates relative proportions between the forelimb and hindlimb.
Calcaneus Length Index (CLI)	Calcaneus length divided by greatest tibia length (CL/TL). Indicates relative proportion between the distal leg and the hindfoot.
Ankle Extensor Index (AEI)	Calcaneus length divided by the sum of calcaneus length and metatarsal 3 length (CL/CL+MT3). Indicates ability of the ankle joint to produce high output force.

Pes Length Index (PES)	Metatarsal 3 length divided by greatest femur length (MT3/FL). Indicates the relative proportion of the proximal and distal aspects of the hindlimb, and the relative size of the hindfoot.

Objectives and Hypotheses

The objectives of this study are to (i) describe forelimb myology and quantify muscle architectural properties in three rare armadillo species and, (ii) assess the functional osteology among xenarthran genera. This study is important to the field of Biology because limb myology, muscle architecture, and bone morphology provide essential postcranial characters for reassessment of evolutionary relationships among The Xenarthra, and these data will ultimately contribute to our understanding of this basal clade by clarifying if the musculoskeletal features observed are ancestral or derived in origin. It is **hypothesized** that quantitative differences in limb form will be predictive of the functional habits observed among cingulates to help resolve the influences of morphology vs. phylogeny in their present taxonomic classifications. Specifically, the anatomical traits quantified will be predictive of the degree of fossorial ability in armadillos with respect to indicating specialization of the limb systems for substrate preference and use. The following outcomes are **predicted**: armadillos with greater fossorial specialization (e.g., *C. truncatus*) will have 1. less complex muscle functional groups with fewer numbers of muscle bellies or heads; 2. limb retractors, elbow extensors, and carpal/digital flexors that are massive with large PCSA; 3. limb retractors and elbow extensors with long muscle moment arms and capacity for large extensor torque application at the shoulder and elbow joints, respectively; 4. fore and hindlimb bones with long *in-levers* for large limb mechanical advantage; and 5. robust fore and hindlimb bones for resistance to bending and large areas of muscle attachment. Collectively, these features confer scratch-digging ability by enhancing mechanical advantage and capability for high out-force application to the substrate.

Last, further evaluation of structure-function and phylogeny in armadillos by thorough quantification of their limb musculoskeletal traits more immediately improves our understanding of xenarthran functional morphology in multiple ways. This study adds to and updates previous, but incomplete, documentations of armadillo myology. It provides representative muscle architectural properties for multiple species of armadillo for which similar data are currently available for only *D. novemcinctus*. And, it provides interpretations for limb bone proportions in relation to substrate preference and substrate use that have only been previously evaluated for extinct/extant species of sloths. In

addition, the postcranial data collected herein will be combined with similar metrics from the limbs of all sloth, anteater, and armadillo genera collected for ongoing studies. To this end, the aggregate assemblage of anatomical characters will be used in a meta-analysis that tests the hypothesis that The Xenarthra is the most basal clade from which all placental mammals emerged.

TABLE 1. Morphometric data for armadillo specimens dissected.

Animal	Origin[a]	Sex	Age	Limb (R/L)	Body Mass (g)
Zp582	Mendoza	M	Adult	R	700.0
Zp583	Mendoza	M	Adult	R	850.0
Zp585	Mendoza	M	Adult	R/L	775.0
Cvell	Mendoza	M	Adult	R/L	625.0
Cvill	Mendoza	F	Adult	R	2460
Ctru	La Paz	M	Adult	R	105.8

[a] All individuals were sourced in Argentina

TABLE 2. Forelimb muscles per limb region; their abbreviations, fiber architecture, and actions in *Z. pichiy*.

Muscle	Abbreviation	Fiber Architecture	Action
Extrinsic			
Panniculus carnosus (+Platysma)	PC	Parallel	Carapace rotation
Trapezius pars cervicalis	TC	Parallel	Scapula elevation, stabilization
Trapezius pars thoracica	TT	Parallel	Scapula stabilization, retraction
Rhomboideus profundus et capitus	RPC	Parallel	Scapula stabilization, protraction
Rhomboideus cervicis	RC	Parallel	Scapula stabilization, protraction
Rhomboideus thoracis	RT	Parallel	Scapula elevation, stabilization, retraction
Omotransversarius	OT	Parallel	Scapula elevation; limb protraction
Serratus ventralis – cervicis[a]	SVC	Parallel	Scapula stabilization; limb protraction/retraction
Serratus ventralis – thoracic	SVT	Parallel	Scapula stabilization; limb protraction/retraction
Latissimus dorsi	LAT	Parallel	Limb retraction
Pectoralis superficialis	PS	Parallel	Limb retraction, adduction
Pectoralis profundus[b]	PP	Parallel	Limb retraction
Subclavius	SC	Parallel	Clavicle/scapula stabilization, rotation
Sternomastoideus[c]	SM	Parallel	Clavicle stabilization; neck lateral flexion
Brachiocephalicus-cleidomastoideus[d]	BCP-CM	Parallel	Clavicle protraction; neck lateral flexion
Shoulder			
Deltoideus pars scapularis	DS	Parallel	Shoulder flexion, limb retraction
Deltoideus pars acromialis	DA	Parallel	Shoulder flexion, limb retraction
Deltoideus pars clavicularis	DC	Parallel	Shoulder flexion, limb retraction
Supraspinatus	SSP	Bipennate	Shoulder extension, limb stabilization/protraction
Infraspinatus[e]	ISP	Bipennate	Shoulder flexion, limb stabilization/retraction

Teres minor	TMN	Parallel	Shoulder flexion, limb stabilization/retraction
Teres major	TMJ	Parallel	Shoulder flexion, limb retraction
Subscapularis	SUB	Multipennate	Shoulder extension, limb stabilization/adduction
Brachium			
Coracobrachialis[f]	CCB	Parallel	Limb protraction, adduction
Biceps brachii	BB	Bipennate	Elbow flexion; shoulder extension, limb protraction
Brachialis	BCH	Unipennate	Elbow flexion
Triceps brachii – angulare	TBA	Parallel	Elbow extension; shoulder flexion, limb retraction
Triceps brachii – longum	TBLO	Parallel	Elbow extension; shoulder flexion, limb retraction
Triceps brachii – laterale	TBLA	Parallel	Elbow extension
Triceps brachii – mediale	TBM	Parallel	Elbow extension
Triceps brachii – mediale accessorium	TBMA	Parallel	Elbow extension
Tensor fasciae antebrachii	TFA	Parallel	Antebrachial fascia tension; elbow extension
Anconeus	ANC	Parallel	Elbow extension
Antebrachium			
Pronator teres	PT	Unipennate	Elbow stabilization; antebrachial pronation
Flexor carpi ulnaris	FCU	Unipennate	Carpal flexion
Flexor carpi radialis	FCR	Unipennate	Carpal flexion, stabilization
Flexor digitorum superficialis[g]	FDS	Unipennate	Flexion digits II–IV
Flexor digitorum profundus – humeral mediale	FDPHM	Unipennate	Flexion digits II–IV
Flexor digitorum profundus – humeral laterale	FDPHL	Unipennate	
Flexor digitorum profundus – ulnar	FDPU	Unipennate	
Flexor digitorum profundus – radial[h]	FDPR	Bipennate	
Extensor carpi radialis[i]	ECR	Bipennate	Carpal extension, stabilization
Extensor carpi ulnaris[j]	ECU	Pennate	Carpal extension, stabilization
Extensor digitorum communis[k]	EDC	Unipennate	Extension digits II–IV

Extensor digitorum lateralis	EDL	Unipennate	Extension digits IV, V
Extensor digiti II[l]	ED2	Unipennate	Extension digit II, III
Abductor digiti I longus	AD1L	Bipennate	Abduction digit I

[a]m. serratus ventralis cervicis was observed as a distinct belly from m. serratus ventralis thoracis in only Zp 583; [b]m. pectoralis profundus was not observed in Zp 585; [c]sternal head of m. sternomastoideus in Zp 585 had moderate pennatation (range: 11–16º); [d]m. brachiocephalicus-cleidomastoideus was observed in only Zp 585; [e]m. infraspinatus was unipennate in Zp 583; [f]m. coracobrachialis was not observed in Zp585; [g]m. flexor digitorum superficialis was bipennate in Zp 585.; [h]pennation not observed for the radial head of m. flexor digitorum profundus in Zp 585 due to poor muscle integrity, but fiber architecture was unipennate in Zp 583 and bipennate in Zp 582; [i]fiber architecture for m. extensor carpi radialis was unipennate in Zp 585; [j]pennation not observed for m. extensor carpi ulnaris in for Zp 585 tdue to poor muscle integrity, but fiber architecture was unipennate in Zp 583 and bipennate in Zp 582; [k]m. extensor digitorum communis was bipennate in m. extensor digitorum communis; [l]muscle also referred to as m. extensor digiti II et III in two individuals (Zp 583, Zp 585) due to its insertion on only MC III.

TABLE 3. Forelimb bone indices: formulae and functional significance.

Index	Definition
Scapular Shape Index (SI)	Greatest scapula dorsoventral width divided by greatest scapula craniocaudal length (SW/SL). Indicates relative scapular width available for intrinsic muscle attachments associated with humeral retraction and shoulder joint stabilization.
Glenoid Fossa Shape Index (GFSI)	Scapular glenoid fossa mediolateral width divided by glenoid fossa craniocaudal length (GFW/GFL). Indicates relative size of glenoid fossa and humeral head articulation.
Scapulohumeral Index (SHI)	Greatest scapula craniocaudal length divided greatest humerus length (SL/HL). Indicates relative size of the proximal and distal elements of the forelimb.
Humeral Head Shape Index (HHSI)	Humeral head mediolateral width divided by craniocaudal depth (HHW/HHD). Indicates relative size of glenoid fossa and humeral head articulation.
Shoulder Moment Index (SMI)	Delto-pectoral crest proximodistal length (or deltoid tubercle) divided by greatest humerus length (DCL/HL). Indicates degree of mechanical advantage of the shoulder joint musculature and the ability to strongly retract the humerus.
Humeral Robustness Index (HRI)	Humerus mid-shaft mediolateral width divided by greatest humerus length (HW/HL). Indicates robustness of humerus its ability to resist bending stress-strain, and relative area available for muscle attachment.
Humeral Epicondyle Index (EI)	Humeral distal epicondylar mediolateral width divided by greatest humeral length (DEW/HL). Indicates relative area available for the origins of carpal and digital flexors and antebrachial pronator musculature.
Humeral Epicondyle Width Index (HEWI)	Humeral distal articular mediolateral width divided by humeral distal epicondylar mediolateral width (DAW/DEW). Indicates relative size between the epicondyles and the trochlea and capitulum.
Humeral Trochlea Depth Index (HTDI)	Humeral trochlea craniocaudal depth divided by greatest humerus length (HTD/HL). Indicates the area available for articulation between the trochlea and ulnar trochlear notch relative to the humerus size.
Humeral Trochlea Length Index (HTLI)	Humeral trochlea proximodistal length divided by humeral distal articular mediolateral width (HTL/HDAW). Indicates the area available for articulation between the trochlea and ulnar trochlear notch relative to the entire distal articulation width of the humerus.
Humeral Capitulum Length (HCLI)	Humeral capitulum proximodistal length divided by humeral distal articular mediolateral width (HCL/HDAW). Indicates the area available for articulation between the capitulum and radial head relative to the entire distal articulation width of the humerus.
Humeral Trochlea/Capitulum Length Index (HTCLI)	Humeral trochlea proximodistal length divided by capitulum proximodistal length (HTL/HCL). Indicates relative size between the capitulum and trochlea and the area available for articulation the radius and humerus and the ulna and humerus.
Brachial Index (BI)	Greatest radius length divided by greatest humerus length (RL/HL). Indicates distal out-lever length and overall mechanical (or velocity) advantage of the forelimb.

Humerus-Radial Length Index (HRLI)	Greatest humerus length divided by greatest radius length (HL/RL). Indicates distal out-lever length and overall mechanical (or velocity) advantage of the forelimb.
Radial Length Index (RLI)	Greatest radius length divided by greatest ulna length (RL/UL). Indicates relative size and the area available for muscle attachment between the radius and ulna.
Radial Shape Index (RSI)	Radial head craniocaudal depth divided by radial head mediolateral width (RHD/RHW). Indicates relative size of radial head and overall area available for articulation with the humeral capitulum.
Alternative Radial Shape Index (ARSI)	Radius mid-shaft craniocaudal depth divided by greatest radial length (RD/RL). Indicates robustness of radius and its ability to resist bending stress-strain, and relative area available for attachment of the carpal and deep digital flexors.
Radial Robustness Index (RRI)	Radius mid-shaft mediolateral width divided by greatest radial length (RW/RL). Indicates robustness of radius and its ability to resist bending stress-strain, and relative area available for attachment of carpal and deep digital flexors.
Olecranon Length Index (OLI)	Ulnar olecranon length divided by greatest ulna length (OL/UL). Indicates the length of the ulnar olecranon process relative to greatest ulna length and the area available for attachment of the elbow extensors.
Fossorial Ability Index (IFA)	Functionalolecranon length divided by functional ulna length [FOL/(FUL)]. Indicates in-lever length and mechanical advantage of elbow extensors to apply large out-force during elbow extension.
Ulnar Trochlear Length Index (UTLI)	Ulnar trochlear notch length divided by greatest ulna length (UTL/UL). Indicates the size of the trochlear notch relative to the ulna and the overall area for articulation with the humeral trochlea.
Ulnar Robustness Index (URI)	Ulna mid-shaft mediolateral width divided by greatest ulna length (UW/UL). Indicates robustness of ulna and its ability to resist bending stress-strain, and relative area available for the attachment of carpal and digital flexors and extensors.
Ulnar Shape Index (USI)	Ulna mid-shaft craniocaudal depth divided by greatest ulna length (UD/UL). Indicates robustness of ulna and its ability to resist bending stress-strain and relative area available for the attachment of carpal and digital flexors and extensors.
Triceps Metacarpal Out-force Index (TMOI)	Functional olecranon length divided by the sum of the functional ulna and metacarpal III length (FOL/FUL+MCL). Indicates amount of out-force applied at distal end of metacarpals per unit triceps in-force.
Metacarpal III Robustness Index (MCRI)	Metacarpal III mid-shaft mediolateral width divided by metacarpal III length (MCW/MCL). Indicates robustness of metacarpal III and its ability to resist bending stress-strain, and relative area available for the attachment of carpal and digital flexors and extensors.
Manus Proportions Index (MANUS)	Proximal phalanx length of digit III divided by metacarpal III length (PPL/MCL). Indicates relative size of phalanges, metacarpals, and palmar surface of manus.
Alternative Manus Proportions Index (AMPI)	Metacarpal III length divided by proximal phalanx length of digit III (MCL/PPL). Indicates relative size of phalanges, metacarpals, and palmar surface of manus.

Proximal Phalanx Robustness Index (PPRI)	Proximal phalanx mid-shaft mediolateral width divided by proximal phalanx metacarpal length of digit III (PPW/PPL). Indicates robustness of metacarpal III and its ability to resist bending stress-strain, and relative area available for the attachment of carpal and digital flexors and extensors.
Relative Manus Claw Length (CLAW)	Manus claw length of digit III divided by the sum of metacarpal III length and proximal phalanx length of digit III [CL/(MCL+PPL)]. Indicates relative proportions of the manus.

TABLE 4. Species, number, substrate preference, and substrate use of the specimens studied for functional osteology.

Species	*N*	Functional Habit	Substrate Use
Tolypeutes matacus (Southern three-banded armadillo)[a,b,]	4	Generalized	Generalized
Zaedyus pichiy (Pichi armadillo)[a,c]	4	Semi-fossorial	Scratch-digging
Chaetophractus vellerosus (Screaming hairy armadillo)[a,d,e]	1	Semi-fossorial	Scratch-digging
Chaetophractus villosus (Big hairy armadillo)[a,f]	6	Semi-fossorial	Scratch-digging
Cabassous centralis (Northern naked-tailed armadillo)[a]	1	Semi-fossorial	Scratch-digging
Cabassous unicinctus (Southern naked-tailed armadillo)[a]	4	Semi-fossorial	Scratch-digging
Dasypus septemcinctus (Seven-banded armadillo)[a,g]	1	Semi-fossorial	Scratch-digging
Dasypus hybridus (Southern long-nosed armadillo)[a]	2	Semi-fossorial	Scratch-digging
Dasypus novemcinctus (Nine-banded armadillo)[a,h]	4	Semi-fossorial	Scratch-digging
Chlamyphorus truncatus (Pink fairy armadillo)[a,i]	2	Fossorial	Scratch-digging
Priodontes maximus (Giant armadillo)[a,j]	3	Fossorial	Scratch-digging

Data sources: [a]Vizcaíno and Milne, 2002; [b]Smith, 2007; [c]Superina and Abba, 2014; [d]Greegor, 1980; [e]Smith*b*, 2008; [f]Smith*a*, 2008; [g]Hamlett, 1939; [h]Olson et al., 2016; [i]Borghi et al., 2011; [j]Toledo et al., 2012

TABLE 5. Functional muscle groups analyzed for mass distribution in the forelimb of *Z. pichiy*.

Functional Groups and Muscles Studied
EXTRINSIC MUSCLES:
Scapula elevator/rotators
Trapezius (parts: cervical, thoracic)
Rhomboideus (heads: profundus/capital, cervical, thoracic)
Serratus ventralis (heads: cervical, thoracic)
Omotransversarius
Subclavius
Scapula/limb retractors
Trapezius thoracica, Rhomboideus thoracis, Latissimus dorsi, Pectoralis superficialis, Pectoralis profundus
Scapula/limb protractors
Rhomboideus cervicis, Rhomboideus profundus et capitis, Cleidocephalicus pars mastoideus, Omotransversarius
Limb adductors
Pectoralis superficialis
INTRINSIC MUSCLES:
Limb retractors (shoulder flexor/stabilizers)
Deltoideus (parts: scapular, acromial), Teres major, Teres minor, Infraspinatus, Triceps brachii (heads: angular, long)
Limb protractors (shoulder extensor/stabilizers)
Coracobrachialis, Deltoideus pars clavicularis, Supraspinatus, Subscapularis, cleidobrachialis, Biceps brachii (long head)
Humeral adductors (shoulder stabilizers)
Coracobrachialis, Subscapularis, Deltoideus pars clavicularis
Elbow flexors
Biceps brachii (heads: long, short), Brachialis
Elbow extensors
Triceps brachii (heads: angular, long, lateral, medial, medial accessory), Anconeus, Tensor fasciae antebrachii
Carpal flexors
Flexor carpi radialis, Flexor carpi ulnaris
Carpal extensors
Extensor carpi radialis, Extensor carpi ulnaris
Digital flexors
Flexor digitorum superficialis, Flexor digitorum profundus (heads: humeral medial, humeral lateral, radial, ulnar)
Digital extensors
Extensor digitorum communis, Extensor digitorum lateralis, Abductor digiti I longus, Extensor digiti II
Pronators
Pronator teres

TABLE 6. Forelimb muscle masses for each of the four species observed.

Muscle	*Z. pichiy*	*Cha. vellerosus*	*Cha. villosus*	*Chl. truncatus*
PC[a]	3.42±0.53	3.58	8.85	--
TC	1.82±0.04	0.77	4.02	0.17
TT	1.18±0.23	0.71	3.70	0.30
RProf et Cap	2.28±0.41	1.61	6.56	0.47
RCerv	1.99±0.61	1.35	5.23	0.39
RT	1.22±0.27	1.66	2.63	0.21
SVC	1.09[b]	0.42	1.26	0.12
SVT	1.04±0.06	0.76	1.96	0.12
LAT	3.93±0.97	3.44	8.16	0.72
PS	3.34±0.79	4.72	14.8	0.62
PP[c]	1.06±0.56	--	--	--
SC	0.53±0.39	0.69	2.39	0.20
SM	1.16±0.12	0.88	3.48	0.27
BCP-CM	0.24[d]	0.32	0.76	0.04
OT	0.23±0.03	0.53	1.07	0.05
DS	1.49±0.44	1.49	2.66	0.25
DA	0.54±0.34	0.37	2.66	0.10
DC	0.53±0.05	0.31	1.11	0.04
SSP	1.51±0.29	1.10	4.00	0.12
ISP	1.04±0.16	0.94	2.40	0.15
TMN	0.10±0.05	0.10	0.20	0.04
TMJ	0.67±0.14	0.61	1.68	0.26
SUB	2.76±0.67	2.18	6.71	0.38
CCB[e]	0.94±0.88	0.07	0.10	--
BB[f]	0.78±0.10	0.75	2.04	0.02
BCH	0.73±0.49	0.39	1.01	0.06

TBA	1.38±0.13	1.24	4.88	0.21
TBLO	3.76±0.58	3.64	13.2	0.62
TBLA	1.60±0.50	1.10	3.90	0.16
TBM	0.42±0.05	0.41	0.92	0.11
TBMA	0.31±0.06	0.29	1.00	0.06
TFA	0.40±0.04	0.32	1.25	0.05
ANC	0.37±0.19	0.47	1.63	0.05
PT	0.50±0.05	0.38	1.16	0.02
PQ[g]	--	--	0.07	--
FCU	0.39±0.05	0.24	1.10	0.05
FCR	0.17±0.09	0.19	0.40	0.01
FDS	0.36±0.01	0.25	0.93	0.03
FDPHM	0.30±0.21	0.43	1.48	0.09
FDPHL[h]	0.24±0.06	0.07	0.22	--
HDPHP[i]	--	--	0.97	--
FDPU	1.09±0.21	1.13	2.53	0.26
FDPR	0.26±0.15	0.22	0.56	0.03
ECR	0.31±0.23	0.40	1.42	0.04
ECU	0.22±0.05	0.20	0.85	0.05
EDC	0.40±0.24	0.48	1.40	0.06
EDL	0.41±0.24	0.32	0.81	0.03
ED2[j]	0.05±0.01	0.02	--	0.01
AD1L	0.21±0.03	0.15	0.29	0.03

[a] mass for m. panniculus carnosus was combined with m. platysma, and it was highly reduced and closely adhered to the skin in *C. truncatus* (and mass was not taken); [b] m. serratus ventralis cervicis is only observed in Zp 583, and its mass was taken with m. serratus ventralis thoracis and is divided equally among both muscles for this study; [c] m. pectoralis profundus is not observed in Zp 585, *C. villosus*, *C. vellerosus*, and *C. truncatus*; [d] m. cleidocephalicus pars mastoidea is observed in only Zp 585; [e] m. coracobrachialis is not observed in Zp 585 or *C. truncatus*; [f] combined mass for the long and short heads of m. biceps brachii; [g] m. pronator quadratus is observed in only *C. villosus*; [h] m. flexor digitorum profundus humeral lateral head is not observed in *C. truncatus*; [i] m. flexor digitorum profundus humeral profundus head is only observed in *C. villosus*; [j] m. extensor digiti II is not observed in *C. villosus*.

TABLE 7. Means (± s.d.) of raw osteological measurements for all armadillo species used for functional index calculations.

Species	SL	SW	GFL	GFW	HL	HHW	HHD	DPL	HW	HTD	HTL	HCL	DAW	DEW
Tolypeutes matacus	48.9±4.7	28.6±5.3	10.3±0.4	5.4±0.4	41.3±3.2	10.1±3.0	10.0±1.2	21.6±4.4	5.1±1.1	4.8±0.7	4.3±0.6	4.1±0.5	10.1±2.1	15.3±0.4
Zaedyus pichiy	51.9±2.8	35.7±3.6	9.7±1.8	5.6±0.5	44.6±1.3	6.9±0.5	9.8±0.7	23.1±1.7	5.6±0.9	5.9±0.6	5.8±0.6	4.8±0.2	11.2±0.9	17.2±0.9
Chaetophractus vellerosus[a]	39.7[b]	32.4	9.1	5.1	39.7	6.1	8.6	19.5	4.1	5.12	5.5	4.4	10.0	15.5
Chaetophractus villosus	64.8±8.7	47.7±5.0	14.3±2.3	7.5±0.4	62.2±3.0	14.0±4.7	15.1±2.3	32.3±4.1	7.7±1.1	8.9±0.9	7.4±1.6	7.6±1.7	17.5±0.8	25.8±2.6
Cabassous centralis	87.6±1.6	55.6±0.2	12.0±2.4	8.4±1.2	57.6±2.2	10.1±0.2	7.0±0.9	38.8±2.3	12.0±0.5	6.3±0.3	6.1±0.4	5.3±0.7	17.5±0.7	29.1±1.8
Cabassous unicinctus	83.6±16.5	55.0±11.9	12.4±2.9	9.7±2.0	59.3±12.5	11.5±2.4	12.9±2.9	34.9±7.0	12.7±1.3	6.8±1.6	7.1±1.3	6.8±1.4	16.8±4.6	28.9±5.3
Dasypus septemcinctus[a]	52.7	39.0	7.2	4.4	43.2	5.3	9.4	21.3	3.8	4.8	3.7	3.9	8.9	13.8
Dasypus hybridus	53.0±8.4	38.6±5.5	8.5±0.7	5.6±0.3	46.6±4.0	6.6±0.3	9.9±1.1	22.1±6.5	5.0±1.6	4.8±0.6	3.8±1.1	4.0±0.3	10.2±0.9	14.9±0.3
Dasypus novemcinctus	81.9±1.7	57.3±1.3	12.0±0.7	8.0±0.4	62.4±2.0	8.4±1.0	13.1±0.8	30.6±1.5	7.7±1.5	6.3±0.5	6.2±0.5	5.8±0.8	14.2±0.4	20.1±0.7
Chlamyphorus truncatus[c]	26.1	22.3	7.2	2.6	18.9	3.8	5.4	9.9	4.1	2.3	2.7	2.4	5.5	11.3
Priodontes maximus	146±6.8	130±7.7	41.1±0.7	18.7±0.5	130±5.9	40.0±1.6	36.4±3.1	80.4±3.4	28.4±5.6	16.2±1.2	12.9±5.8	13.4±1.1	38.9±0.2	59.0±1.2

Means (± s.d.) of raw osteological measurements for all armadillo species used for functional index calculations.

Species	RL	RW	RD	RHL	RHW	UL	FUL	UW	UD	OL	UTL	OTL	MCL	PPL	CL
Tolypeutes matacus	32.0±2.9	2.7±0.2	2.8±0.2	7.4±0.2	3.7±0.5	48.0±4.6	32.8±3.3	2.7±0.3	5.2±0.2	12.4±2.7	6.5±0.9	15.2±1.3	7.8±2.6	5.2±1.1	28.0±3.6
Zaedyus pichiy	28.1±0.9	3.1±0.2	2.5±0.4	6.5±0.5	3.8±0.7	42.4±3.2	27.7±2.0	3.2±0.4	5.8±0.4	11.4±2.5	8.1±1.2	14.6±2.5	12.4±1.3	4.7±2.3	18.5±3.1
Chaetophractus villosus	38.2±2.6	3.8±0.5	4.9±0.7	10.2±0.7	5.7±0.6	62.0±2.7	38.6±2.2	4.8±0.8	8.6±0.4	20.4±3.4	11.8±1.1	23.4±2.6	17.0±2.6	6.7±3.4	28.5±6.9
Chaetophractus vellerosus[a]	24.9	3.0	2.1	5.3	3.1	41.0	25.0	2.5	5.5	12.9	8.4	16.0	12.4	6.8	8.5[d]
Cabassous centralis	35.1±1.1	4.8±0.4	4.0±0.3	9.7±0.6	8.7±1.1	61.9±2.1	35.5±0.3	5.5±0.1	9.9±1.9	22.8±0.6	9.9±1.2	26.4±1.8	16.5[c]	11.0[c]	45.6±8.1
Cabassous unicinctus	35.7±5.6	5.8±1.1	4.3±0.8	10.8±1.6	7.6±1.2	63.5±11	32.1±5.9	5.7±0.6	10.0±2.1	27.3±5.6	13.9±2.7	31.3±6.0	17.1±3.2	12.7±4.9	39.9±5.8
Dasypus septemcinctus[a]	28.9	2.5	3.8	6.7	3.4	48.2	29.1	2.0	5.0	16.3	5.9	19.1	11.5	3.9	14.6
Dasypus hybridus	30.4±6.1	4.4±0.9	2.6±0.7	6.9±0.8	4.4±0.01	44.9±0.1	28.6±0.7	3.5±1.6	5.7±0.4	12.6±2.3	6.4±0.6	16.4±0.8	11.7[c]	2.3[c]	19.0[c]
Dasypus novemcinctus	43.2±1.2	7.0±0.4	3.8±0.5	10.7±0.8	5.9±0.7	69.7±1.4	41.1±1.0	6.2±1.6	7.4±0.2	24.9±1.7	8.5±0.5	28.7±1.0	17.5±0.3	8.3±0.4	19.9±1.8
Chlamyphorus truncatus	10.5±0.6	1.8±0.4	1.1±0.1	2.9±0.04	2.6±0.2	21.7±1.3	10.8±0.8	1.8±0.9	3.4±0.6	10.5±1.7	4.0±0.2	11.0±0.6	4.4±2.0	3.5[c]	17.6[c]
Priodontes maximus	72.2±0.8	10.8±0.5	9.2±1.0	24.5±1.5	15.0±0.4	132±3.4	75.8±4.5	14.6±0.6	24.8±2.6	47.4±1.2	21.4±1.5	56.3±2.7	19.7±3.5	28.0±3.2	104±5.0

[a]Only one specimen used for this study
[b]Scapular acromion was completely fractured specimen due to previous damage
[c]Only one measurement each for this species
[d]Claw of digit III was fractured due to previous damage

TABLE 8. Means (± s.d.) of functional osteological indices for all armadillo species.

Species	SI	GFSI	SHI	HHSI	SMI	HRI	HEI	HEWI	HTDI	HTLI	HCLI	HTCLI	BI	HRLI
Tolypeutes matacus	0.62±0.1	0.53±0.04	1.17±0.1	1.00±0.2	0.52±0.1	0.13±0.03	0.37±0.03	0.66±0.1	0.12±0.02	0.45±0.1	0.41±0.1	1.07±0.2	0.78±0.03	1.29±0.04
Zaedyus pichiy	0.69±0.05	0.59±0.11	1.16±0.04	0.71±0.1	0.52±0.03	0.13±0.02	0.39±0.02	0.65±0.04	0.13±0.01	0.52±0.1	0.43±0.03	1.21±0.1	0.63±0.02	1.59±0.1
Chaetophractus vellerosus[a]	0.82[b]	0.56	1.00[b]	0.71	0.49	0.10	0.39	0.65	0.13	0.55	0.44	1.25	0.63	1.60
Chaetophractus villosus	0.75±0.10	0.54±0.1	1.04±0.1	0.91±0.2	0.52±0.1	0.12±0.02	0.42±0.05	0.69±0.1	0.14±0.01	0.42±0.1	0.43±0.1	1.02±0.3	0.61±0.03	1.63±0.1
Cabassous centralis	0.64±0.01	0.70±0.04	1.52±0.03	1.45±0.15	0.67±0.01	0.21	0.51±0.01	0.60±0.01	0.11±0.00	0.35±0.01	0.30±0.05	1.17±0.2	0.61±0.00	1.64±0.01
Cabassous unicinctus	0.66±0.05	0.79±0.05	1.41±0.07	0.89±0.03	0.59±0.05	0.22±0.03	0.49±0.03	0.58±0.1	0.11±0.00	0.43±0.1	0.41±0.05	1.04±0.1	0.61±0.04	1.65±0.1
Dasypus septemcinctus[a]	0.74	0.62	1.22	0.57	0.49	0.09	0.32	0.64	0.11	0.42	0.44	0.96	0.67	1.50
Dasypus hybridus	0.73±0.01	0.65±0.1	1.13±0.1	0.67±0.05	0.47±0.1	0.11±0.03	0.32±0.02	0.69±0.05	0.10±0.00	0.37±0.1	0.39	0.94±0.2	0.65±0.1	1.55±0.2
Dasypus novemcinctus	0.70±0.01	0.67±0.05	1.31±0.04	0.65±0.1	0.49±0.03	0.12±0.03	0.32±0.02	0.71±0.04	0.10±0.01	0.44±0.03	0.41±0.05	1.10±0.1	0.69±0.03	1.45±0.05
Chlamyphorus truncatus	0.86[a]	0.37[a]	1.38[a]	0.72[a]	0.53[a]	0.30[a]	0.60[a]	0.49[a]	0.12[a]	0.50[a]	0.44[a]	1.14[a]	0.53[a]	1.87[a]
Priodontes maximus	0.89±0.1	0.46±0.01	1.13±0.1	1.11±0.1	0.62±0.01	0.17[b]	0.46±0.02	0.66±0.01	0.12±0.01	0.33±0.15	0.35±0.03	0.94±0.4	0.56±0.02	1.80±0.1

Means (± s.d.) of functional osteological indices for all armadillo species.

Species	RLI	RSI	ARSI	RRI	OLI	IFA	UTLI	URI	USI	TMOI	MCRI	MPI	AMPI	PPRI	CLAW
Tolypeutes matacus	0.67±0.02	2.04±0.3	0.09±0.01	0.08±0.01	0.26±0.04	0.46±0.02	0.14±0.03	0.06±0.01	0.11±0.01	0.35±0.00	0.53±0.1	0.52±0.1	1.99±0.4	1.11±0.6	2.06±0.4
Zaedyus pichiy	0.67±0.05	1.78±0.4	0.09±0.01	0.11±0.01	0.27±0.05	0.53±0.1	0.19±0.02	0.08±0.01	0.14±0.02	0.36±0.05	0.21±0.03	0.38±0.2	3.01±1.2	1.02±0.3	1.09±0.2
Chaetophractus vellerosus[c]	0.61	1.72	0.08	0.12	0.31	0.64	0.21	0.06	0.13	0.43	0.17	0.55	1.83	0.47	0.44[d]
Chaetophractus villosus	0.62±0.02	1.80±0.3	0.13±0.02	0.10±0.02	0.33±0.05	0.61±0.1	0.19±0.01	0.08±0.01	0.14	0.41±0.05	0.22±0.03	0.33±0.1	3.16±0.7	1.12±0.4	1.37±0.6
Cabassous centralis	0.57±0.00	1.12±0.1	0.11±0.01	0.14±0.01	0.37±0.00	0.75±0.05	0.16±0.01	0.09±0.00	0.16±0.03	0.62±0.1	0.36[a]	0.67[a]	1.50[a]	0.82[a]	1.87[a]
Cabassous unicinctus	0.56±0.02	1.43±0.15	0.12±0.01	0.16±0.02	0.43±0.04	0.98±0.15	0.22±0.04	0.09±0.01	0.16±0.01	0.64±0.1	0.37±0.1	0.97±0.45	1.57±0.3	0.62±0.05	1.59±0.3
Dasypus septemcinctus[c]	0.60	1.98	0.13	0.09	0.34	0.66	0.12	0.04	0.10	0.47	0.29	0.34	2.95	1.08	0.95
Dasypus hybridus	0.68±0.1	1.55±0.2	0.09±0.01	0.14±0.00	0.28±0.05	0.57±0.04	0.14±0.01	0.08±0.04	0.13±0.01	0.39±0.15	0.33[a]	0.20[a]	5.03[a]	2.09[a]	1.35[a]
Dasypus novemcinctus	0.62±0.01	1.84±0.2	0.09±0.01	0.16±0.01	0.36±0.02	0.70±0.03	0.12±0.01	0.09±0.02	0.11±0.01	0.49±0.02	0.29±0.02	0.47±0.02	2.13±0.1	0.68±0.05	0.77±0.1
Chlamyphorus truncatus	0.48±0.00	1.01±0.1	0.11±0.01	0.17±0.03	0.45[a]	1.04±0.02	0.18±0.00	0.14±0.05	0.20±0.05	0.73±0.1	0.41±0.2	1.16[a]	0.86[a]	0.61[a]	2.74[a]
Priodontes maximus	0.55±0.01	1.63±0.1	0.13±0.01	0.15±0.01	0.36±0.01	0.75±0.1	0.16±0.01	0.11±0.01	0.19±0.02	0.59±0.1	1.05±0.2	1.43±0.1	0.70±0.1	0.53±0.1	2.20±0.2

[a]Only one specimen used for this study
[b]Scapular acromion was broken off specimen due to previous damage
[c]Only one measurement used for this species
[d]Claw of digit III was fractured due to previous damage

TABLE 9. Stepwise DFA Wilk's lambda scores, F-statistics, and significance for functional index data relating substrate use.

Step	Functional Index	Wilk's Lambda	F-Statistic	*P*
1	BI	0.476	9.923	0.012
2	USI	0.091	40.083	<0.001
3	RRI	0.041	54.222	<0.001
4	SMI	0.014	106.778	<0.001
5	OLI	0.007	138.106	<0.001
6	SHI	0.003	236.371	<0.001

Lambda value for the last step represents the amount of variance remaining
BI, Brachial Index; USI, Ulnar Shape Index; RRI, Radial Robustness Index; SMI, Shoulder Moment Index; OLI, Olecranon Length Index; SHI, Scapulohumeral Index

TABLE 10. Stepwise DFA Wilk's lambda scores, F-statistics, and significance for index data relating digging habit specialization substrate use.

Step	Functional Index	Wilk's Lambda	F-Statistic	*P*
1	BI	0.157	21.517	0.001
2	HRLI	0.010	30.715	<0.001
3	UTLI	0.004	28.305	<0.001
4	CLAW	0.001	32.022	<0.001
5	MCRI	<0.001	40.144	<0.001
6	GFSI	<0.001	51.496	<0.001

Lambda value for the last step represents the amount of variance remaining
BI, Brachial Index; HRLI, Humerus-Radial Length Index; UTLI, Ulnar Trochlear Length Index; CLAW; Relative Manus Claw Length; MCRI, Metacarpal Robustness Index; GFSH, Glenoid Fossa Shape Index

TABLE 11. Comparative forelimb muscle traits in *Z. pichiy* and other armadillos

Trait	*Zaedyus pichiy*	*Tolypeutes matacus*[a,b]	*Dasypus novemcinctus*[c,d,e]	*Euphractus sexcinctus*[d,f,g]	*Chaetophractus vellerosus*	*Chaetophractus villosus*[g]	*Chlamyphorus truncatus*[bd,g,h]
Origin of trapezius pars cervicalis	First dermal ring of carapace; base of cranium	Scapular shield and first dermal ring of carapace	Cervical/thoracic vertebrae via aponeurosis	Cervical vertebrae via aponeurosis	First dermal ring of carapace; base of cranium	Junction of scapular shield and first demal ring of carapace; base of cranium	Base of cranium
Distinct head of rhomboideus profundus	Absent	Present	Absent	Absent	Absent	Absent	Absent
Omotransversarius	Present	Absent	Absent	Present	Present	Present	Present
Brachiocephalicus: cleidomastoidea	Present	Present	Absent	Present	Present	Present	Present
Brachiocepalicus: cleidocephalicus	Absent	Absent	Absent	Absent	Absent	Absent	Absent
Coracobrachialis	Present	Present	Present	Present	Present	Present	Variable[i]
Biceps brachii – short head	Absent	Present	Variable	Present	Present	Present	Absent
Brachioradialis	Absent	Absent	Absent	Absent	Absent	Absent	Absent
Triceps brachii – medial accessory (# of triceps heads)	Present (6)	Present (variable)[j]	Variable (4)	Present (5)	Present (6)	Present (6)	Present (4–6[k])
Distinct head of triceps brachii long head	Present	Variable[j]	Absent	Absent	Present	Present	Present
Pronator quadratus	Absent	Absent	Absent or reduced	Absent	Absent	Present	Absent or reduced
Flexor digitorum profundus (# of humeral bellies)	2	2	2	2	2	3	1
Digits served by flexor digitorum superficialis	To digits II-IV	To digis II-IV	To digits I–III	To digits II, III	To digits II, III	To digit II, III[l]	To digits I, III
Number of digits on forefeet	5	3-4	4	5	5	5	5

Data sources: [a]Butcher et al. (unpublished data); [b]Murie (1872); [c]Miles (1941); [d]Macalister (1875); [e]Olson et al. (2016); [f]Galton (1869); [g]Windle and Parsons (1899); [h]Hyrtl (1855); [i]Hyrtl (1855) did not observe m. coracobrachialis in *Chl. truncatus*; [j]Butcher et al. (unpublished data) described two distinct heads of the m. triceps brachii long head in one individual and only one head in another individual; [k]Macalister (1875) observed 3 scapular heads and one humeral head in *Chl. truncatus*; [l]Windle and Parsons (1899) observed the m. flexor digitorum superficialis to serve to only digit III in *Cha. villosus*

Fig. 1 Schematic diagrams of forelimb osteological measurements taken from the **a** scapula, **b** humerus, **c** ulna, **d** radius, and **e** manus. SL, greatest scapula length; SW, greatest scapula width; GFL, glenoid fossa length; GFW, glenoid fossa width; HL, greatest humerus length; HW, humerus mid-shaft width; DCL, humeral delto-pectoral crest length; HCL, humeral capitulum length; DEW, humeral distal epcondylar width DAW, humeral distal articular width; HTL, humeral trochlea length; HHW, humeral head width; HHD, humeral head depth; HTD, humeral trochlea depth; RL, greatest radius length; RD, radius mid-shaft depth; RW, radius mid-shaft width; RHL, radial head length; RHW, radial head width; UL, greatest ulna length; UW, ulna mid-shaft width; OL, ulnar olecranon length; UTL, ulnar trochlear notch length; FUL functional ulna length; UD, ulna midshaft FOL, functional olecranon length; depth; MCL, metacarpal III length; MCW, metacarpal III width; PPL, proximal phalanx length of digit III; PPW, proximal phalanx width of digit III; CL, manus claw length of digit III.

Ā

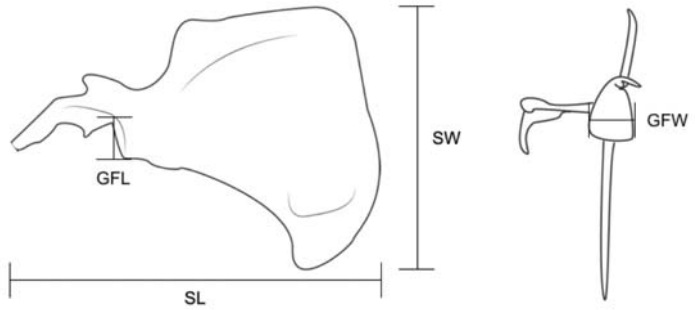
GFL
SW
SL
GFW

À

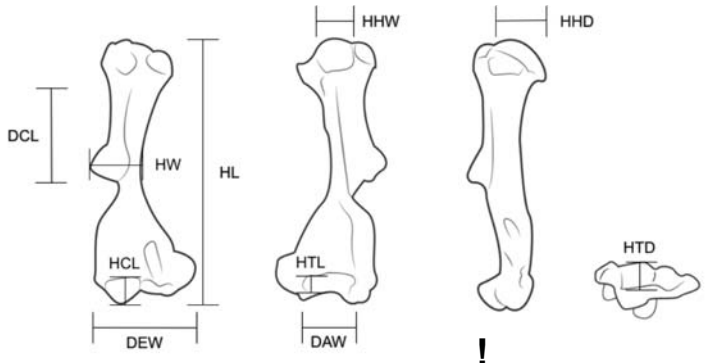
DCL
HW
HL
HCL
DEW
HHW
HTL
DAW
HHD
HTD

!

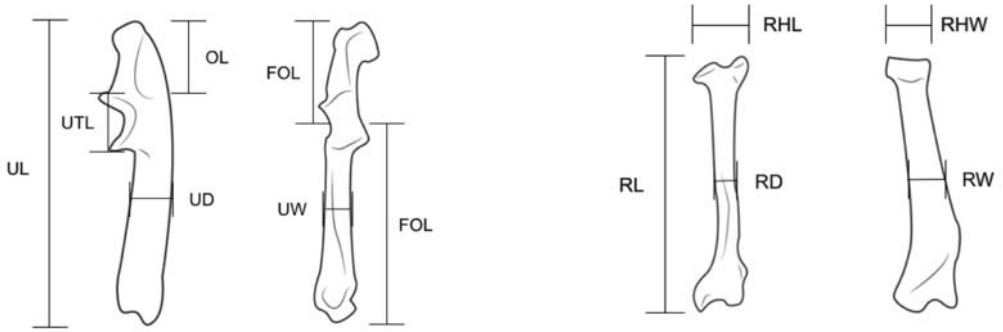
UL
UTL
OL
UD
FOL
UW
FOL
RHL
RL
RD
RHW
RW

"

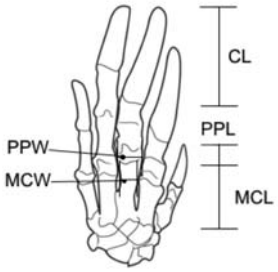
CL
PPL
PPW
MCW
MCL

Fig. 2 Photographs of forelimb muscle topography of *Z. pichiy* for **a** lateral and **b** medial views. Muscle abbreviations are listed in Table 2.

Ā

Lateral forelimb view

À

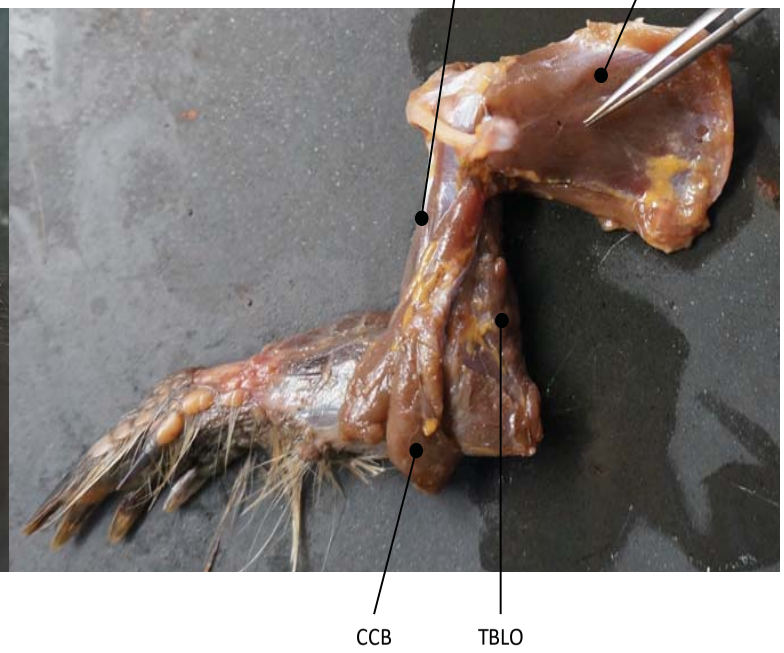

Medial forelimb view

Fig. 3 Muscle map diagrams of *Z. pichiy* for **a** lateral and **b** medial scapula (and clavicle). Muscle abbreviations are listed in Table 2.

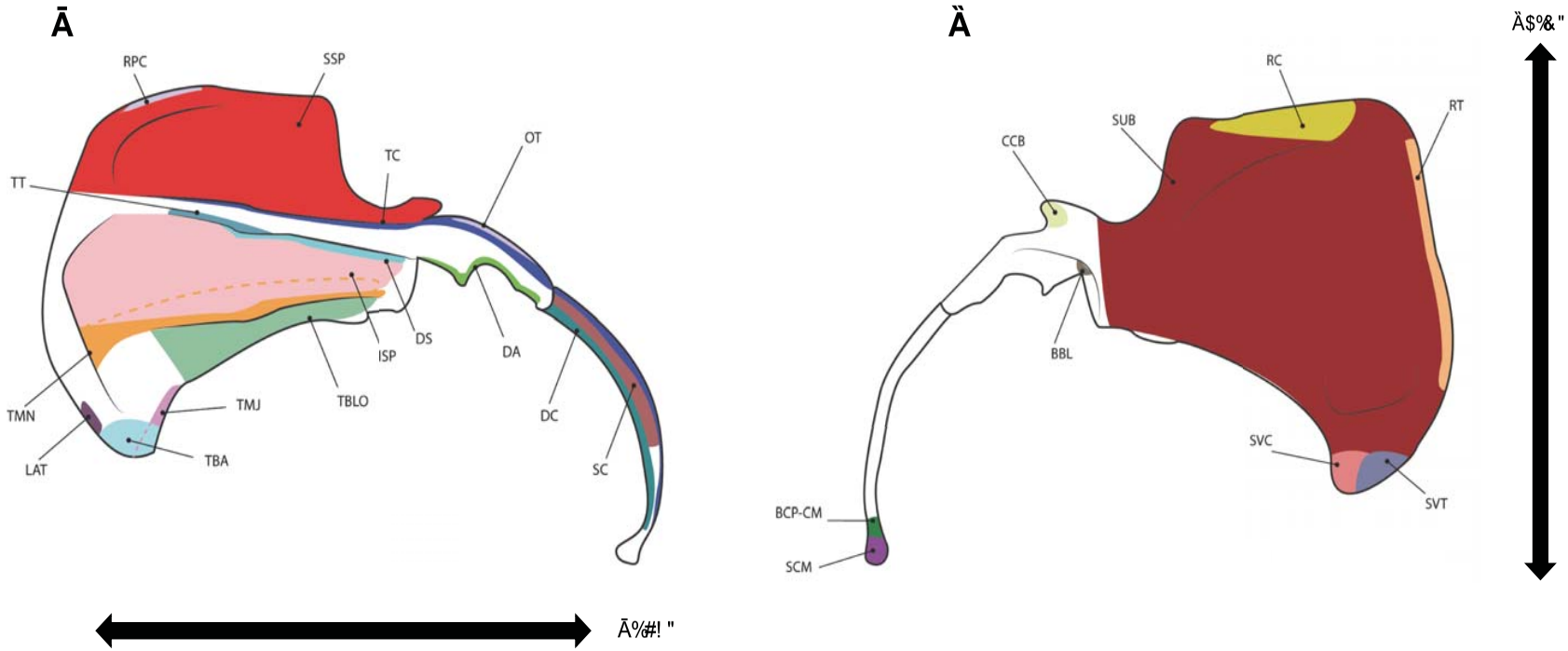
Ā
RPC
SSP
TC
OT
TT
DS
ISP
DA
TMN
TMJ
TBLO
DC
LAT
TBA
SC
Ā%#! "
À
RC
RT
SUB
CCB
BBL
SVC
SVT
BCP-CM
SCM
Ä$%&"

Fig. 4 Muscle map diagrams of *Z. pichiy* for **a** cranial, **b** caudal, **c** lateral, and **d** medial humerus. Muscle abbreviations are listed in Table 2.

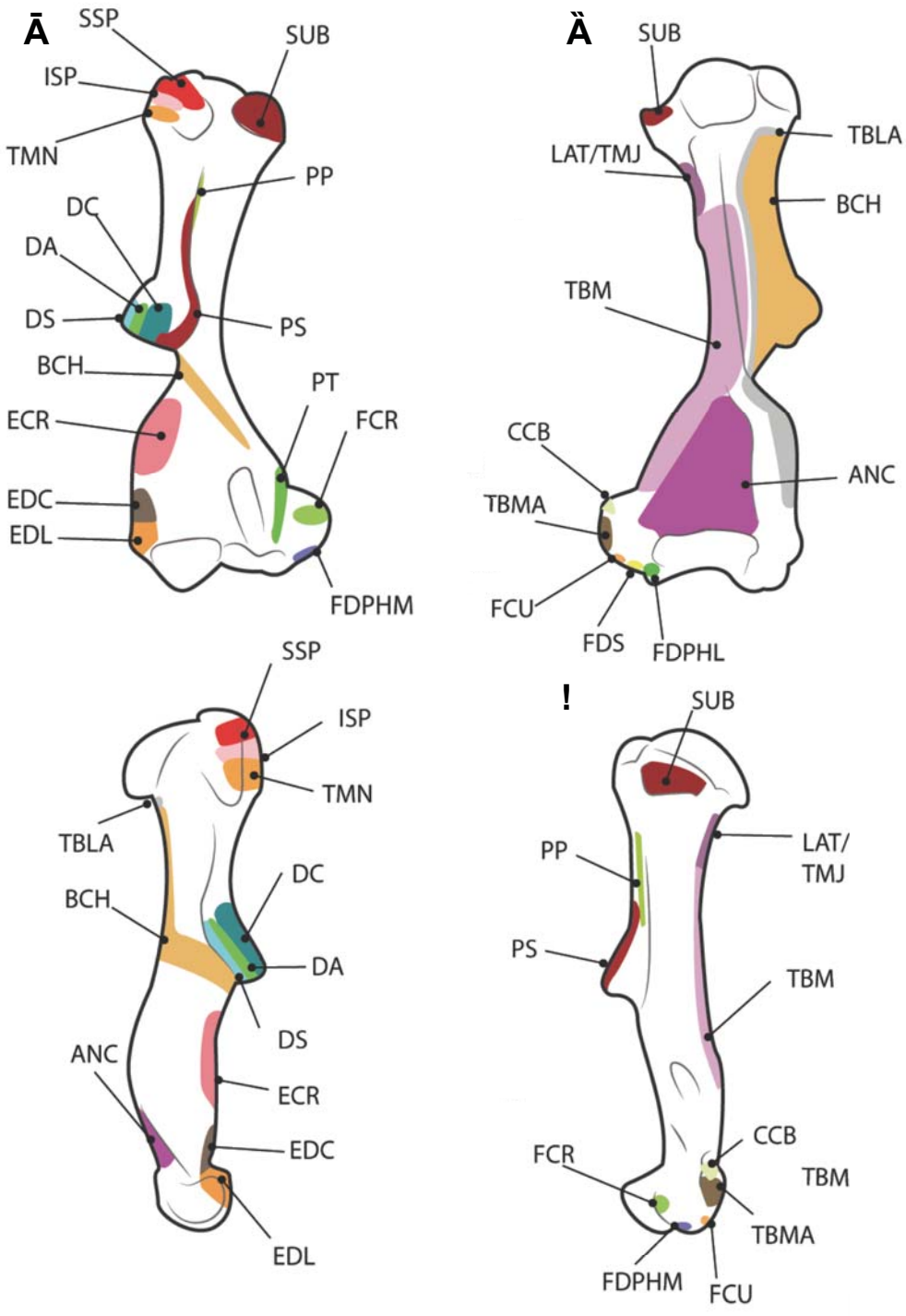
Ā
SSP
SUB
ISP
TMN
PP
DC
DA
DS
PS
BCH
PT
ECR
FCR
EDC
EDL
FDPHM
À
SUB
TBLA
LAT/TMJ
BCH
TBM
CCB
ANC
TBMA
FCU
FDS
FDPHL
SSP
ISP
TMN
TBLA
DC
BCH
DA
DS
ANC
ECR
EDC
EDL
!
SUB
LAT/
TMJ
PP
PS
TBM
CCB
FCR
TBM
TBMA
FDPHM
FCU

Fig. 5 Muscle map diagrams of *Z. pichiy* for **a** lateral ulna, **b** medial ulna, **c** lateral radius, and **d** medial radius. Muscle abbreviations are listed in Table 2.

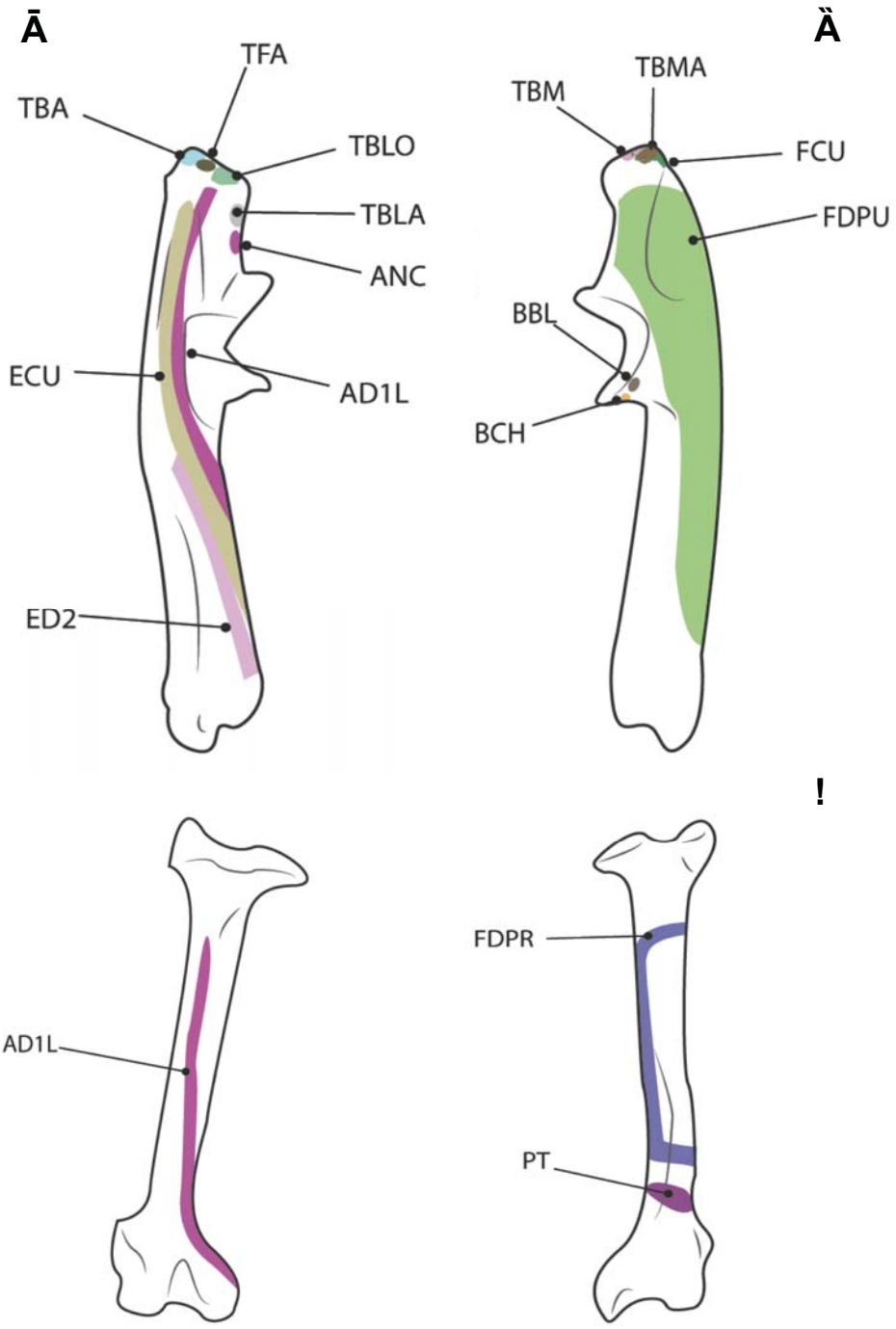
Ā
TFA
TBA
TBLO
TBLA
ANC
ECU
AD1L
ED2
À
TBMA
TBM
FCU
FDPU
BBL
BCH
!
AD1L
FDPR
PT

Fig. 6 Muscle map diagrams of *Z. pichiy* for **a** palmar and **b** dorsal manus. Muscle abbreviations are listed in Table 2.

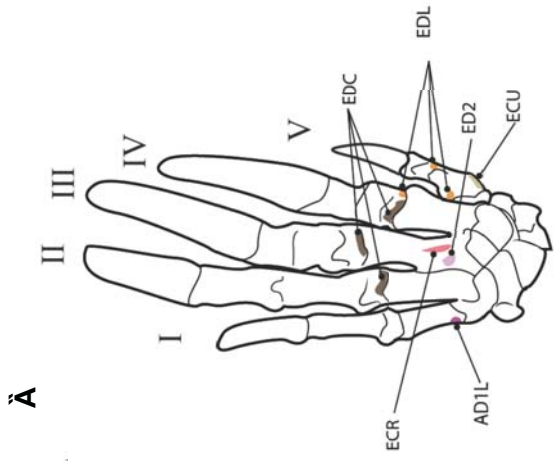
Ā
I
II
III
IV
V
EDC
EDL
ED2
ECU
ECR
AD1L

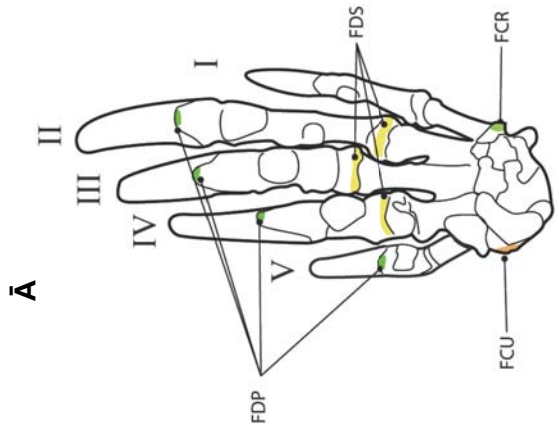
Ā
I
II
III
IV
V
FDS
FCR
FDP
FCU

Fig. 7 a Distribution of functional group muscle mass to total forelimb muscle mass for *Z. pichiy*. Total forelimb muscle mass was calculated for the summed mass of all individual muscles studied. Proximal-to-distal muscle group mass is expressed as a percentage, with *bars* representing means for each functional group. *Error bars* represent the s.d. (standard deviation). Muscles with synergistic functions are combined into one functional group. Biarticular muscles are also included in more than one functional group. **b** Distribution of select functional group muscle mass to total forelimb muscle mass compared between *Z. pichiy*, *Cha. vellerosus*, *Cha. villosus*, and *Chl. truncatus*. Functional groups for comparison include the limb retractors, elbow extensors, digital flexors, and carpal flexors. Total forelimb muscle mass was calculated the summed mass of all indicidual muscles studied. Proximal-to-distal muscle group mass is expressed as a percentage, with *bars* representing means for each functional group. Biarticular muscles are included in more than one functional group.

6

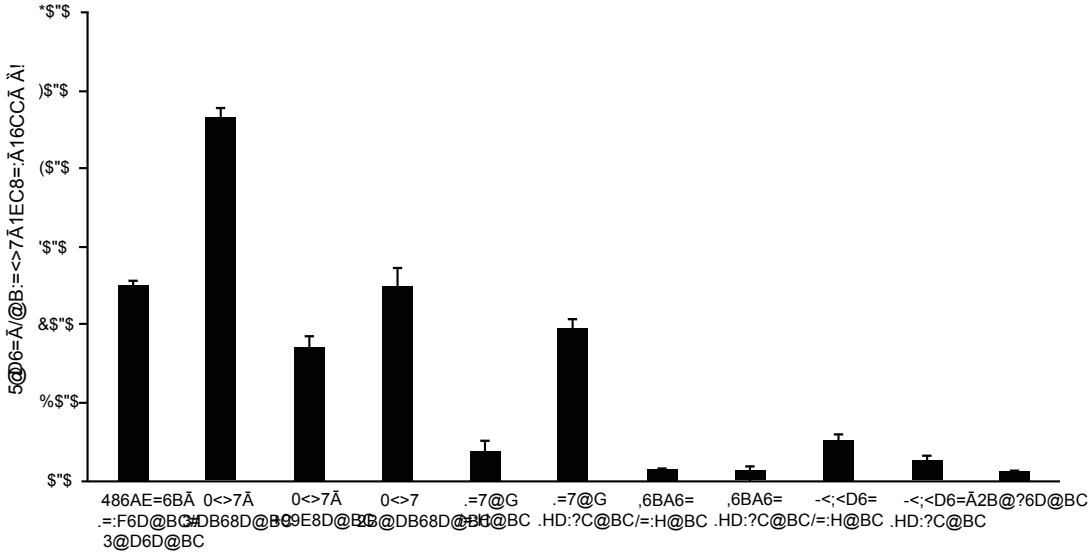
*$"$
)$"$
($"$
'$"$
&$"$
%$"$
$"$
5@D6=Ā/@B:=<>7Ā1EC8=:Ā16CCĀ Ā!
486AE=6BĀ 3@D6D@BC
0<>7Ā3:DB68D@BC
0<>7Ā3:DB68D@BC
0<>7 3@DB68D@BC
.=7@G .HD:?C@BC
.=7@G .HD:?C@BC/=:H@BC
,6BA6= Ā/=:H@BC
,6BA6= .HD:?C@BC/=:H@BC
-<;<D6= .HD:?C@BC
-<;<D6=Ā2B@?6D@BC

7

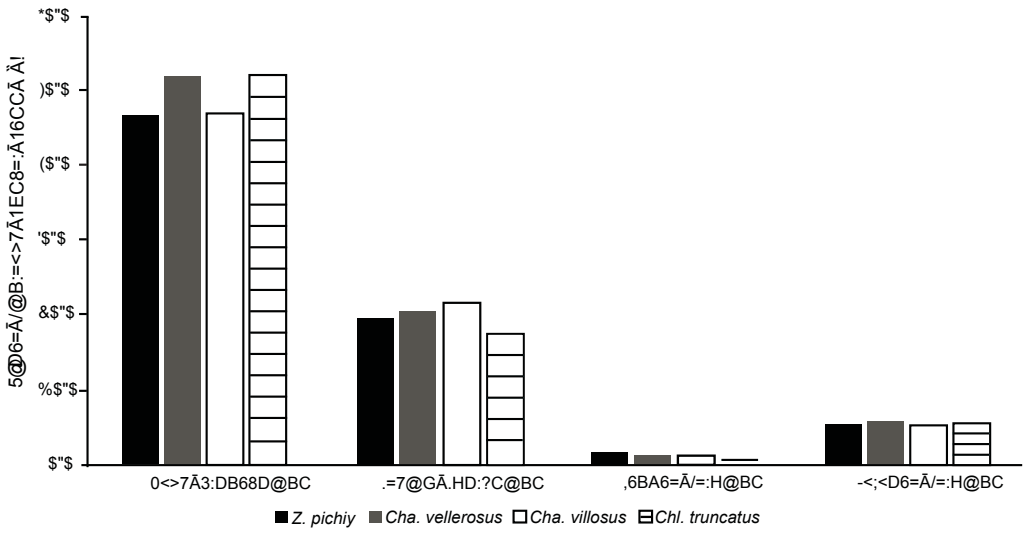
*$"$
)$"$
($"$
'$"$
&$"$
%$"$
$"$
5@D6=Ā/@B:=<>7Ā1EC8=:Ā16CCĀ Ā!
0<>7Ā3:DB68D@BC
.=7@GĀ.HD:?C@BC
,6BA6=Ā/=:H@BC
-<;<D6=Ā/=:H@BC
Z. pichiy
Cha. vellerosus
Cha. villosus
Chl. truncatus

Fig. 8 Allometry of humeral dimensions in armadillos. Allometric scaling regressions for **a** humerus length and mass, **b** humerus length and width, and **c** humerus length and depth. Under the null hypothesis of isometry, length and mass are expected to scale with a slope of 0.33 and length to length (i.e., width and depth) with a slope of 1.00. Data are log transformed and plotted on standard axes (in mm and g). Solid lines indicate the fitted Model 2 regression, whereas the dashed lines correspond to the 95% confidence intervals. Scaling coefficients (b: slope) and R^2 are shown for each relationship. Species (N=11) analyzed are identified by their symbol in the legend.

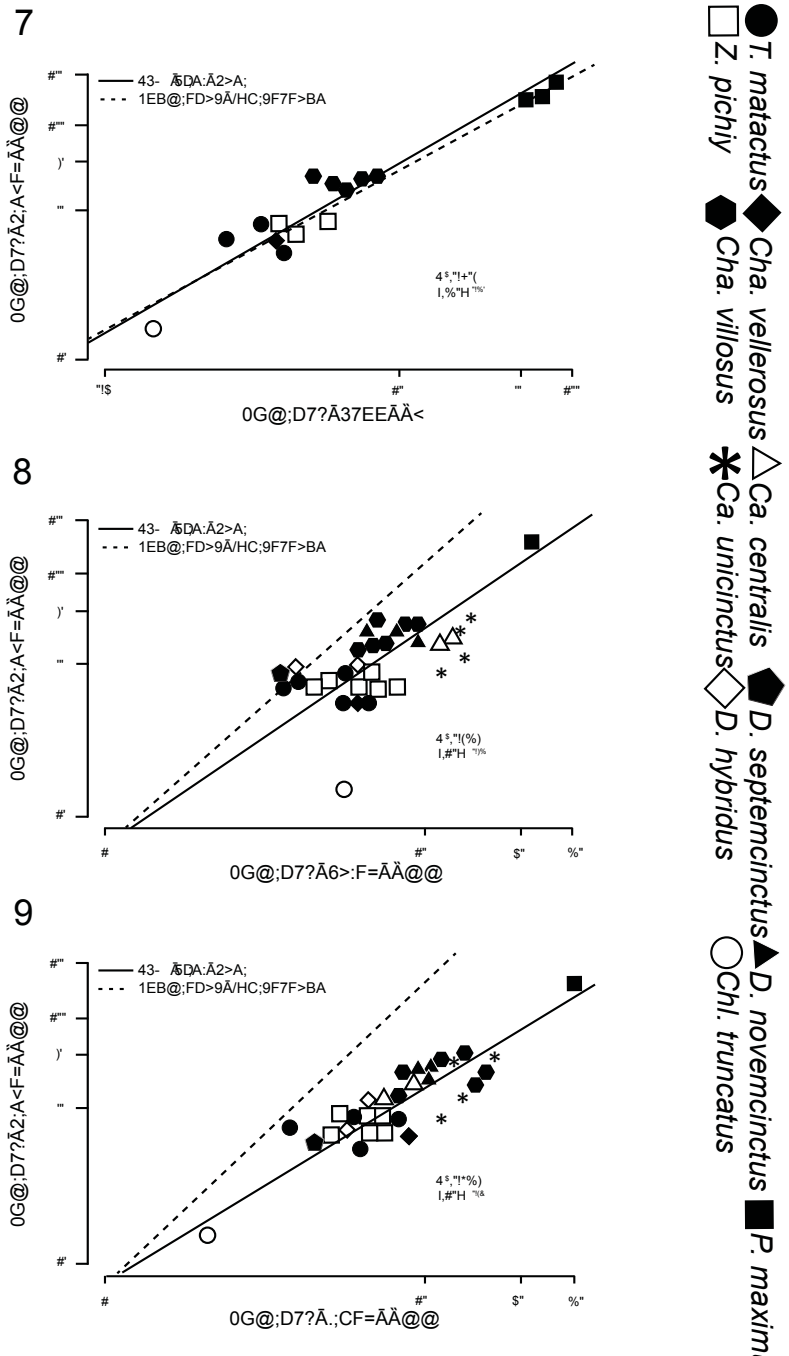
7
8
9
0G@;D7?Ã37EEÃÀ<
0G@;D7?Ã6>:F=ÃÀ@@
0G@;D7?Ã.;CF=ÃÀ@@
0G@;D7?Ã2;A<F=ÃÀ@@
T. matactus
Cha. vellerosus
Ca. centralis
D. septemcinctus
D. novemcinctus
P. maximus
Z. pichiy
Cha. villosus
Ca. unicinctus
D. hybridus
Chl. truncatus

Fig. 9 Stepwise Discriminent Function Analysis predictions for membership to **a** substrate use and **b** functional habit categories. Bar colors and fill patterns for all stacked columns are defined in the legends in each panel.

a

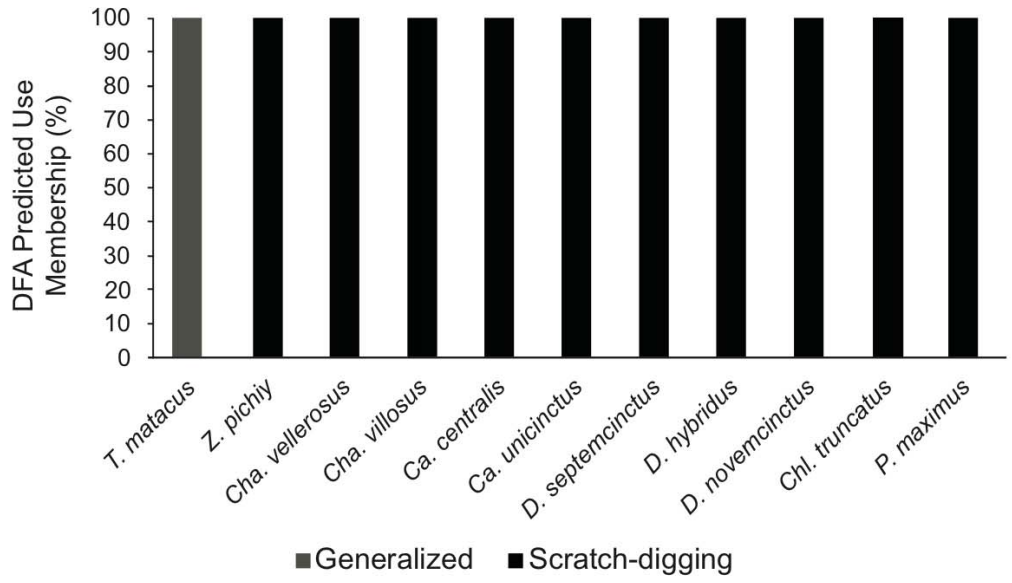
DFA Predicted Use Membership (%)
100
90
80
70
60
50
40
30
20
10
0
T. matacus
Z. pichiy
Cha. vellerosus
Cha. villosus
Ca. centralis
Ca. unicinctus
D. septemcinctus
D. hybridus
D. novemcinctus
Chl. truncatus
P. maximus
Generalized
Scratch-digging

b

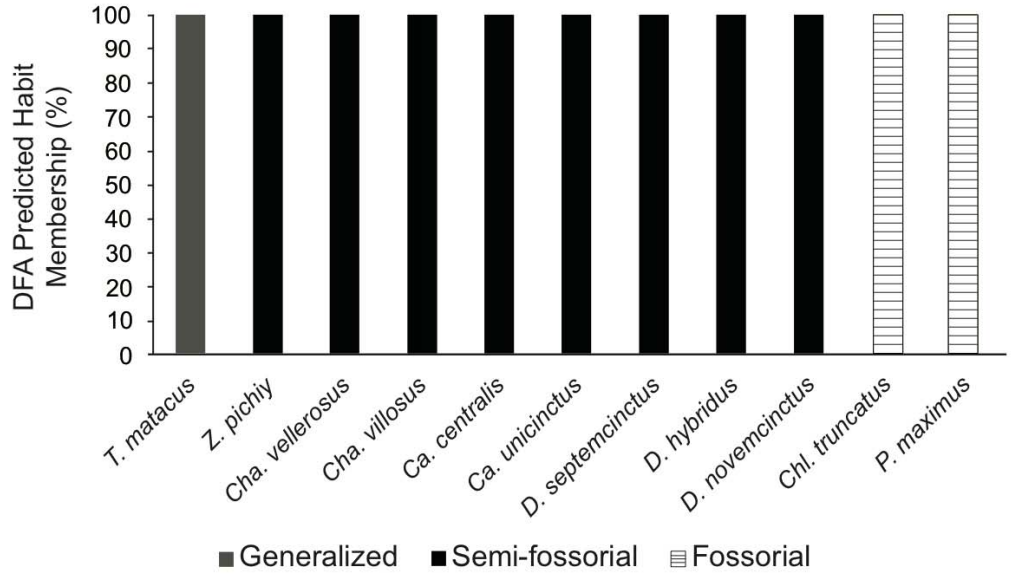
DFA Predicted Habit Membership (%)
100
90
80
70
60
50
40
30
20
10
0
T. matacus
Z. pichiy
Cha. vellerosus
Cha. villosus
Ca. centralis
Ca. unicinctus
D. septemcinctus
D. hybridus
D. novemcinctus
Chl. truncatus
P. maximus
Generalized
Semi-fossorial
Fossorial